MONDRAGON UNIBERTSITATEA

GOI ESKOLA POLITEKNIKOA

FACULTY OF ENGINEERING

PH.D. DISSERTATION

Towards data-driven predictive maintenance for industrial robots

Author:

Unai IZAGIRRE AIZPITARTE

Supervisors:

Dr. Urko ZURUTUZA ORTEGA

Dr. Luka ECIOLAZA ECHEVERRIA

Applied Engineering PhD Program

Computer and Electronics Department

Faculty of Engineering

Mondragon Unibertsitatea

Arrasate

April 2021

Familiari esker eta familiarentzat.

Acknowledgments

I want to thank my supervisors Urko Zurutuza and Luka Eciolaza for all their help, advice and reviews during the course of my PhD degree. I also want to thank to my colleagues Javi, Iñigo, Markel, Julen and Oscar for they support. Your company made the PhD much more enjoyable in the good times and much more bearable in the bad ones.

I want to specially thank Imanol Andonegui for his constant and clear advises, for his outstanding implication, as well as for the technical support. This PhD thesis would not have been possible without him. I will always be grateful for what you have done these years and admire the passion and rigour with which you face any scientific challenge.

Muchas gracias a todos los compañeros de la planta de montaje bruto de Mercedes-Benz Vitoria Ani, Suber, Mónica, Fede, Pascual, Luis, Arantza, Armentia y Bazán, por haberme hecho sentir uno más del equipo. Gracias a Aniceto Alonso por la gran implicación, el conocimiento y la ayuda que me ha ofrecido todo este tiempo. A Javier Bustamante por los consejos, la creatividad y por definir siempre un horizonte claro hacia donde avanzar. Y en especial a Jon, Adrian y Toni, por todos los momentos compartidos en el día a día, tanto dentro de la fábrica como fuera de ella.

Azkenik, eskerrik beroenak familiari. Zuen laguntzari esker izan dut indarra tesia bukatzeko eta tesiaren aurretik eta geroago etorriko direnei ere aurre egiteko. Eskerrik asko beti erreferente izateagatik. Eta zuri Mai, bihotzez, distantzia ezerezean uztea lortzen duzu beti. Mila esker guztiagatik.

Declaration

Hereby I declare that this document is my original authorial work, which I have worked out on my own. All sources, references, and literature used or excerpted during elaboration of this work are properly cited and listed in complete reference to the due source.

Unai Izagirre Aizpitarte
Arrasate, April 2021

Abstract

The automation of industry in general and the use of industrial robots in assembly lines in particular has considerably increased in the last two decades. Although industrial robots have received significant attention from academic research, there is a lack of contributions focused on the predictive maintenance of these complex systems. In the era of the fourth industrial revolution, improvements in industrial sensorization, data analysis and cyber-physical infrastructures, allow to address the predictive maintenance of industrial robots from a data-driven perspective. This research work reports on experimental evidence of reliable data-driven techniques for the predictive maintenance of industrial robots. This thesis presents four main contributions: the diagnosis of the health status of an industrial robot using vision-based techniques, the feasibility of using torque sensors to diagnose the conditions of industrial robots in real industrial environments, the optimization of the standby pose of robots with genetic algorithms and the design and implementation of a practical data acquisition network for real world industrial scenarios, respectively.

keywords:
Industrial robots, Predictive Maintenance, Prognosis and Health Management, Energy Efficiency, Data Analysis, Cyber-Physical Systems, Industry 4.0

Laburpena

Industria automatizazioak orokorrean eta zehazki muntaketa-kateetan robot industrialen erabilerak gorakada handia izan du azken bi hamarkadetan. Nahiz eta mundu akademikoak sakon jorratu duen robotika, ikerketa hutsune nabaria dago sistema konplexu hauen mantenketaren arloan. Gaur egungo sentsorizazio teknologiek, datuen analisiak eta infraestruktura ziber-fisikoen aurrerakuntzek, ikerketa hutsune hau betetzeko datuen analisian oinarritutako soluzioak proposatzea ahalbidetzen dute. Lan honetan jorratzen den ikerketa robot industrialen mantenketa prediktiboan datza. Horretarako, datuen analisian oinarritutako ikerketaz baliatuz. Tesian zehar hurrengo lau ekarpen nagusi aurkeztuko dira: Robot industrialen osasun egoeraren diagnosia ikusmen teknikak erabiliz, torke sentsoreen erabilgarritasunaren azterketa roboten osasunaren diagnosirako, roboten itxarote posizioaren optimizazioa algoritmo genetikoak erabiliz eta industrian inplementagarria den roboten monitorizaziorako sare arkitektura baten diseinu eta inplementazioa.

keywords:
Industrial robots, Predictive Maintenance, Prognosis and Health Management, Energy Efficiency, Data Analysis, Cyber-Physical Systems, Industry 4.0

Resumen

La automatización de la industria en general y el uso de robots industriales en líneas de montaje en particular ha aumentado considerablemente en las últimas dos décadas. Aunque los robots industriales hayan recibido una atención significativa por parte del mundo académico, existe una cierta falta de contribuciones en cuanto al mantenimiento predictivo de estos complejos sistemas. En la era de la cuarta revolución industrial, las mejoras en tecnologías de sensorización, el análisis de datos y las infraestructuras ciber-físicas permiten abordar este problema con soluciones basadas en el análisis de datos. Este trabajo de investigación se centrará en el estudio y desarrollo de técnicas de análisis de datos para avanzar en el mantenimiento predictivo de los robots industriales. La tesis presenta cuatro contribuciones principales: El diagnóstico del estado de salud de un robot industrial mediante técnicas de visión, la viabilidad de utilizar sensores de par motor para diagnosticar las condiciones de los robots industriales en entornos reales, la optimización de la posición de espera de los robots con algoritmos genéticos y el diseño e implementación de una arquitectura de red práctica para la adquisición de datos de robots en escenarios industriales reales.

keywords:
Industrial robots, Predictive Maintenance, Prognosis and Health Management, Energy Efficiency, Data Analysis, Cyber-Physical Systems, Industry 4.0

Contents

List of Figures

List of Tables

Acronyms

Part I

Foundation and Context

Chapter 1

Introduction

This thesis is grounded on two main pillars: The evolution of maintenance in the manufacturing industry as a consequence of the fourth industrial revolution and the prediction of mechanical faults in industrial robots. These two pillars describe, on the one hand, the context in which this research work takes place and on the other hand, the particular use case in which the study focuses. Since the advent of first cyber-physical systems, the automation and monitoring of industrial processes and machinery has grown accordingly. With this regards, maintenance strategies have undergone a drastic evolution.

Historically, maintenance was only performed correctively. After detecting a fault or a malfunction, the machine was repaired or removed from the production line and a new one was introduced [66]. As the knowledge of the industrial processes and components increased, the corrective maintenance was slowly replaced by Preventive Maintenance (PM). PM builds upon the theory that maintenance should be performed before the fault and not after. All in all, adopting a preventive maintenance strategy leaded to a big change for the industry as maintenance was no longer a passive work, but an active one. In PM, the knowledge of the behaviour of a machine or component is used to schedule maintenance activities and prevent future failures. Nowadays the reality of manufacturing industry is that preventive and corrective maintenance are still the most widely used strategies.

However, the continuous monitoring of machinery using robust and reliable sensors, is changing the way maintenance work is scheduled: from traditional knowledge and mathematical model-based preventive maintenance, to data acquisition and real condition-driven Predictive Maintenance (PdM). Instead of relying on fixed schedules, it is now possible to monitor the health status of a certain component or system by analysing acquired sensor data and to identify future trends in order to diagnose a potential future fault. Therefore, this all enables a more efficient maintenance, which is only applied when needed [25].

Prescribing maintenance solutions for the predicted failures has recently become a new promising research field [40]. The main idea of this new method is not only to predict a certain failure but also to suggest an optimal set of maintenance actions as a response. This new maintenance strategy is called Prescriptive Maintenance (PsM). Maintenance and Industry 4.0 are naturally merging, giving birth to Maintenance 4.0 as argued by Galar et. al in [20].

According to the International Federation of Robotics (IFR), the worldwide operational stock of industrial robots has increased year by year since 2009 and it is expected to keep increasing 1.1.

Even though industrial robots are a fundamental part for assembly lines, there is a significant lack of scientific research in predictive or prescriptive maintenance for robots compared to other industrial components such as bearings, gears, electric motors, etc. The complexity of an industrial robot makes it difficult to predict a mechanical fault using the traditional mathematical model-driven approaches.

Although some researchers have mentioned the feasibility of using data-driven approaches for robot PdM, there is still no consensus on how to address the issue i.e. Which sensors work best for a particular scenario and robot type? Which data acquisition techniques are more robust for a real industrial environment? Which methodology should be applied to acquire reliable data? Are questions that will have to be responded in order to achieve an optimal maintenance policy for industrial robots. Therefore, this thesis works around these questions to shed some light in the field of industrial robot predictive maintenance.

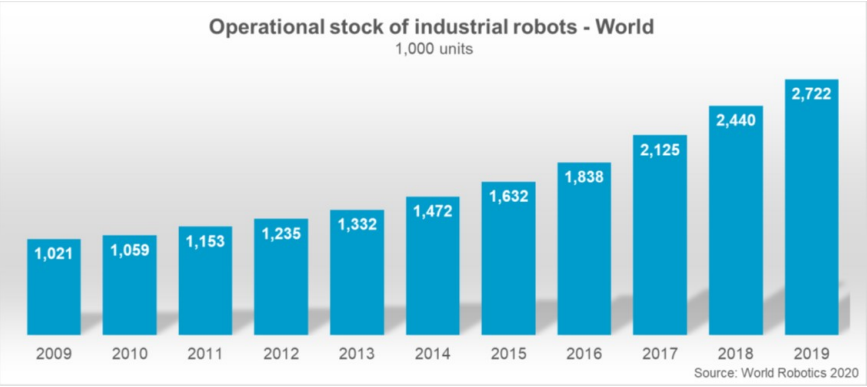

Figure 1.1: Operational stock of industrial robots according to the International Federation of Robotics (IFR).

Part II

Research Topic

Chapter 2

Research Topic

The main goal of the thesis is to advance in the predictive maintenance of industrial robots. As the literature review of the following chapter illustrates, data-driven approaches show promising results. Thus, the research will be focused on data-driven solutions for industrial robot predictive maintenance. This chapter defines the research hypotheses and the technical objectives to be completed.

2.1 Hypotheses

The following list enumerates the hypotheses of the research work:

1. *Visual-based monitoring systems provide enough accuracy to detect deviations beyond the tolerance limits of industrial robots.*

2. *Torque sensors can effectively be used to detect medium and long term mechanical deterioration in industrial robot joints.*

3. *An inefficient standby pose significantly decreases the remaining useful life of an industrial robot.*

4. *Optimising an industrial robot's standby pose can significantly reduce its energy consumption in a production line.*

5. *Common industrial assets offer enough technology to effectively assess the health status of industrial robots in real world production lines.*

2.2 Objectives

The following list enumerates the technical objectives to be accomplished to answer to all the previously exposed hypothesis:

1. To perform a critical review of the state of the art in industrial robot predictive maintenance.

2. To select the most promising sensing methods for an effective industrial robot health assessment.

3. To design and implement experiments to validate the feasibility of the selected methods.

4. To propose a methodology for the detection and prediction of industrial robot failures.

5. To study the relationship between the standby or *Home* pose of robots and their failures.

6. To optimise the standby pose of an industrial robot in order to extend it's remaining useful life and reduce it's energy consumption.

7. To develop a practical and reliable data acquisition network infrastructure that stores industrial robot signals to assess their health status.

2.3 Brief description of the publications and contributions

The research work is assembled in a total of four articles. Three of them have already been published and the fourth is currently (December, 2020) undergoing a peer review process. Each research article focuses on accomplishing on one or two technical objectives and ultimately answers to at least one of the hypothesis listed above.

Article 1: Towards manufacturing robotics accuracy degradation assessment: a vision-based data-driven implementation *(Accepted 07 July 2020, Robotics and Computer Integrated Manufacturing)*

In this manuscript we study the feasibility of using visual-based data-driven solutions for robot health assessment. The main contribution resides on the use of binary squared fiducial markers to detect robot pose degradation. We monitored a faulty robot and succeeded to identify the joint that induced the pose deviation using fiducial markers. In addition, we trained machine learning models to predict the deviation of the end tool using images captured by a camera located in one side of the robot. Answering to the first hypothesis of the thesis, these results show that binary

squared fiducial markers do indeed offer enough precision to detect deviations beyond the tolerance limits of industrial robots.

Article 2: A Methodology and Experimental Implementation for Industrial Robot Health Assessment via Torque Signature Analysis *(Accepted 03 November 2020, Applied Sciences)*

In the second article we study the feasibility of joint torque signals to assess medium and long term degradation in industrial robot joints. We analyse and compare torque signals in healthy and faulty robot joints with different loads. Moreover, we perform an exhaustive mechanical inspection to identify the root cause of the robot failure. Finally, with the knowledge acquired from the experiments and the mechanical inspection carried out, we present a practical methodology based on torque signature analysis to assess the health status of industrial robots in real world production lines. This article answers to the second hypothesis of the thesis. The results demonstrate that torque sensors can effectively be used to detect medium and long term mechanical deterioration in industrial robot joints.

Article 3: Torque-based methodology and experimental implementation for industrial robot standby pose optimization *(Accepted 09 October 2020, The International Journal of Advanced Manufacturing Technology)*

The main contribution of the third article resides on the optimization of the standby pose of industrial robots for RUL enhancement and energy consumption reduction. We perform a descriptive analysis of robot data captured in an automotive body shop assembly line and conclude that the standby pose of industrial robots has a significant impact in the reduction of the RUL of these complex systems. The standby pose of industrial robots has been traditionally ignored by researchers and practitioners. However, a non-optimal standby pose reduces the RUL of industrial robots in manufacturing assembly lines. We implement an evolutionary optimization algorithm to find an optimal standby pose for industrial robots that effectively reduces the torque applied by robot joints. The results of the article answer to the third and fourth hypotheses. The second and third articles demonstrate that an inefficient standby pose increases the temperature of the joints and therefore decreases the RUL of industrial robots in real world production lines. In addition, we show that optimising the standby pose of industrial robots significantly reduces their energy consumption.

Article 4: A practical and synchronized data acquisition network architecture for industrial robot predictive maintenance in manufacturing assembly lines *(Under peer review, IEEE Transactions on Industrial Informatics)*

The fourth article answers to the fifth and last hypothesis. It presents a practical data acquisition network architecture for industrial robots. The contribution is a necessary preliminary step towards an effective predictive maintenance for these complex systems. The proposed architecture and methodology uses well-known industrial assets to acquire robot signals in a synchronized, clean and scalable way. The data acquisition is synchronized with the robot routines in order to detect anomalies and identify possible malfunctions. We implement the architecture in a real automotive assembly line and the results show that it can automatically acquire reliable robot signals and effectively assess the health status of industrial robots in real world scenarios.

Part III

State of The Art

Chapter 3

Literature review

The following chapter provides a literature review and a theoretical background for the thesis. It will also be helpful to understand the path followed throughout the research work. This chapter begins by analysing the characteristics of different maintenance strategies. It will then briefly describe industrial robot fundamentals, with a special focus on maintenance. Afterwards, some remarkable model-driven and data-driven approaches for condition monitoring will be presented. The chapter highlights the differences and the similarities between these two approaches. The last section will review the most relevant academic contributions in industrial robot condition monitoring. Finally, the last section will summarize the main conclusions and will critically discuss the state of the art.

3.1 From corrective to prescriptive maintenance

Manufacturing industry has undergone a remarkable change in its maintenance strategy. Corrective, preventive, predictive and prescriptive maintenance are the four main strategies that the industry has applied to face the inevitable deterioration of industrial assets. In today's manufacturing companies, several or even all four of them need to coexist. Although predictive and prescriptive maintenance are gaining relevance, it is necessary to keep in mind that industrial components keep failing every day. Hence, it is still essential to prepare for those eventual failures and to apply corrective and preventive maintenance.

3.1.1 Corrective Maintenance

Corrective Maintenance (CM) focuses on making sure that the installation (assembly line, processes, machinery, personnel, etc.) is in the best possible situation to properly react to the eventual failure, even though no action is taken until the failure occurs [4]. D.S. Dhillon proposed the following steps to apply an effective CM strategy [13]:

1. Fault recognition.
2. Localization of the failure.
3. Diagnosis.
4. Repair of the affected component/s or item/s.
5. Checkout and returning the system to normal behaviour.

The purpose of CM is to minimize the Mean Corrective Maintenance Time (MCMT) [13] which is given by

$$T_{mcm} = \frac{\sum \lambda_j T_{cmj}}{\sum \lambda_j} \tag{3.1}$$

where:

T_{mcm} = Mean Corrective Maintenance Time,
T_{cmj} = Corrective maintenance time of the jth equipment/system element,
λ_j = Failure rate of the jth equipment/system element.

By definition CM is performed after the failure and it is a reactive action. In an ideal world where all the equipment's failures can be prevented or predicted CM would not be needed [59]. As nowadays reality is yet far from there, concrete actions and policies are still vital for manufacturers to react efficiently to unexpected failures. Bevilacqua et al. emphasized in [4] the importance of corrective maintenance after analysing the best maintenance strategies for an oil refinery.

3.1.2 Preventive Maintenance

PM is always applied before the failure. It comprises the set of actions and decisions taken to keep the equipment and the installation in the best possible state in order to avoid failures. An effective PM finds the balance between keeping the machinery healthy by performing maintenance interventions and reducing the cost of these interventions. The fewer PM activities are executed, the lower the cost. However, reducing PM activities increases the risk of an unexpected failure.

It is fundamental for maintenance engineers and personnel to know and understand the life cycle of an asset to schedule maintenance activities. Moreover, as maintenance resources are limited, it is crucial to optimize the scheduling of those activities. The optimization of PM intervention scheduling is one of the most important aspects of an effective PM strategy [14]. Several academic surveys have reviewed the contributions in optimal PM policy [62, 63, 41, 12].

3.1.3 Predictive Maintenance

PdM has emerged as a consequence of two main factors. On the one hand, the lack of effectiveness of PM, i.e. if PM actions are executed too prematurely, it becomes highly inefficient. On the other hand, the recent technological advances allow the robust acquisition and analysis of large amounts of data. Which permits to implement Big Data infrastructures and advanced data analysis techniques and assess the predictive maintenance of complex systems from a data-based perspective. These two factors are deeply rooted in the Industry 4.0 philosophy and are paving the way towards the future of maintenance. The merge of the Industry 4.0 paradigm with the maintenance world has recently created the Maintenance 4.0 concept.

The estimated cost for unnecessary or inappropriate preventive maintenance is up to 60.000 million dollars per year only in the U.S. [43]. This represents the 33% of the total maintenance cost of the country [43]. The purpose of PdM is to improve the efficiency of maintenance by capturing data with sensors, extract tendencies and assess the health status of the machines. Therefore, a PdM based strategy acts whenever the real conditions of the machinery require it, wasting as few resources as possible in unnecessary interventions.

There are three main steps that have to be followed to implement an effective PdM strategy: Root Cause Analysis (RCA), anomaly detection and Remaining Useful Life (RUL) prediction. With RCA, the main source of a given failure is identified. The objective of this first step is to detect the cause of a given failure [34] and determine the best ways in which changes in that particular cause of failure can be monitored. When the cause of a failure is identified and effectively monitored, it is time to detect anomalies in the monitored data. The objective of the second step (anomaly detection) is to detect anomalies in the monitored data to infer deviations in the normal behaviour of a given system and infer impending failures. An in depth survey of anomaly detection techniques and use cases can be found in [10]. Finally, once the RCA and anomaly detection phases are completed, the third step estimates the remaining useful life of the monitored asset and predicts failures based on historical data and the knowledge acquired in the previous steps. An overview of remaining useful life prediction techniques can be found in [47] and [56].

The success of each step is directly conditioned by the previous steps. If the root cause for a given failure cannot be identified, it is very difficult to monitor the health status of a given asset. Following the steps, if the health status of an asset cannot be monitored, it is not possible to detect anomalies or deviations in its normal behaviour and finally predict future failures. Therefore, the overall quality of a PdM system, directly depends on the effectiveness of its individual steps.

In the last decade there has been a remarkable increment in predictive maintenance research contributions, mainly divided into two groups: scientific reports that frame the role of predictive maintenance, define the methodology and analyse theoretical aspects of this field [64, 69, 58, 35]. And publications that present successful PdM use cases e.g. wind turbines [21, 33], induction motors [32, 7], bearings [2, 19, 22], etc.

3.1.4 Prescriptive Maintenance

The current digital transformation is pushing the maintenance of the industrial assets beyond predictive maintenance. According to Anari et al. [1] PsM extends prediction of failures. Sensing technology, expert knowledge and predictive analytics are reaching the point where decision-making support systems can be built to suggest optimal course of action to take in real time, based on the current state of the assembly line [46]. Hence, PsM focuses on suggesting what maintenance actions to take, based on the current state of the machinery, historical data analysis and expert knowledge modelling.

Matyas et al. suggested methodologies in [40] for an effective PsM implementation but real application in assembly lines will require more work by researchers and practitioners. Recently, Karner et al. [30] presented an industrial PsM use case for a steel plate manufacturer.

3.2 Model-driven approaches for condition monitoring

Physical model-driven condition monitoring depends on mathematical models that describe the behaviour of a system. These mathematical models are built by domain experts based on their knowledge and historical data. As illustrated in figure 3.1, sensor data is compared with model-generated data. If the information of the sensor and the physical model is inside certain limits, it is assumed that the system has a normal behaviour. When a certain threshold is exceeded, there is something unusual happening in the system. However, in order to build models that describe complex and non-linear systems, there are some assumptions that have to be considered such as constant speeds, lubricant temperatures, constant loads, etc. These necessary assumptions might distance the behaviour of the model from the real system.

To mention some remarkable model-driven based contributions, Kacprzynski et al. developed a physical model for gas turbine condition monitoring and prognosis [29]. Oppenheimer et al. developed a physical model for cracked rotor shafts [48]. Echavarria et al. used wind turbine models for fault diagnosis [16, 17] and Feng et

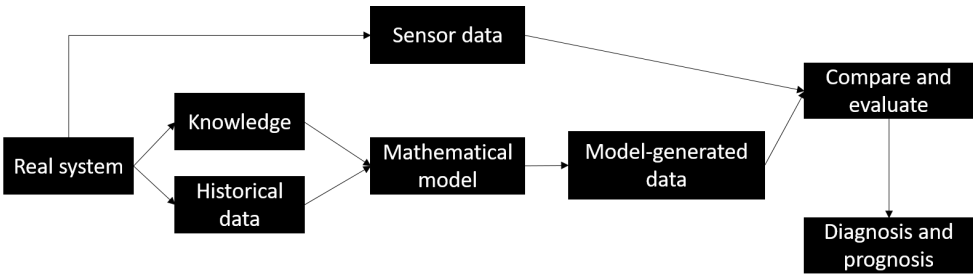

Figure 3.1: Physical model-driven maintenance.

al. implemented wind turbine gearbox models in [18]. Finally, Cheng et al. built planetary gearbox models in [11].

3.3 Data-driven approaches for condition monitoring

Data-driven approaches rely on statistical and/or machine learning methods to extract patterns and trends on historical and real time sensor data in order to predict possible future failures. This method does not require any mathematical model, so there are no assumptions or approximations made. Data-driven techniques for machine condition monitoring, are mainly divided between statistical and machine learning approaches. However, the process followed in the two approaches is essentially the same. First of all, the features that describe the behaviour of the system are identified and collected with sensors. Then, statistical and/or machine learning analysis is performed with these data features to detect patterns and trends. Finally, this data patterns are analysed to assess the health status of the machinery and predict possible failures, malfunctions or anomalies.

3.3.1 Statistical based condition monitoring

Statistical techniques study the statistical characteristics (mean, median, variance, etc.) of the features obtained and thus describe their normal or expected behaviour. When there are deviations that exceed predefined limits, it is assumed that the current behaviour of the system is anomalous.

Heng et al. [27] studied the application of sound pressure and vibration signals to detect defects in a rolling element bearing using well known statistical parameters such as the crest factor and the distribution of moments including kurtosis and skew. Zhao et al. [71] used multivariate empirical mode decomposition (EMD) for rotating machinery condition monitoring. Sohn et al. [57] monitored a fast patrol boat with statistical pattern recognition. They used time series analysis combining Auto-

Regressive (AR) and AR eXogenous (ARX) as inputs and an outlier analysis with the Mahalanobis distance measure. Gearbox condition monitoring has also been monitored using statistical methods such as Kernel principal component analysis [26] or local mean decomposition [38]. Si et al. [56] conducted an extensive review of recent modelling developments for estimating the RUL using statistical data driven approaches.

Although statistical based techniques may not be as suitable as machine learning techniques for highly non-linear systems, they are faster to compute and therefore are useful when a fast response is needed. Moreover, statistical based techniques are white box methods. In the sense that all the results can be clearly traced and explained. This is not always the case with machine learning methods.

3.3.2 Machine learning based condition monitoring

Machine learning based condition monitoring uses machine learning algorithms to extract features, identify patterns and trends in the data, and predict the future behaviour of the analysed system. Machine learning algorithms learn to describe the behaviour of the monitored system, creating a model based on the collected data. Once a machine learning model is selected, the first step is the *Training* phase. In this first phase, the model is created and optimized with the training data. Then the accuracy of the model is tested in the *Testing* phase, which consists on measuring the predictive accuracy of the model using previously unseen data.

Depending on how the *Training phase* is performed, machine learning algorithms are subdivided into two groups: unsupervised algorithms and supervised algorithms. Unsupervised algorithms do not need any additional information about the data they are modelling. They are able to create a model from raw data. Unsupervised learning is mainly used for clustering and anomaly detection. For condition monitoring, a typical approach would be to create a *normal behaviour* cluster that would include all the data obtained when the machine is in a healthy state. Then, once the algorithm is trained to identify the healthy behaviour, the algorithm would detect any new incoming data that does not fit in the cluster. This would mean that the machine is not acting in the same way as in its normal state. This method was used for bridge structural health monitoring by Khoa et al. [31] or for an induction motor fault detection system in [55] and [49]. Another way to use unsupervised algorithms is for feature extraction. When there is too much sensor information, these algorithms can be used to detect the most relevant features [36, 37] or perform dimensionality reduction [23].

Supervised algorithms differ from unsupervised algorithms in the way they create the model. While unsupervised algorithms require only raw data to describe the

behaviour of a system, supervised algorithms need some extra information about the data. When implementing supervised algorithms, the training of the algorithm has to be supervised. Explicitly identifying which data corresponds to healthy machines and which data corresponds to faulty machines. Thus, the algorithm will learn to identify if new data belongs to the first group or to the second. This type of algorithms are called supervised classification algorithms. Widodo et al. [67] published a survey about the use of a well-known machine learning algorithm called Support Vector Machine (SVM) for classification in machine condition monitoring and fault diagnosis. Deep Belief Learning based health status classification was used in [60] for aircraft engine health diagnosis and electric power transformer health diagnosis.

Supervised algorithms can also be used for non-linear regression (supervised regression models). In this case the algorithm outputs a numerical value instead of classifying the input into different groups. The numerical value can be used in condition monitoring as a representation of the health status of the machinery or even to predict it's RUL. Saha et al. [54] proposed this method for battery health monitoring. Bohouche et al. [8] used online Support Vector Regression (SVR) for speed rolling condition monitoring. Support Vector Regression was also used by Benkedjouh et al. [3] for cutting tool machine RUL prediction. Yang et al. [70] used regression models to predict several steps ahead of the current machine condition using Decision Trees and Neuro-Fuzzy systems. Finally, the modelling of a *normal behaviour* and the identification of anomalies based on deviations can also be performed with a supervised learning approach. Following this approach, a one-class supervised learning model was proposed by Michau et al. [42] to model critical and complex systems under limited information.

3.4 Industrial robot fundamentals for maintenance

In this section, I will mention some basic yet important aspects for industrial robot maintenance. The most common robots used in the manufacturing industry are robots with 6 Degrees of freedom (DOF). These robots are designed to withstand years of continuous work and handle loads up to 200kg. Industrial robots are made up of two parts: the controller and the physical structure of the manipulator chain. This thesis focuses on the physical structure of the manipulator rather than on the *Controller*

The physical structure is mainly comprised of metallic rigid-bodies and revolute movable components, hereafter referred as links and joints, respectively. Most common robotic arm manipulators are comprised of six joints and each one of thses joints has a brushless electric motor connected to a complex speed reducing gear box. The

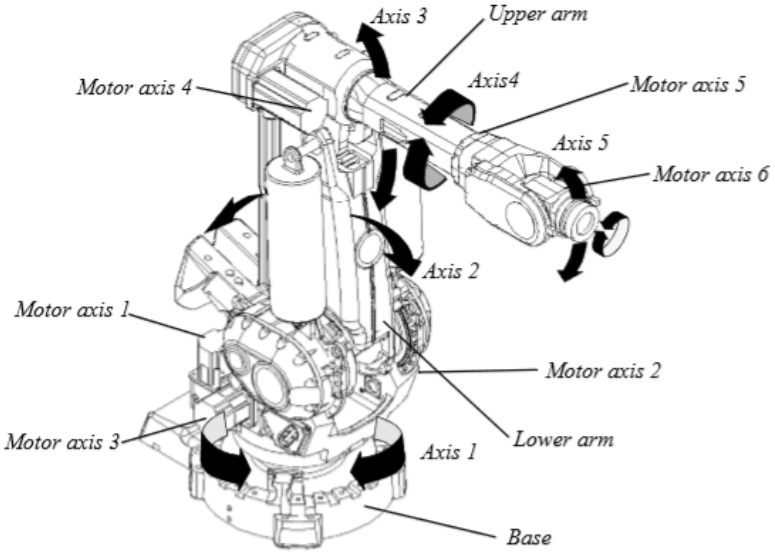

Figure 3.2: Industrial robot schematic (ABB IRB 6400 model).

links are rigid metal pieces that connect the joints serially, forming the structure of the robot. An schematic of a 6 DOF industrial robot is shown in figure 3.2. Physical failures in an industrial robot can therefore occur in any joint, in the speed reducers, in the motors, in the electrical connections or in the links.

The motors and the speed reducers are different in all the joints. The first two joints (the ones closer to the robot base) are specifically designed to work with higher loads than the rest of the joints. The reason is that they support the dynamical coupling of the whole manipulator body. Although it might be reasonable to assume that the first joints suffer more friction than the rest and thus are more prone to failure, the empirical evidence of an automotive plant with more than 600 industrial robots shows the opposite. In this automotive plant, the historical data of the industrial robot's failures collected for more than twenty years shows that 98,51% of the robot joint failures occurs in the 5th and 6th joints. Therefore, this thesis will make special emphasis on diagnosing and studying the failures of those two joints.

The speed reducers of the joints are high precision reduction gears (see figure 3.3). Although the design of the reducers is different for each joint, all of them share important tribological aspects that are explained in the following paragraphs in order to better understand the degradation process of industrial robots.

The true contact between two solid materials occurs at certain points, not on the entire apparent surface. These points at which actual contact takes place are called asperities. Figure 3.4 shows two solid surfaces before being in contact and after

Figure 3.3: Nabtesco RV-N reduction gear. An example of speed reducers used in robot joints [45].

making contact when a certain load is applied. In general, the contact of two materials creates elastic deformations on the surfaces and the material returns to its initial state after deformation. However, plastic deformation my also occur in asperities [5]. Therefore the material might not always return to its initial state and thus be permanently deformed.

In robot joints, the contact surfaces are not in direct contact because of the lubrication. Therefore, wear is caused by fatigue and to by abrasion or adhesion. The fatigue of the surface, is caused by the stress transmitted through the lubricant membrane. This fatigue wear occurs long before there is significant material detachment or attachment. With this regards B. Bhushan suggests in [5] to calculate the RUL of well lubricated components as a function of revolutions and not by measuring the amount of debris or material detachment. It is important to realise that wear is not a property of the material such as friction, but the response of a system to certain conditions. Therefore, all the characteristics of the system, robot trajectory, load, speed, temperature, type of

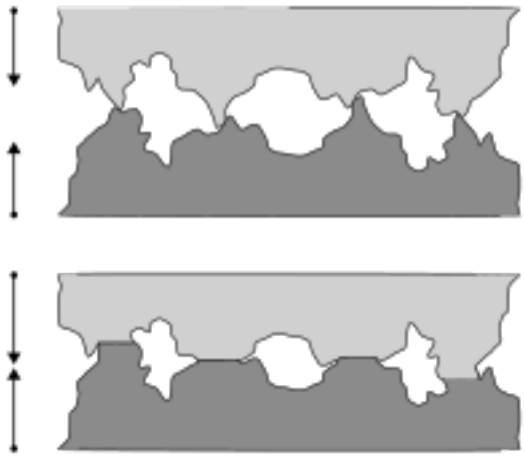

Figure 3.4: Asperities before a load is applied (up) and after applying a certain load (down) [68]

lubrication, design of the reducers, etc. have a certain impact on the wear of a robot.

3.5 Industrial robot condition monitoring

Although health status analysis for industrial robots has not been studied as extensively as other machinery or industrial components such as motors, gearboxes, gears, etc. There are some studies that address the problem building mathematical models and others by implementing data analysis. The mathematical model of a robot has some inherent inaccuracies. When building such models, there are some assumptions and approximations that have to be made, such as constant speeds, the weight of the loads, the temperature of the lubricant, etc. [9]. These necessary approximations distance the model from the real behaviour of the robot. Therefore, data-driven approaches might be more suitable for these complex systems [50]. In addition, the expansion of the Industrial Internet of Things (IIoT) and Big Data in the era of smart manufacturing continue to push the way towards useful and reliable data analysis solutions [61].

A.A. Jaber [28] developed an embedded system for industrial robot condition monitoring using accelerometers on the flange of the robot. He also addressed the lack of research in industrial robot condition monitoring compared to other industrial components. He detected a mechanical failure in the gears of the robot joints, removing gear teeth and comparing the vibration data captured before and after removing them. The drawback of using accelerometers for robots in real assembly lines is that it is hard to isolate external vibrations from vibration caused by the robot's malfunction.

To try to overcome this issue, acoustic emission sensors were used in [39] to detect a faulty rolling bearing on a welding robot joint. Both accelerometers and acoustic emission sensors are intrusive in the sense that they have to be attached to the structure of the robot. This can become a serious inconvenience in real assembly lines, because a sudden detachment of one of these sensors could cause a defect in the quality of the manufactured product or even stop the production line.

Lubricant or wear debris analysis is also commonly used for industrial robot joint condition monitoring. It consist on analysing the wear particles inside the oil that lubricates the joints. As extensively illustrated in [5], any mechanical element working in contact with another mechanical element will deteriorate regardless of design. The deterioration of the robot joints produces metallic debris in the lubricant and therefore the deterioration grade of the joint's gearboxes can be estimated by analysing the amount of metallic debris. However, this method has some drawbacks such as the requirement of an advanced laboratory equipment, the time required for the analysis, and the need to completely stop the robot in the production line [15].

Qiao et al. [50, 52, 51] recently proposed a new methodology for robot health assessment based on vision-based tracking. They suggested to attach a known 3D object to the flange of the robot and using a vision-based tracking system with cameras to diagnose the repetitiveness and thus health of the robot. They also remark the need to analyse the robot as a whole in a holistic way, in order to build an effective health assessment methodology. In other words, the need to assess the health status of the robot as a unique complex system rather than analysing its components separately.

Bittencourt et al. studied in [6] the feasibility of using torque data for industrial robot and repetitive machinery condition monitoring. However, instead of measuring the torque at the joints, they estimated it by measuring the consumed electric current. The torque required in each joint is directly proportional to the current flowing through the motors in each joint. Thus, the higher the torque that the robot requires to manipulate a given load, the more electric current each joint will require. In their study, Bittencourt et al. used kernel density estimates and the Kullback-Leibler distance calculation to detect deviations in the repeatability of a robot's joint torque [6]. They considered both real data from accelerated wear tests and data obtained with simulations.

3.6 Critical review

Maintenance is evolving as condition monitoring technologies do. The development of better sensors, better data acquisition infrastructures and data analysis techniques drive

this evolution. Although there is a lot of literature devoted to condition monitoring and Prognosis and Health Management (PHM) for industrial components, industrial robots have not received as much attention. The main reason for this gap lies on the complexity of industrial robots. The complexity and non-linearity of these complex systems, make it difficult to address the problem with a traditional physical model based approach.

The interaction between the different components inside the robot and the great versatility offered by the robots themselves with different tools, trajectories, etc. create a highly non-linear system. Moreover, the behaviour and health status at each joint has a high impact on the whole kinematic chain.

Data-driven approaches offer a solution regardless of the physical model. Instead, data-driven models focus on the analysis of patterns and trends in data collected by sensors. The feasibility of this approach to identify patterns and predict trends in non-linear systems has already been demonstrated. In addition, recent contributions in the detection of failures and CM of industrial robots with data-driven approaches [28] have shown promising results.

Accelerometers have been used in CM for a wide variety of machines and components. However, trajectory dynamics in which a 6 DOF industrial robot operates are much greater than a common industrial mechanical component. Furthermore, the constant external vibrations of a real assembly line can make it very difficult in practice to distinguish between vibrations caused by an internal failure of the robot and vibrations caused by external elements.

Acoustic emission sensors can be used to deal with external vibration problems, but they are expensive and can be intrusive for deployment in a real industrial environment. Just in the same way as accelerometers, if these sensors are installed on the outside part of the robot's armature, there is a risk of detachment and they could end up falling into the production line.

In this sense, torque sensors are much less intrusive and there is no risk for them to fall into the production line, as they are installed inside the robot's structure. Torque sensors measure the effort of the joints. Hence, a mechanical deterioration that increments the effort of a joint, is expected to produce an unusual behaviour in the applied torque. Torque deviation analysis seems to be a very promising strategy to diagnose the health status of the joints and predict future failures.

Another way to approach the diagnosis of the health status of an industrial robot is to measure it's repeatability or it's positional deviations. As suggested by Qiao et al. [50] vision-based position measuring systems could in principle diagnose the accuracy of an industrial robot. The vision-based approach needs external equipment such as

cameras or laser trackers to measure the position of the robot. Nevertheless, they do not require additional sensors attached to the robot's structure.

According to the literature review carried out in this chapter, the author concludes that torque sensors and vision-based accuracy measuring inspections are very promising approaches for industrial robot predictive maintenance and health monitoring. Therefore, following chapters will focus on developing data-driven predictive maintenance approaches for industrial robots, based on torque measurements and vision-based techniques.

Part IV

Results

Chapter 4

Results

This chapter presents and discusses the obtained results. These results are organized according to the logical path followed throughout the thesis. In the first two sections, vision-based and torque-based solutions are implemented and evaluated according to their accuracy and feasibility to assess industrial robot health status. Then, a special attention is given to robot standby pose optimization, as a non-optimal standby pose is demonstrated to have a severe impact in the reduction of the remaining useful life of industrial robots in real manufacturing assembly lines. Finally, a practical and automated data acquisition network architecture is proposed and implemented in a real automotive assembly line as a necessary step forward towards the implementation of effective large-scale predictive maintenance strategies in the context of Industry 4.0. The network architecture reported to effectively acquire synchronized robot data signals, which is essential to easily detect robot faulty states.

4.1 Accuracy degradation assessment: a vision-based data-driven implementation

In this section we report on a vision-based data-driven methodology for industrial robot health assessment. Based on the conclusions extracted from the literature review, the first approach towards industrial robot's health assessment will consist on a vision-based data-driven measuring system. The following sections will provide an experimental evidence of the usefulness of the methodology on a system comprised of a 6-axis industrial robot, two monocular cameras and five binary squared fiducial markers.

In the experimental implementation, a fiducial marker system tracks the deviation of the end-effector of an industrial robot along a fixed non-trivial trajectory. The trajectory deflection is monitored using three gradually increasing weights attached to the end-effector. When the robot is loaded with the maximum allowed payload, a deviation of $0.77\,\mathrm{mm}$ is identified in the Z-coordinate of the end-effector. In addition, five supervised learning regression models are trained to predict the final pose of the robot. Such models predict the deviation of the end-effector, using the pose estimation provided by the visual tracking system. As a result of this study, the procedure is proven to be a stable, robust, rigorous and reliable tool for robot trajectory deviation estimation and it even allows to identify the mechanical element producing non-kinematic errors. In summary, the proposed methodology is therefore a novel approach that uses fiducial marker based vision systems to assess the accuracy degradation and repeatability of an industrial robot with different loads.

The experiments were carried out using a 6 Degrees of Freedom (DOF) industrial robotic manipulator ABB IRB 120, which maximum payload was limited to 3 Kg. The robot has an slight looseness in the gear of the second joint, which is expected to cause a certain lack of precision. We placed fiducial markers at the rigid links of the robot, as shown in Fig. 4.1. To track the position of these fiducial markers and avoid occlusions during the robot trajectory we used two monocular cameras as it is shown in Fig. 4.2.

The camera labelled as camera *A* (see Fig. 4.2) calculates the pose of these markers located on the side-viewed links of the manipulator, i.e. markers 1, 2, 3 and 4. While camera *B*, calculates the pose of the end-effector. An independent platform was build to isolate the cameras from the robot and prevent mechanical vibrations. A flat halogen red lamp illumination and a non-collimated red diode bright field illumination were used to optimize image acquisition on *A* and B cameras, respectively.

During the experimental data acquisition, the robot executes a closed non-trivial

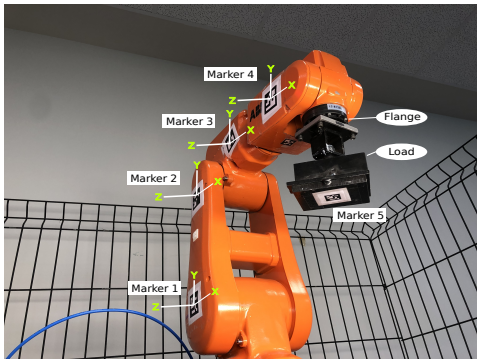

Figure 4.1: The experimental setup showing the markers used to track the relative pose of the manipulator.

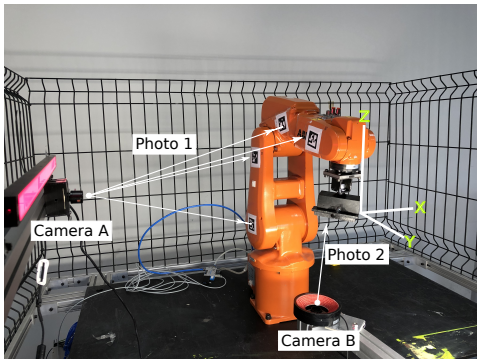

Figure 4.2: The position of the cameras and the coordinate system of the end-effector.

trajectory and meantime cameras *A* and *B* capture images of the markers at fixed time-stamps. The experimental procedure is schematically depicted in Fig. 4.3.

We conducted a total of three experiments following this same process. We increased the weight attached to the end-effector in each of the experiments to study the behaviour of the manipulator using different loads. The first experiment was

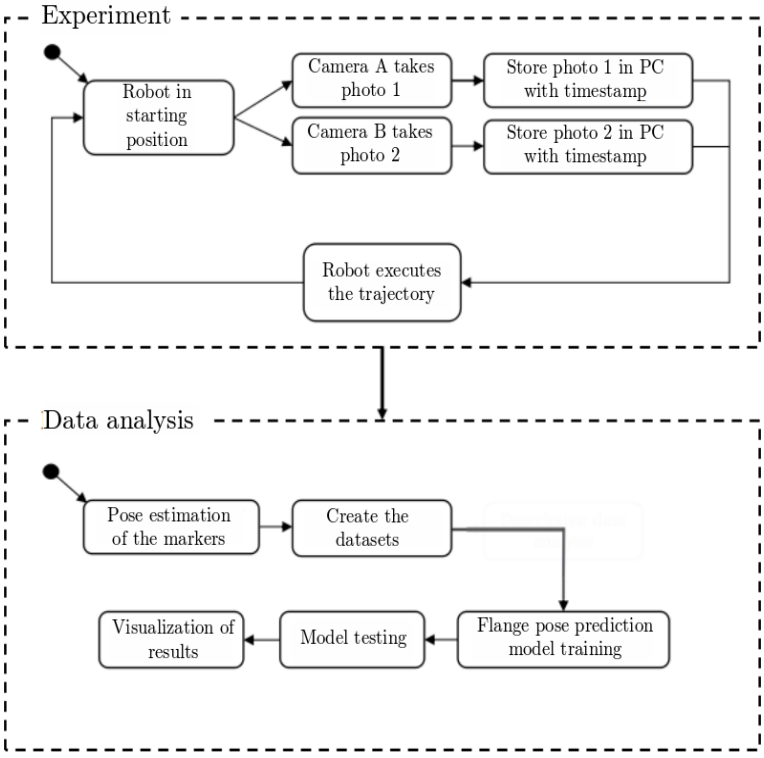

Figure 4.3: Flow chart of the experimental procedure.

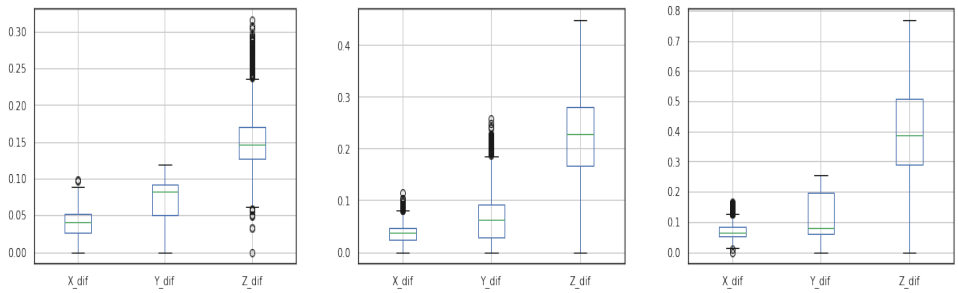

carried out without any extra load, leaving the flange free. In the second and third experiments the load was 1.5 Kg and 3 Kg (the maximum payload), respectively. Each experiment saves 1500 images. After completing the experiments, we obtained three datasets with the positions (*X*, *Y* and *Z*) and rotations (R_x, R_y and R_z) of all these markers.

The analysed data contains the position in millimeters (*X*, *Y* and *Z*) and the rotation in radians (R_x, R_y and R_z) of every marker (see Figure 4.1). Those values are obtained from the images and stored in the datasets. Figure 4.4 shows the dispersion of the coordinates of the end-effector using boxplots and scatter plots. Each dot in the scatter plot represents the actual position deviation (in *Z* and *Y* coordinates) of the end-effector. The coloring of the graphs represents the transient status of the experiments, from dark blue dots (the deviation of the flange when the experiment starts) to brown dots (the deviation of the flange when the experiment ends). The data shown in the first boxplot and scatter plot corresponds to the first experiment. The data of the second and third experiments is shown in the second and third boxplots and scatter plots respectively.

As it is shown in figure 4.4, the greatest dispersion occurs in the Z_{tool} coordinate (*Z* axis in the tool coordinate frame, figure 4.2) in the 3 cases. In the first two experiments the end-effector has an ascending tendency and in the third experiment, when the load equals the maximum payload, the end-effector descends in the negative *Z* direction. Note that the deviation in the Z coordinate increases significantly as weight is added to the flange. The robot deviated the most from its initial position ($0.77\,\mathrm{mm}$) in the third experiment.

To foresee the source of the pose deviation in the *Z* coordinate, an analysis of the *R-squared* was conducted where $R\epsilon[0,1]$ and

$$R^2 = 1 - \frac{SS_{res}}{SS_{tot}}. \tag{4.1}$$

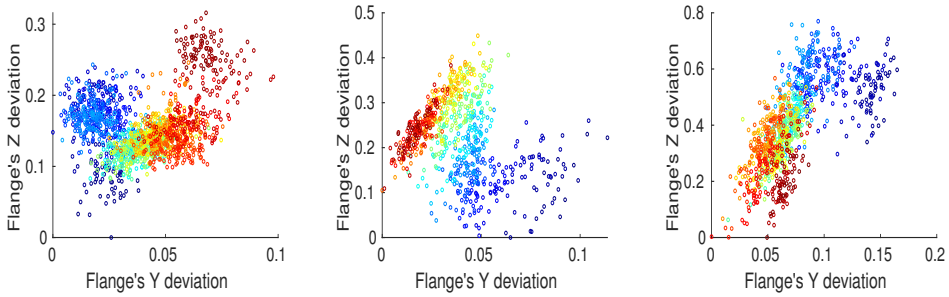

Figure 4.4: Deviation in the flange of the robot in the *X*, *Y* and *Z* coordinates with 0Kg, 1.5Kg and 3Kg respectively.

SS_{res} is given by

$$SS_{res} = \sum_i (f_i - \bar{y})^2 \tag{4.2}$$

where $\bar{y}$ is the mean of observed values associated to f_i predicted or modeled values. SS_{tot} is the total sum of squares and it is given by

$$SS_{tot} = \sum_i (y_i - \bar{y})^2. \tag{4.3}$$

The vertical displacement of the robot in the *Z* coordinate is controlled by joints 2 and 3, so the deviation must be originated in one of those two joints (or in both of them). To identify the origin of the deviation, the coordinates of the first four markers that are related to the robot's vertical movements have been compared with the flange's displacement in Z. The R_z, *X* and *Y* coordinates of the markers, as it can be seen in figure 4.1, are in charge of directing the movement of the flange in it's *Z* coordinate. In summary, the R-square coefficient between R_z, *X* and *Y* coordinates of the first four markers and the *Z* coordinate of the flange were calculated. The results are shown in tables 4.1, 4.2 and 4.3.

	Rz & flange *Z*	*X* & flange *Z*	*Y* & flange *Z*
Marker 1	0.037	0.002	0.003
Marker 2	**0.308**	**0.316**	**0.345**
Marker 3	0.038	0.037	0.117
Marker 4	0.009	0.108	0.030

Table 4.1: R-squared values between first 4 markers' R_z, *Z* and *Y* and flange's *Z*. (0Kg)

	Rz & flange Z	X & flange Z	Y & flange Z
Marker 1	0.053	0.226	0.264
Marker 2	0.010	0.248	**0.273**
Marker 3	0.135	0.110	0.263
Marker 4	**0.245**	**0.398**	0.234

Table 4.2: R-squared values between first 4 markers' R_z, Z and Y and flange's Z. (1,5Kg)

	Rz & flange Z	X & flange Z	Y & flange Z
Marker 1	0.028	0.001	0.061
Marker 2	**0.576**	**0.682**	**0.667**
Marker 3	0.142	0.504	0.376
Marker 4	0.538	0.623	0.368

Table 4.3: R-squared values between first 4 markers' R_z, Z and Y and flange's Z. (3Kg)

In the first experiment, marker 2 obtains the highest *R-square* values (table 4.1) with a significant difference. In the second experiment, markers 2 and 4 score the highest scores (table 4.2). Finally, in the third experiment, marker 2 is again the marker with highest coefficient values (table 4.3). This results show that markers 2 and 4 have the greatest relationship with the deviation of the flange. The marker 2 scores the most significant relationship with the flange compared to the rest of the markers specially when the flange is left free with no load attached to it or when the load is the maximum.

These results are in line with expectations, as markers 2 and 4 are the two most separate markers from the points where the vertical movement of the robot originates (joints 2 and 3) as can be seen in figure 4.1. Which means that, a rotation in joint 2 will be more noticeable in marker 2 than in marker 1, even though it affects both markers' pose.

As a result of the analysis, joint 2 was identified as the origin of the flange deviation. The reasons that led us to that conclusion were: first of all, if the deviation was originated in joint 3, there would be no correlation between marker 2 and the final deviation of the flange. This correlation would only be appreciable in the 4th marker, which is not the case. Second, if the source of the deviation were both joints (2 and 3) in a similar way, marker 4 would have a much higher correlation with the flange than marker 2, because the deviation of both joints could be appreciable in this 4th marker (the deviation of the 3rd joint plus the deviation propagated from the 2nd joint).

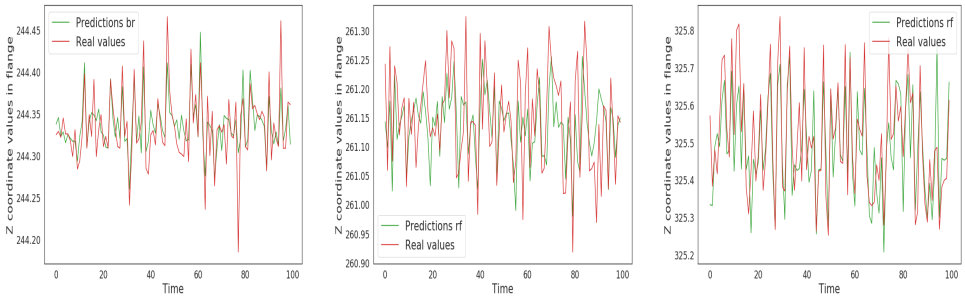

Figure 4.5: Predictions of the flange's Z coordinate position and real values with 0, 1.5 and 3kg of load respectively.

Therefore, the fact that it is mainly the 2nd marker the one that scores the greatest R-squared coefficient values in most of the cases and with different loads, suggests that the source of the deviation in the Z coordinate of the flange is located in the 2nd joint.

After evaluating the relationship between the poses of the robot's side markers and the deviation of the flange, six regression models were trained to predict the position of the flange in the Z coordinate. We trained the models using the information of the pose of the four markers (the position and the rotation in$X$ Y and Z of every marker) as independent variables and the position in the Z coordinate of the flange as the dependent variable to be predicted.

In figure 4.5 a comparison of the actual position of the flange in the Z coordinate and the position predicted by the models that obtained the highest accuracy is presented (bayesian ridge in the first experiment and random forest in the second and third).

To evaluate the prediction accuracy of the models, the Mean Absolute Error (MAE) and the Root Mean Squared Error (RMSE) were calculated. MAE and RMSE are both widely used metrics for error measuring in statistics. MAE is given by

$$MAE = \frac{\sum_{i=1}^{n} |y_i - x_i|}{n} \tag{4.4}$$

and RMSE by

$$RMSE = \sqrt{\frac{\sum_{i=1}^{n} (y_i - x_i)^2}{n}} \tag{4.5}$$

where y_i is the set of predicted values and x_i is the set of real values.

To see whether our models captures the behaviour of the system or not, we established a baseline prediction by calculating the moving average of the real data. That is, we calculated the RMSE and MAE errors we would obtain if we used the moving average value to predict the position of the flange in the Z coordinate. As previously mentioned, we optimized the window size of the moving average model to

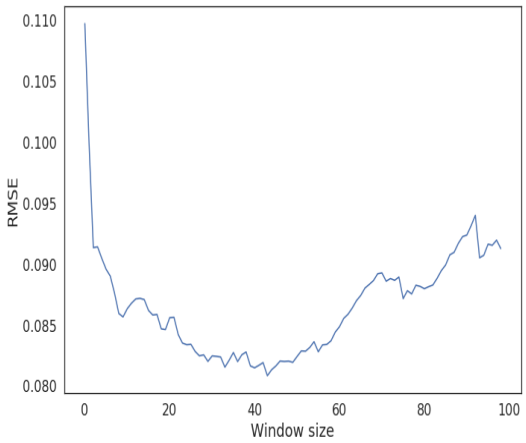

Figure 4.6: Learning curve of the moving average windows size in the experiment with 1,5Kg of load.

chose the window with the highest prediction accuracy for every experiment. We then compared the results with the rest of the models. In figure 4.6 we show the learning curve of the moving average obtained by reducing the RMSE error as the window size increases (second experiment). When the window size is about 40, the RMSE error stops decreasing and the model does not score better results. This value obtained by optimizing the windows size is then compared with the results of the rest of the models. The comparison is shown in tables 4.4, 4.5 and 4.6.

	RMSE	MAE
Moving Average	0.04162	0.03094
Random forest	**0.02540**	0.02152
SVR	0.04148	0.03477
LASSO	0.03946	0.02883
Multi-layer perceptron	0.15250	0.12415
Bayesian ridge	0.02763	**0.02140**

Table 4.4: Error of the trained models with no extra load.

	RMSE	MAE
Moving Average	0.08142	0.064390
Random forest	**0.06557**	**0.02152**
SVR	0.07154	0.05670
LASSO	0.08391	0.06806
Multi-layer perceptron	0.17636	0.13704
Bayesian ridge	0.06648	0.05297

Table 4.5: Error of the trained models with 1,5Kg.

	RMSE	MAE
Moving Average	0.16102	0.13129
Random forest	0.09765	**0.02152**
SVR	0.10546	0.08506
LASSO	0.15757	0.12729
Multi-layer perceptron	0.28744	0.23893
Bayesian ridge	**0.08845**	0.07093

Table 4.6: Error of the trained models with 3Kg.

The effectiveness and feasibility of some of the implemented models can be seen both in the graphs and in the improvement of the error with respect to the baseline error in the tables. The Random Forest, Support Vector Regression and Bayesian Ridge models obtain the best results and the error of the moving average is improved in the three cases. Multi-Layer Perceptron obtains the worst results.

4.2 Methodology and experimental implementation for industrial robot health assessment with torque signature analysis

As concluded in the literature review, both vision-based and torque measuring systems are promising approaches for robot predictive maintenance and health assessment. After presenting a vision-based approach in the previous chapter, we will now proceed to study the feasibility of a torque measuring based methodology for industrial robot joint health assessment.

The main idea of this approach is to analyze the data collected with torque sensors when the robots are in a healthy state. This data will be then compared with data extracted from mechanically damaged robots. The objective is to conclude whether torque sensors are useful for diagnosing and predicting medium-long term mechanical deterioration in industrial robots or not. The feasibility of the methodology will be tested with a real industrial use case by analysing a healthy industrial robot and a damaged one. Furthermore, an in depth mechanical inspection will be performed in order to detect the origin of the mechanical deterioration.

4.2.1 Experimental Design and Implementation

An experiment was carried out to compare the torque applied by a faulty robot joint and a healthy one. If the mechanical wear has a significant effect in the effort of the joint, the hypothesis is that the faulty joint would require higher torque than a healthy joint to execute a given trajectory. Therefore, the methods selected to identify a faulty joint should focus on measuring the increment of the torque applied in the robot joints, whether they are statistical methods or machine learning models. Figure 4.7 describes the process of the experimental procedure carried out. First, a faulty robot wrist was removed from an automotive assembly line after years of uninterrupted work. The faulty robot caused a sudden stop in the production line and it was replaced by a new one. The experiment was performed using a 6 DOF industrial robot (ABB IRB 6400r), two robot wrists (the faulty wrist and the new one), two loads representing the 15% and 90% of the maximum payload of the robot and four torque sensors, two sensors for each wrist, located in the 5th and 6th joints. These sensors are factory built-in torque sensors and the robotic systems uses them in the control feedback-loop. The ABB IRB 6400r is a widely used industrial robot in the automotive industry with a maximum payload of 200Kg.

A non-trivial fixed trajectory was programmed in order to excite the robot joints. First of all, the faulty wrist was installed in the ABB robot in a laboratory facility, out

of the production line. Then, the programmed trajectory was executed three times with three different loads each time. The loads represented the 0%, 15% and 90% of the maximum payload of the robot. We executed the trajectories and collected the torque data with a sampling rate of $100\,\mathrm{ms}$. Afterwards, the faulty wrist was removed and the new one installed in the same ABB robot. The trajectory was repeated again three times with the same three different loads in each repetition. Therefore we collected the data of the torque applied in the 5th and 6th joints throughout the six trajectory executions (three with the faulty wrist and tree with the new wrist).

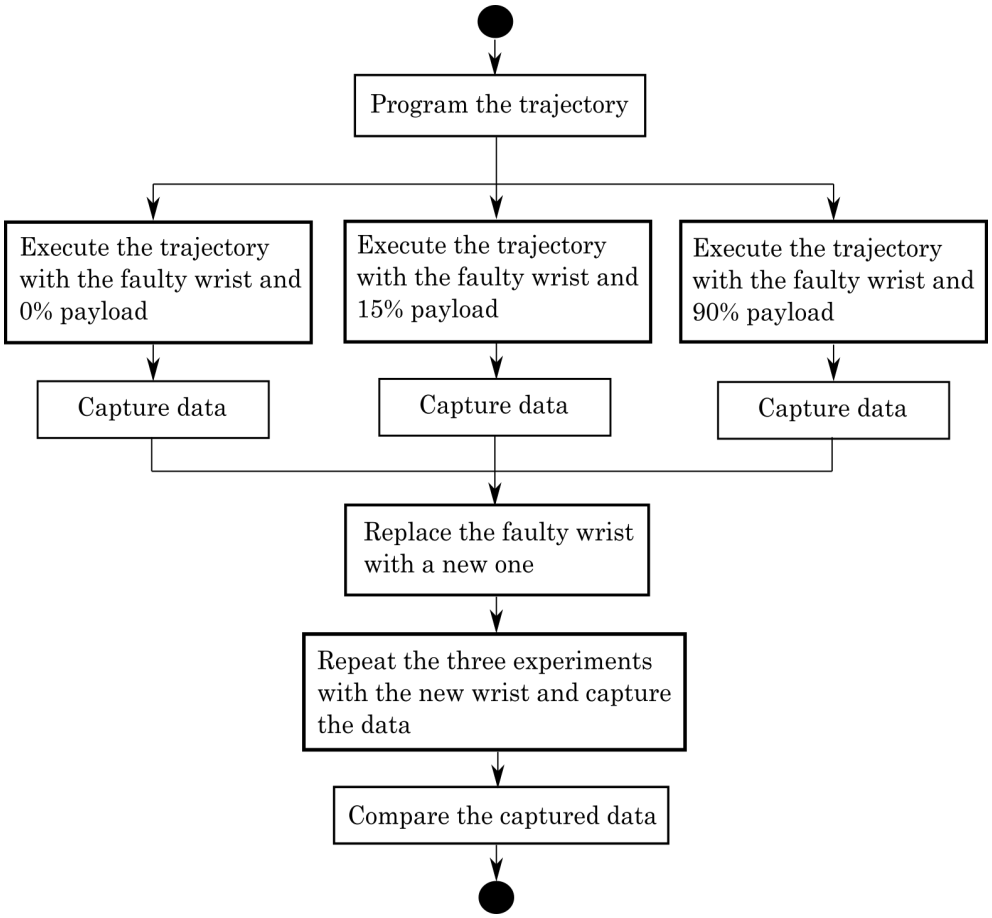

Figure 4.7: flowchart of the experimental procedure carried out.

After completing all these trajectories, torque signals were acquired and stored in csv files following the format specified in Table 4.7. The signals were stored as floating point numbers and using the standard unit (Nm) for the torque. We used the TCP/IP communication protocol to connect with the robot controller and capture the torque signals, which is an Industry 4.0 communication standard. The TCP/IP protocol is suitable for Industry 4.0 and Big Data scenarios, as it is able to interconnect large

number of devices [65]. Some researchers have used the OPC-UA communication protocol [44] which is built on top of TCP/IP for data acquisition in industrial scenarios. The data shown in Figures 4.8 and 4.9 disclose an evident increment in the torque of the faulty wrist's 5th joint. This increment is clearly appreciable in all the three experiments and throughout the execution of the whole trajectory, therefore the effort required by the motor of the 5th joint was higher than expected with any of the three loads and in any robot pose or movement. In contrast, the torque of the 6th joint does not change significantly in any experiment.

Table 4.7: Example of the torque data captured by one robot in one experiment E.g. The column name *Torque_joint_5_A* refers to the torque acquired in the 5th joint of robot *A* (faulty robot).

Observation	**Time (s)**	**Torque_Joint_5_A (Nm)**	**Torque_Joint_6_A (Nm)**
1	0	0.819	-1.045
2	0.100	4.08	2.109
3	0.200	9.007	4.323
4	0.300	10.118	6.137
...	...	...	...

The increment in the torque is measured by first calculating the absolute value of the acquired signals. The absolute value of the torque in each joint is then integrated to calculate the total amount of torque applied throughout the whole trajectory in all the experiments. Once the total applied torque is calculated, the percentage of increase between the two wrists is calculated. Tables 4.8 and 4.9 show the results of the 5th and 6th joints respectively.

Table 4.8: Total torque of the 5th joint of the new and faulty wrists. *Load 1*, *Load 2* and *Load 3* represent the 0%, 15% and 90% of the maximum payload respectively.

	New (Nm)	**Faulty (Nm)**	**Increase**
Load 1	19,567	42,830	118.88%
Load 2	21,224	46,451	118.86%
Load 3	62,235	124,703	100.37%

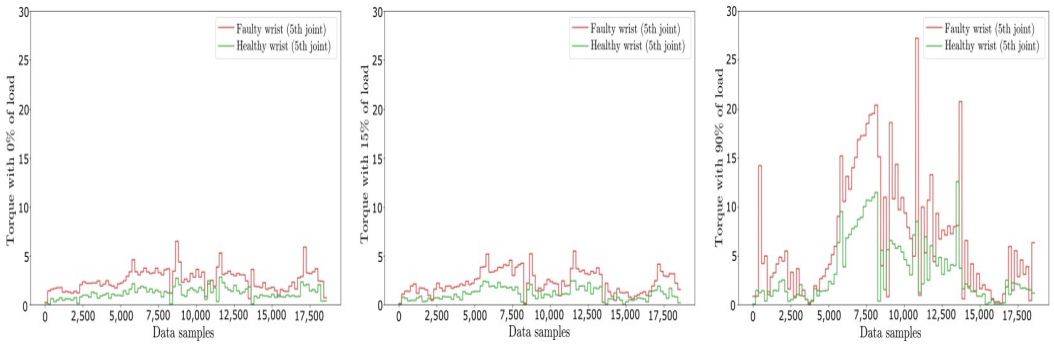

Figure 4.8: Torque values of the 5th joint in a faulty wrist and in a healthy wrist with different loads and same trajectory.

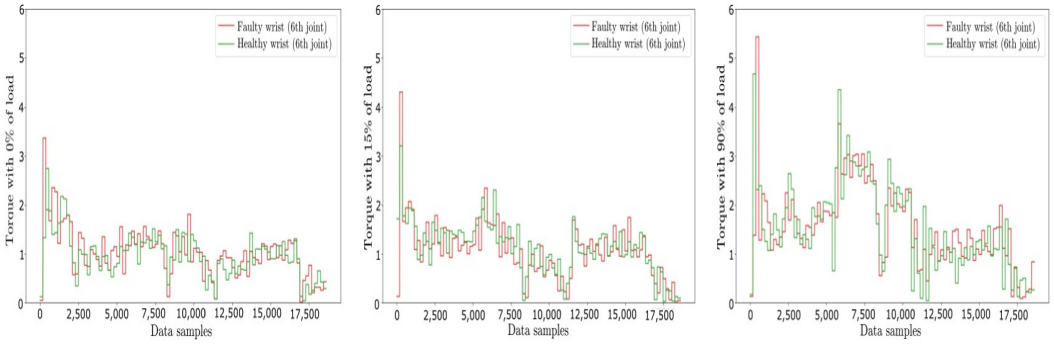

Figure 4.9: Torque values of the 6th joint in a faulty wrist and in a healthy wrist with different loads and same trajectory.

Table 4.9: Total torque of the 6th joint of the new and faulty wrists. *Load 1*, *Load 2* and *Load 3* represent the 0%, 15% and 90% of the maximum payload respectively.

	New (Nm)	**Faulty (Nm)**	**Increase**
Load 1	17,910	19,039	6.31%
Load 2	20,852	19,982	−4.17%
Load 3	28,671	28,970	1.04%

The increment in the torque is homogeneous, i.e., The torque increases in the whole trajectory and not only in certain movements or positions. The fact that the torque increases in the whole trajectory and not only in certain poses, reveals that the deterioration affects to the entire movement of the joint. The results also show that at the time of the failure, the electric consumption of joint 5 in the faulty wrist was at least twice as high as expected for a healthy joint.

Although the acquired data effectively detects the wear in the joint, the detected increment is not enough on its own to deduce a root cause of the fault. Thence, we

conducted a root cause analysis with an in-depth mechanical inspection in order to identify the cause.

4.2.2 Root Cause Analysis of the Faulty Joint

Mechanical Inspection

The first step of the mechanical inspection consisted on disassembling the faulty wrist. The 5th joint of the wrist is composed of an electric motor and a speed reducer. First, we inspected the gears of the speed reducer, shown in Figure 4.10. We did not find any evidence of wear or pitting in the surface of the gears and there was no apparent damage in the gears that could cause the significant increment detected in the torque. The lubricant oil of the reducer was extracted and analysed in the process of disassembling the faulty wrist. We confirmed that the lubricant was within the quality tolerance limits as no metallic debris was found in the oil.

Afterwards, we examined the motor of the 5th joint. An increment such as the one detected in the experiment could be caused due to a significant decrease in the motor's coil resistance. We measured the resistance of the coil using an ohmmeter and compared it with the resistance of the coil of a new motor. The resistance values in both coils were identical. Hence, the motor's coil was dismissed as the cause of the joint fault.

After analysing the condition of the speed reducer and the motor, we inspected the brake of the motor. The brake of the 5th joint is a permanent magnet brake that stops the motor when the robot is shut down or when an emergency stop is required. As illustrated in the schematic of Figure 4.11 this kind of brakes have three main parts: a metallic armature, a field coil and a neodymium (NdFeB) permanent magnet. The brake works in the following way: when the robot shuts down or makes an emergency stop, there is no voltage applied to the coil and the permanent magnet attracts the armature, stopping the rotation of the motor. In contrast, if the robot controller applies 24V to the field coil of the brake, it produces a magnetic field compensating the magnetic field created by the permanent magnet and the motor is released.

We measured the resistance of the brake's coil and compared it with the resistance of a completely new coil. In both cases the values reached $15.4\,\Omega$. Therefore, the coil of the brake could not be the cause of the detected torque increment.

Finally, we inspected the permanent magnets of the brake. The permanent magnets used in this brake are squared NdFeB magnets. We noticed a slight deformation in the corners of the magnets, as some magnetic particles were detached from them. We

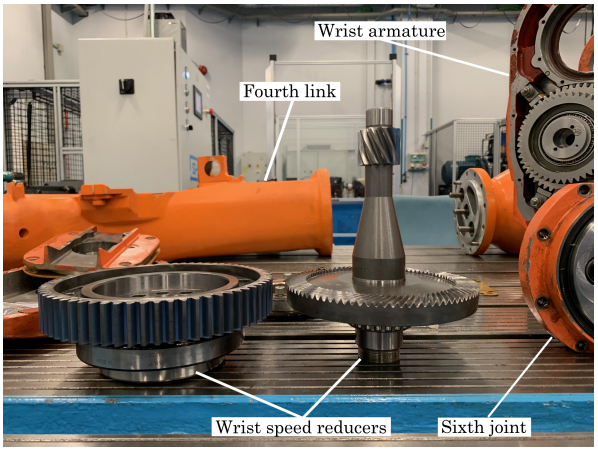

Figure 4.10: Mechanical inspection of the gears, bearings and motors of the wrist.

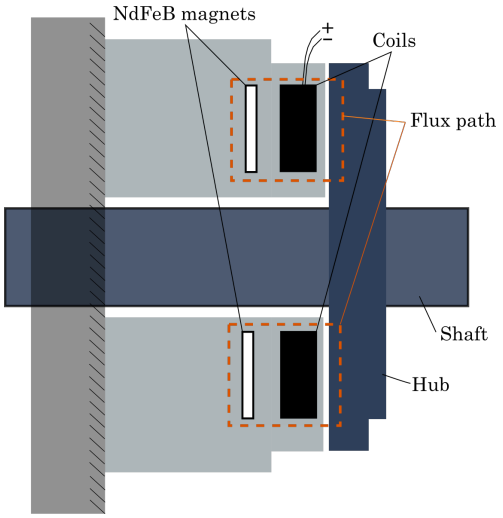

Figure 4.11: Schematic of the motor brake.

found the particles filling the space where the magnets are located. Figure 4.12 shows the permanent magnets inside the brake of the faulty joint compared to a completely new brake. In addition, Figure 4.12 shows that the colouring of the brake's armature was changed. These kind of stainless steel armatures, have a metallic light silver colour when manufactured. However, the inspected brake had a reddish coloring as a consequence of oxidation.

We performed two tests to diagnose the health status of the permanent magnets. The first test consisted on measuring the M(H) hysteresis curve of the magnets. Then, we magnetized the permanent magnets and measured again the M(H) hysteresis curve after the magnetization. The results of the tests are shown in Figure 4.13.

There is a 24% loss from $0.814\,\mathrm{T}$ before magnetization to $1.071\,\mathrm{T}$ after the mag-

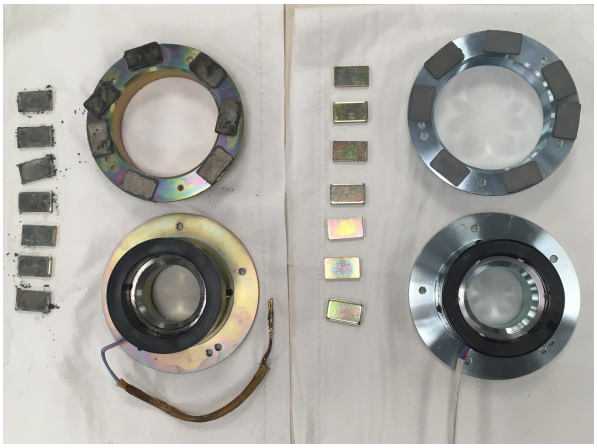

Figure 4.12: The motor brake of the faulty joint and its permanent magnets (**left**) compared to a completely new motor brake (**right**).

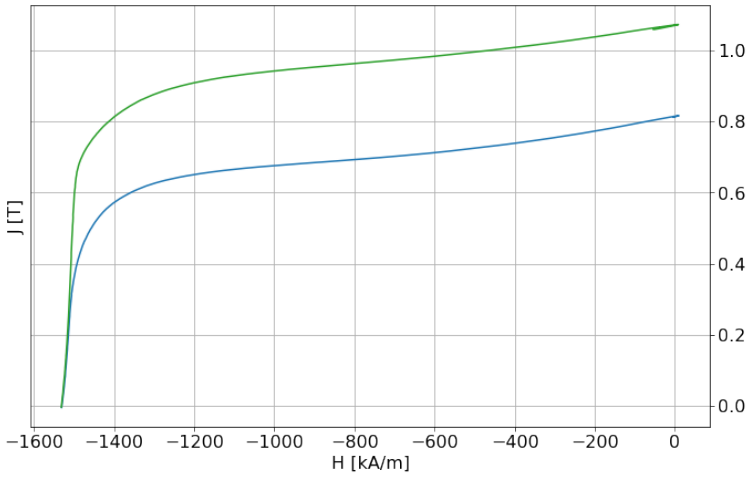

Figure 4.13: Magnetic hysteresis curve of the motor brake's permanent magnet before (blue) and after (green) magnetization.

netization. This significant magnetic field loss has a direct impact in the malfunction of the motor's brake. As a consequence, the brake constantly resists the movement of the motor. This produces the torque increment in the 5th joint throughout the whole trajectory identified in Section 4.2.1.

The second test consisted on measuring the magnetic hysteresis curve at different temperatures. Figure 4.14 shows the different M (H) curves at 26, 80, 100 and 120 °C and Table 4.10 shows the magnetic properties of the permanent magnet at these temperature regimes. Br (T) is the residual induction or flux density, that is the magnetic induction corresponding to zero magnetizing force in a magnetic material after saturation. Hci (kA/m) is the intrinsic coercive force of a material and indicates

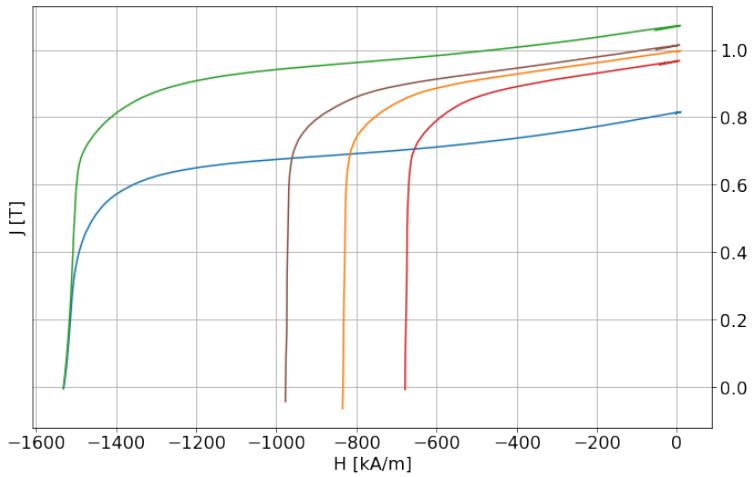

Figure 4.14: Magnetic hysteresis curve of the permanent magnet at 26 (green), 80 (brown), 100 (orange) and 120 °C (red).

its resistance to demagnetization.

There are two additional considerations that have to be taken into account. The technical specifications of the 5th joint's motor indicates that the surface temperature of the motor can reach up to 140 °C. Therefore, the temperatures inside the motor brake could be even higher than the temperatures reached in the test. Moreover, in the recently published work by M. Haavisto [24] the time dependent demagnetization of NdFeB permanent magnets is extensively investigated. She experimentally proved that this type of magnets can be demagnetized if exposed to higher than 80 °C for a long period of time. This conclusion is especially relevant for industrial robots working in assembly lines for years uninterruptedly.

These results of the tests, the mechanical inspection carried out, the state of the motor brake, as well as the previously mentioned PhD dissertation [24], give us enough evidence to conclude that the temperatures inside the motor of the 5th joint of the robot, reached high enough temperatures for sufficient time to produce a magnetization loss in the permanent magnets of the motor brake. This caused the failure in the wrist and the increased torque values shown in Section 4.2.1.

4.2.3 The Health Assessment Program Methodology

Based on the results of the previous sections, we propose a methodology for diagnosing the health status of industrial robot joints with torque signature analysis. The diagram representing the methodology can be seen in Figure 4.15. The main idea behind the proposed methodology is that a joint that suffers a mechanical degradation will require

Table 4.10: Magnetic properties of the permanent magnet at the measured temperatures.

T (°C)	Br (T)	Hci (kA/m)
26	1.071	1531
80	1.013	976.9
100	0.9957	833.4
120	0.9668	678.5

higher torque to execute a certain trajectory than a healthy one. As the time goes by, the mechanical elements attached to the motor (i.e., The brake and the reducer) will inevitably suffer mechanical deterioration. This will require higher effort to execute the same trajectory. To illustrate the methodology, let's say that a robot R_1 executes a certain program P_1 and needs to apply torque T_1 in a joint to complete the trajectory. If there is any mechanical deterioration, the system will be less efficient, but the robot controller will make sure that this deterioration does not affect the accuracy of the robot. Even if the accuracy remains invariant, to finish the same program P_1 the required torque now (T_2) will be higher than before ($T_2 > T_1$).

We therefore propose to use a specific trajectory-tool combination in the robots of the production line to assess their current health status. As described in the diagram of Figure 4.15 robots will execute a predefined non-trivial trajectory with a known load and they will require a certain amount of torque in each joint to complete this trajectory. To acquire torque data in all the joints, the trajectory must use the whole set of joints comprising the robot manipulator. We will call *Health Assessment Program* (*HAP*) to that predefined trajectory-load combination. These two specifications will always have to remain unchanged in order to make a fair comparison of the results. However, an advantage of the methodology is that the precise shape, center of mass and inertia of the load are not required to be known or modeled.

The first step is to execute the trajectory with the robot attaching the corresponding load. The torque of each joint will be recorded during the the whole process, producing a digital *signature* of the torque of each joint. This initial torque data or *signature* will be used as a reference for that particular robot. This initial data will be stored with an identification number of the robot. Whenever we want to analyse the mechanical deterioration of the joints of that robot, we will run the *HAP* again and compare the previously stored values with the recently acquired ones. If there is no change in the torque values, we can conclude that there is no significant mechanical deterioration in the joints yet. In contrast, if there is some increase in the torque of a certain joint, it will mean that the motor of that joint is requiring more effort than expected. The proposed

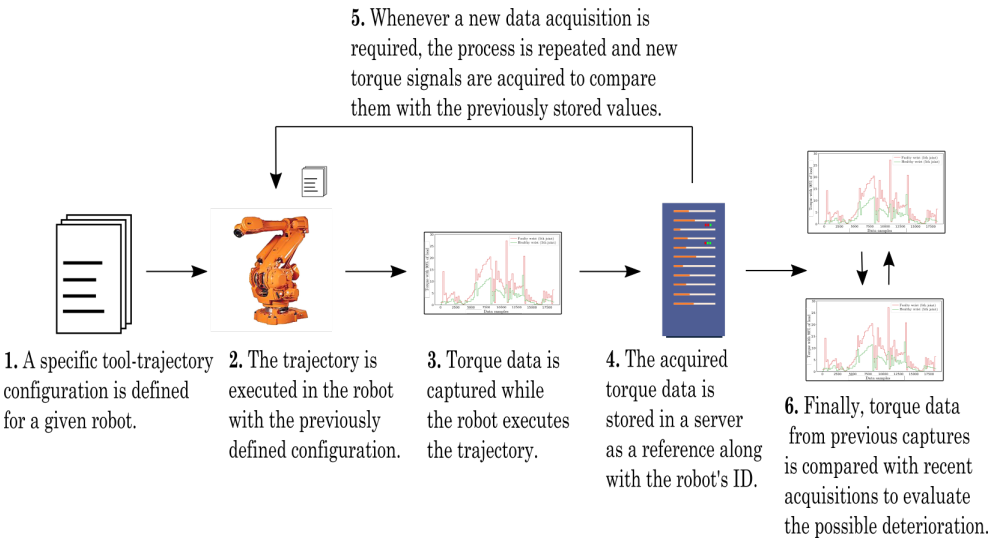

Figure 4.15: Diagram of the proposed methodology. First, the trajectory and tool are defined. Then, the program is executed and torque data is acquired. The recorded data is stored in a server as a reference along with the robot's ID. The process is periodically repeated and the new signals are compared with previously recorded ones to diagnose a possible deterioration.

methodology is applicable to any joint or industrial robot and it is not necessary to take the robot off the production line to diagnose it. Which is a significant advantage compared to existing condition monitoring techniques.

4.3 Genetic algorithms for industrial robot standby pose optimization

After analysing the feasibility of visual and torque based methodologies for industrial robot health assessment, the following section will highlight the importance of the standby pose in industrial robots. Section 4.2 showed that the overheating of the motors can demagnetize the magnets of the brakes. When a robot waits on the assembly line before working on the next product, the motors inside the joints hold the standby pose of the robot. the effort of the motors and therefore their temperature is determined by the weight of the tool, the shape of the tool and the pose of the robot. Some robots spend a large portion of the total operational time waiting for the next product. If this waiting is done in an inefficient standby pose it can lead to unnecessary overheating, decreasing the RUL of the joints. Moreover, the extra effort required to hold a non-optimal pose produces unnecessary electric consumption.

There are three main methods to reduce the temperature of industrial robot joints: decreasing the weight of the tool, optimizing the trajectory or optimizing the standby pose. This thesis will be focused on the third method, as a preliminary study conducted in a real automotive manufacturing line demonstrates its influence in the reduction of the robots lifetime. The standby pose is also commonly called *Home* pose. As mentioned before, it is the stationary pose of the robots when they wait for the next product in an assembly line. While the robots wait, the motors inside the joints apply torque to hold the tool in the pose they are programmed to. The amount of torque required in each joint will be higher or lower depending on the programmed pose and the tool.

Minimizing the total torque applied by the robot in a standby pose, reduces the temperature of it's joints and the required electric consumption. Hence, first of all it increases the remaining useful life of it's joints and secondly, it reduces the electric consumption. Although sustainability has not been considered in the optimization of industrial processes until very recently, in the last few years there is an increasing need to reduce the electric consumption in factories and transforming the industry to a more sustainable sector.

4.3.1 Preliminary study

Researchers and practitioners have paid little attention to the efficiency of the standby pose of industrial robots compared to the efficiency of the trajectories. However, in real manufacturing assembly lines, industrial robots spend between 20% and 80% of the total operational time waiting in a stationary or standby pose for the next product,

depending on their work regime. In this section, as well as in section 4.3.4 we will highlight the importance of optimizing the robot pose in real industrial scenarios.

There are two main reasons to optimize the standby pose of industrial robots. The first reason is to increment the useful life of industrial robots. If the effort of a joint is reduced, the electric current of its motor and thus its temperature will also decrease. The temperature directly affects the useful life of the components inside the joints, such as the permanent magnets of the brakes, the wires of the coils, etc.

The second reason, is that there is a significant electric consumption saving potential. As a consequence of the climate crisis, there is an increasing need to reduce energy consumption in industry. As the use of robots in manufacturing production lines increases, it is necessary to develop and implement methods that minimize the electrical consumption of these systems. By minimizing joint torque, the motors inside the joints require less electric current to hold a stationary pose. As a result, the total electric consumption of assembly lines could be significantly reduced, especially in highly automated factories e.g. Automotive body shop assembly lines.

A preliminary study was conducted in a real automotive production line by collecting the historical failure data of 621 industrial robots to illustrate the importance of the standby pose in robot failures. The data collected consists of the pose of robot joints while being stationary and information about whether the robot had a failure in a particular joint or not. In table 4.11 we show the difference in the mean standby orientation of the fifth joint of all the robots. The data in the first row corresponds to robots that have failed in the fifth joint and the second row corresponds to robots that have never failed. We measured the orientation in degrees, which ranges between 0° and 90°. Figure 4.16 shows and schematic of an industrial robot wrist (5th and 6th joints) and a representation of the angles used in the study. As shown in the figure, 0° represents absolute verticality to the ground in the 5th joint and 90° represents total horizontality to the ground.

	Orientation of 5th joint (°)
With failure	71.39
Without failure	62.22

Table 4.11: Standby orientation mean with recorded historical failures and without failures in the fifth robot joint.

These preliminary results show that robots waiting in a standby pose closer to the horizontal plane with reference to the ground, tend to fail more frequently in the 5th joint than robots whose stationary pose is closer to the vertical plane.

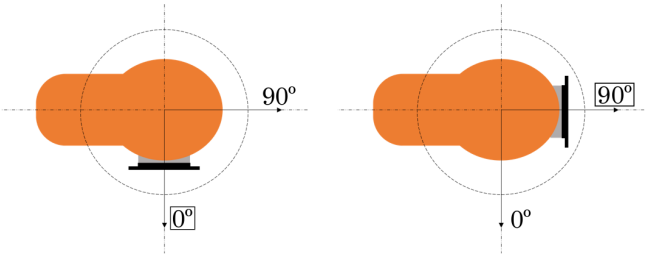

Figure 4.16: Schematic of the 5th and 6th joints (wrist) of a robot and the corresponding degrees used to represent the verticality and horizontality of the 5th joint.

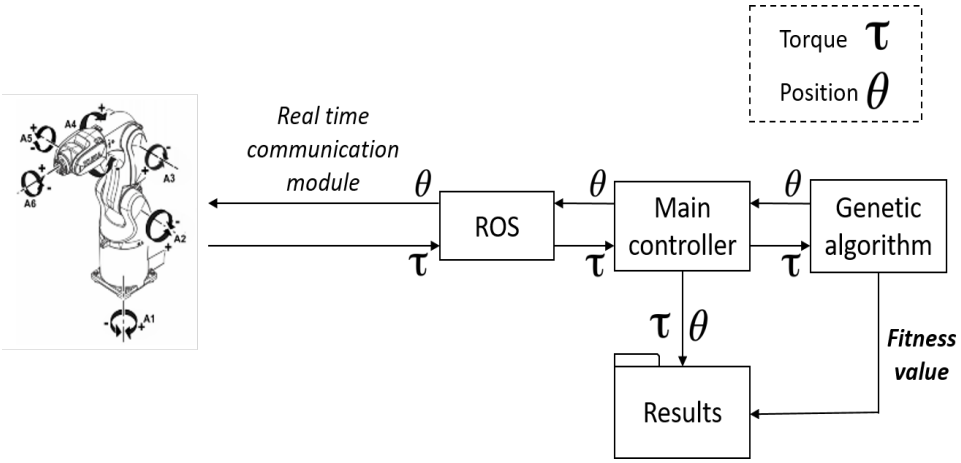

Figure 4.17: Diagram of the data acquisition modules.

4.3.2 Experimental implementation

We optimized the standby pose of a Kuka KR3 robot and used The Robot Operating System (ROS) [53] as a communication and control interface between the robot and a laboratory computer. We used real-time communication with a frequency of 12ms in order to ensure a reliable data acquisition process. The genetic algorithm was developed from scratch with the Python programming language. The architecture of the data acquisition process is shown in figure 4.17.

The experimental process starts by defining a set of 40 random joint angles (the initial population) in the Genetic algorithm module. These angles are sent to the main controller, which moves the robot to the first random pose and waits until the movement has finished. When the robot reaches the desired pose, the controller waits approximately half a second for the robot to stabilize and then, it captures the torque of all the six joints for another half a second. We calculate the median of the captured torques in each joint to eliminate non-gaussian noises, frequent in non-linear and dynamic industrial machinery. These torque values are stored in a file alongside the

angles of the joints and the scored fitness value. The fitness value is calculated based on the total torque applied to hold the current pose. The more torque is applied, the higher the fitness score. Therefore, the genetic algorithm selects the angles with the lowest fitness score. In each epoch or iteration, the best 20 individuals (poses) are selected as the parents of the next generation. The next generation is created by crossover, mixing the genes (joint angles) of the selected parents. A mutation ranging between 0 and 0.05 radians is randomly introduced in every 1 out of 4 new individuals to maintain genetic diversity and avoid local minima. Following this process iteratively, each generation of individuals reduces the torque applied by the robot compared to the previous generation until the algorithm converges in an optimal solution.

Our methodology allows to easily apply physical constraints to the search space of the genetic algorithm. The constraints are implemented for two main reasons: to avoid the collisions between the robot and nearby physical obstacles and to avoid singularity poses. The algorithm rejects the angles that are in conflict with the physical constraints i.e. every new generation of poses that the algorithm creates is checked to ensure that the new individuals satisfy the specified constraints. The constraints are defined by calculating the forward kinematics equations of the industrial robot with every new generation of individuals.

Although we decided to minimize the total torque of the robot, it is also possible to minimize the torque of a certain joint or group of joints, or even to implement a multi-objective optimization algorithm with multiple objectives to optimize e.g. to maximize the torque of a joint while minimizing the torque of another one. In our case, we developed a multi-objective minimization algorithm to minimize both the sum of the torques in joints 1, 2 and 3 and the sum of the torques in joints 4, 5 and 6 separately.

4.3.3 Results

Each of the two optimization objectives i.e. sum of torques in joints 1, 2 and 3, and sum of torques in joints 4, 5 and 6, had its own fitness function. Figure 4.18 shows the fitness function of the two optimization objectives (Fitness1 and Fitness2) throughout the whole optimization process, as well as the sum of these two fitness functions (FitnessTot).

The genetic algorithm minimizes faster the fitness functions in the first 100 iterations than in the rest of the process. Afterwards, from iteration 100 to iteration 200 the fitness functions are minimized slower reaching a convergence point. Finally, the genetic algorithm reaches an optimal solution and converges approximately in

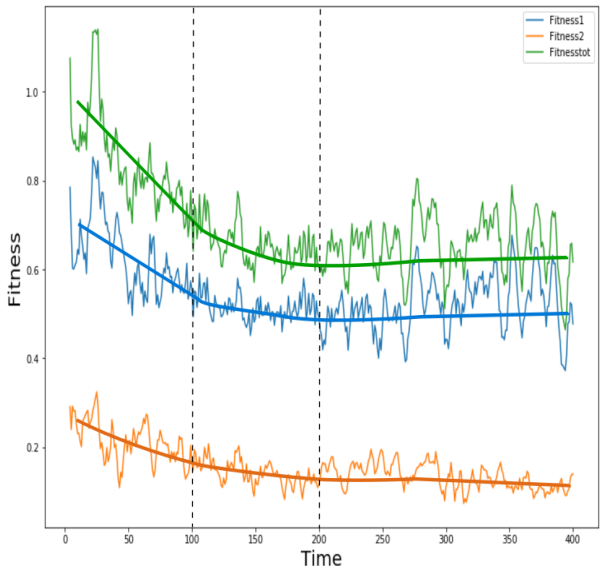

Figure 4.18: Fitness function value of joints 1, 2 and 3 (Blue), joints 4, 5 and 6 (Orange) and the sum of the two fitness values (Green).

the 200th iteration. Figure 4.19 shows the angles of each joint in radians while the optimization algorithm was executing. The lines in the figure represent the joint angles in each iteration, until the algorithm eventually finds the optimal standby pose.

The optimal standby pose in which the robot applies the minimum torque to hold the pose is shown in figure 4.20. The achieved pose is logically coherent, as the robot reaches a pose of equilibrium. The center of gravity of the whole systems stays as close as possible to the base of the robot. Therefore, the motors of the joints require the minimum amount of effort to hold the optimized pose.

The methodology is applicable to any robot and tool configuration. Every robot and tool will have its own optimal pose depending on the dimensions and center of gravity of the whole system. The algorithm will find the minimum torque-demanding pose regardless of the attached tool and without any additional code modification. To demonstrate the applicability of the methodology in different robots, we optimized the standby pose of a large ABB IRB 6400r industrial robot, following the same process described in this manuscript.

The optimization potential is more appreciable with large industrial robots, as they carry very heavy loads in assembly lines. Figures 4.21, 4.22 and 4.23 show the robot with a load of 140 kg in the default standby pose, in an extended pose and in the optimized pose respectively. The total torque applied in these three poses is shown in table 4.12. The robot applies 3.27 times more torque in the extended pose than in the

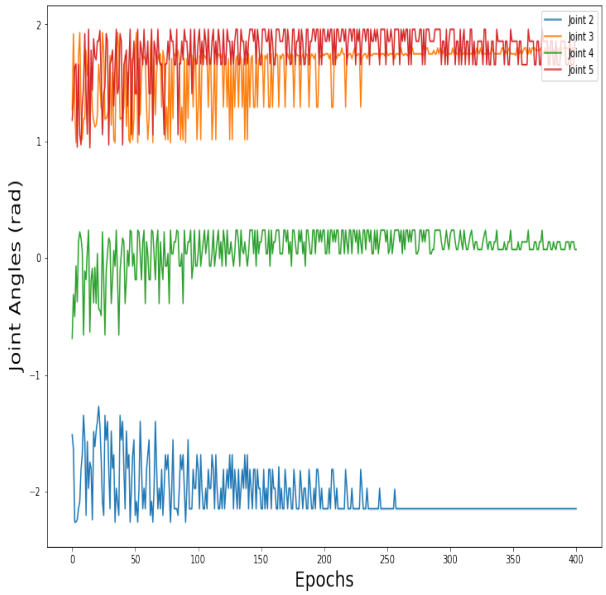

Figure 4.19: The angle value (rad) of each joint while the optimization algorithm was in execution. The angles of joints 1 and 6 were removed from the figure for clarity.

Figure 4.20: The optimal standby pose obtained by minimizing the total torque applied by the joints with the multi-objective genetic algorithm.

optimal pose. This increment in the torque is a key factor for robot maintenance as pointed out in section 4.3.1, especially for highly critical robots such as those located in assembly line bottlenecks.

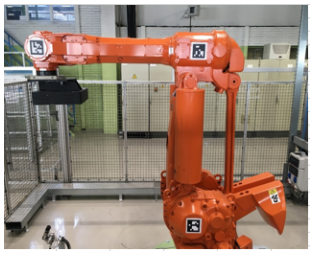

Figure 4.21: Standard pose.

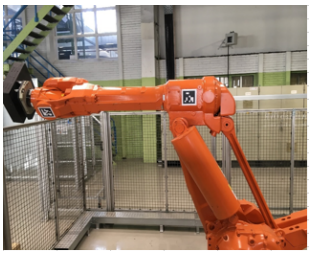

Figure 4.22: Extended pose.

Figure 4.23: Optimized pose.

pose	**Applied torque (Nm)**
Standard	7.764
Extended	17.413
Optimized	5.333

Table 4.12: Torque required by an ABB IRB 6400r robot with a load of 140Kg in three different poses.

4.3.4 Implementation in a manufacturing assembly line

We implemented the methodology in a real automotive manufacturing assembly line to measure the real optimization potential on industrial production working conditions. We selected a robot that had a particularly high failure frequency compared to the rest of the robots. In addition, the workstation of this robot was identical to an adjacent station. Which means that the work of this particular station was duplicated in another contiguous station and the robots of both stations executed the same work in parallel. These conditions allowed us to optimize the waiting pose of one robot and compare it's torque minimization with respect to the robot that executed the same work in the contiguous station.

The selected robot had a spot welding gun attached to the flange and carried a total load of $165.7\,\mathrm{Kg}$. We optimized the standby pose of the robot by implementing the presented methodology. The pose in which the robot waits for the next product was therefore modified to minimize the total torque applied in the joints. The period of time that robots spend waiting for the next product on automotive assembly lines depends on many factors: the state of the assembly line, the production rate, the trajectories that the robots have to execute, their location on the line, etc. Hence, the influence of the standby pose optimization on the energy efficiency and the increase of the robot's RUL will also depend on all these factors that determine its working regime.

Once we optimized the pose, we monitored the torque of all the joints in both

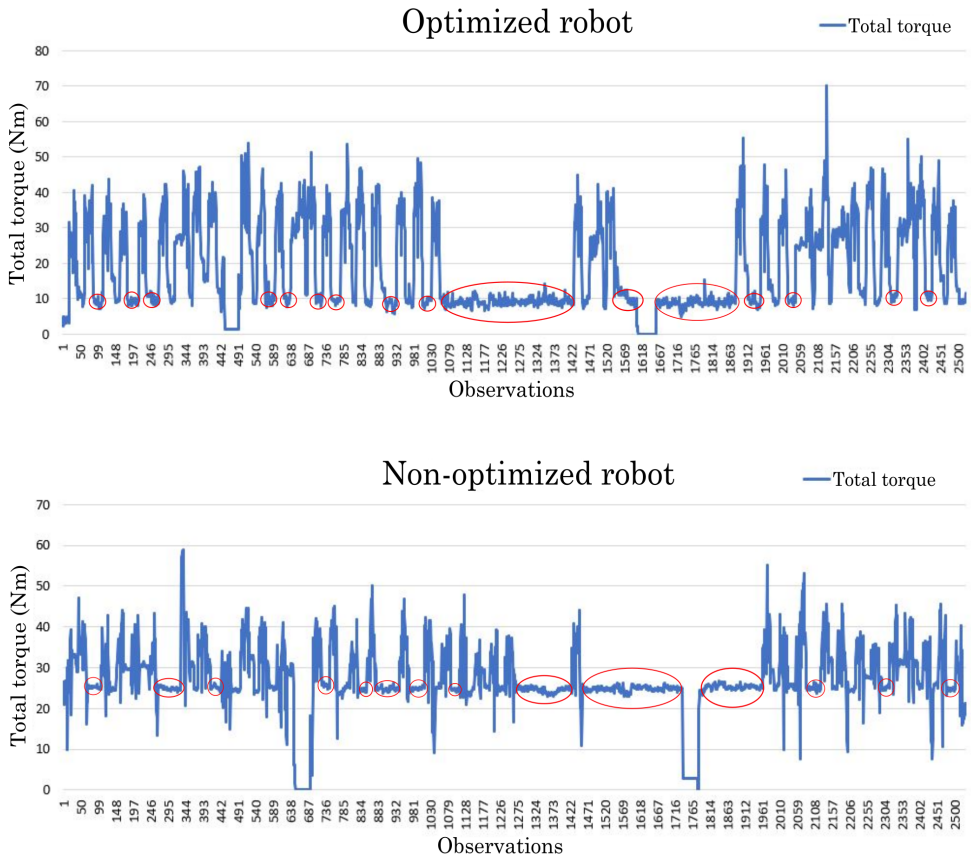

Figure 4.24: Total torque of the optimized and non-optimized robots respectively. The red circles identify examples of periods of time in which the robots wait in their standby pose.

robots (the optimized robot and it's homologous in the contiguous workstation). The monitoring was carried out over approximately two hours in normal production conditions. Figure 4.24 shows the total torque applied (the sum of the torque of the 6 joints) by the optimized and non-optimized robots.

The torque minimization potential is significant as shown in the figures. The circles indicate specific periods of time in which the robots wait in a standby pose. The standby pose highly influences the median and mean values of the total torque in industrial robots. The median and mean values of the total torque in the optimized robot were $11.28\,\mathrm{Nm}$ and $18.56\,\mathrm{Nm}$ respectively. In contrast, the median and mean values of the non-optimized robot were $25.38\,\mathrm{Nm}$ and $27.06\,\mathrm{Nm}$ respectively, which implies a 31.37% reduction of the average total torque applied by the optimized robot in normal production conditions. It is evident from these results that the optimization of the standby pose can significantly affect the total torque applied by industrial robots

in real world scenarios and therefore requires special attention from maintenance personnel.

4.4 A practical and synchronized data acquisition network architecture for industrial robot predictive maintenance in manufacturing assembly lines

This section presents a network architecture and a methodology for industrial robot data acquisition. It consists on a non-intrusive and scalable robot signal extraction architecture, easily applicable in real manufacturing assembly lines. All the infrastructure needed for the implementation of the architecture is based on traditional well-known industrial assets. The data acquisition is synchronized with the execution of robot routines using common Programmable Logic Controllers (PLC) to obtain comparable data batches. A network architecture that acquires comparable and structured data over time, is a crucial step to advance towards an effective predictive maintenance of these complex systems, in terms of effectively detecting time dependent degradation. The architecture is implemented and tested in a real automotive manufacturing assembly line. The results show the potential of the solution to detect robot joint failures in real world scenarios.

4.4.1 Data acquisition network architecture

Figure 4.25 shows the architecture of the proposed network. The network is divided in five layers: data acquisition, control, external sensors, robot metadata, data storage and analysis and visualization layers. One of the benefits of the proposed solution is that the implementation of the architecture does not require additional infrastructure than the usual found in a conventional automated production line.

Data acquisition layer

The data acquisition layer is the subnet that records the data from the robots and stores it in the data server. Nowadays robot controllers can send internal signals through TCP socket communication to an external receiver. This feature has to be enabled in the controller by specifying the internal signals to collect e.g. speed, resolver angle, torque, etc.

The signals can be acquired on demand. When the socket communication is enabled in the robot controllers, the data can be transmitted continuously or on demand when an external agent establishes connection. In our case, the *data server* decides when to start and end the acquisition and from which robot.

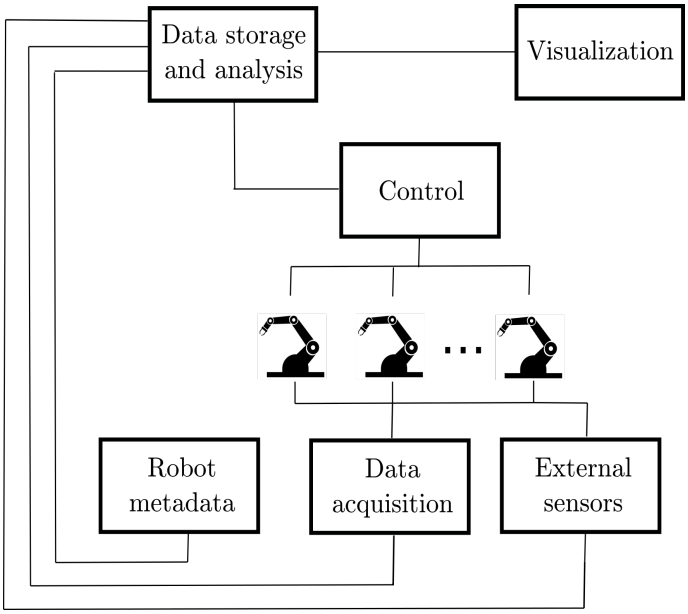

Figure 4.25: The data acquisition network architecture. The control layer is used to synchronize the acquisition of robot signals with additional external sensors, as well as with the executed routines.

Control layer

Depending on the work they have to perform, the PLCs know which routine is each robot executing and when. This is crucial to synchronize the data acquisition and it is the core of our proposal.

The difference between collecting data continuously and on demand is essential when the purpose of the data collection is to build predictive models. Specially for industrial robots, as their behaviour changes drastically depending on the routine they are executing. If the data acquisition process is done in a way in which every stream of data has a certain robot and routine assigned to it, the data will be comparable and representative of that particular robot and routine binomial.

Therefore, this architecture enables the data recording either continuously or discontinuously and synchronized. Each of these forms has its benefits. On the one hand, if the data is collected continuously, it describes the entire operational behavior of the robot. Including all the routines and the periods in which the robot waits standstill for the execution of the next routine. Depending on the robot, this standstill waiting time can be even longer than the actual execution of it's routines.

On the other hand, if the data is discontinuously and synchronously collected, the acquisition is only be performed when the robots execute certain routines. As a result, there is no recording while the robot waits standstill, but the data from a

certain routine is directly comparable over time. This ability to compare the data of a robot-routine binomial over time is the key enabler for detecting anomalies and predicting medium and long-term wear. Therefore, the implementation of a data acquisition network architecture that supports both continuous and synchronized data extraction is a necessary preliminary step for building feasible predictive models.

External sensors layer

The signals collected from the data acquisition layer consist of internal robot signals. However, if there is more information to be recorded with additional external sensors, the data captured with the external sensors will be transmitted trough this layer. Examples of additional external sensors could be acoustic emission sensors, oil debris sensors, thermal images, etc.

A powerful benefit of the proposed architecture is that even if the external sensors are not intelligent enough to capture data on demand, the server will know which information stream coming from the external sensors merges with the internal robot signals of the data acquisition layer. The merging is possible by using the timer of the control layer to save the data that is acquired online with the external sensors. In this way, the control layer establishes the exact period of time when the data acquisition has to be performed in both layers. This synchronization is possible by using the PLCs of the control layer.

Robot metadata layer

The robot's metadata is used to classify the data acquired in the rest of the layers. The metadata contains information of the tool that each robot is holding and its weight, their maximum payload, the standby or waiting pose of each robot, the history of faults and its frequency, etc. The signals recorded in a faulty state of a given robot can be very similar to those recorded in the healthy state of another one. Therefore, By adding the metadata, it is possible to compare the acquired data between robots that have similar working regimes and therefore detect anomalies in robots that should be behaving in the same way.

Data storage and analysis layer

The *data storage and analysis* layer consists of a server responsible for storing and analysing the data acquired from the *data acquisition*, *additional sensors* and *robot metadata* layers. The server communicates with the PLCs to decide when to start collecting the data in each robot and merges the acquired signals with the appropriate

additional information. As mentioned in the *control layer* section, although we propose to collect the data on demand, it is also possible to monitor and store the data continuously e.g. if we want to store the behaviour of a robot uninterruptedly both when it executes routines and when it waits in a standby pose. The diagram of the database that stores robot signals and robot metadata is shown in figure 4.26. Where each table stores the following information:

- *Routines:* Defines which routine is recorded in each robot.
- *Robot_Signals:* Defines which signals are recorded in each robot (resolver angle, speed or torque).
- *Robot_Description:* Stores the metadata of each robot (ID number, IP address, model, location in line, load, date of last failure, attached tool, etc.)
- *Data_Raw:* Stores the data that comes directly from the *Data acquisition layer*. We do not clean or process the data before storing it in this table.
- *Statistical_Summaries:* After processing the data stored in the *Data_Raw* table, we store the results of the statistical analysis and summaries of each routine in this table. Each line of the table saves an statistical descriptive summary of all the acquired raw data.
- *RUL_Estimation:* Finally, once the data analysis is carried out, the results of the Remaining Useful Life (RUL) are calculated using the current health status of each robot and it's historical failure records. This table stores a RUL estimation for each robot based on the results of the data analysis.

In our case, the data analysis is implemented in the same server where the data is stored. However, it is also possible to separate these functionalities in two different servers, one for data storage and the other one for the data analysis and model implementation, as long as the communication between each other is guaranteed.

Visualization layer

The visualization layer consists in data visualization software and infrastructure. It visualizes the results extracted from the analysis and the predictions calculated with the models. Our architecture permits to analyse and visualize robot data at two independent levels: at an individual scale with predictive maintenance models and RUL estimation for individual robots, and at a general scale with a global visualization of the robot fleet.

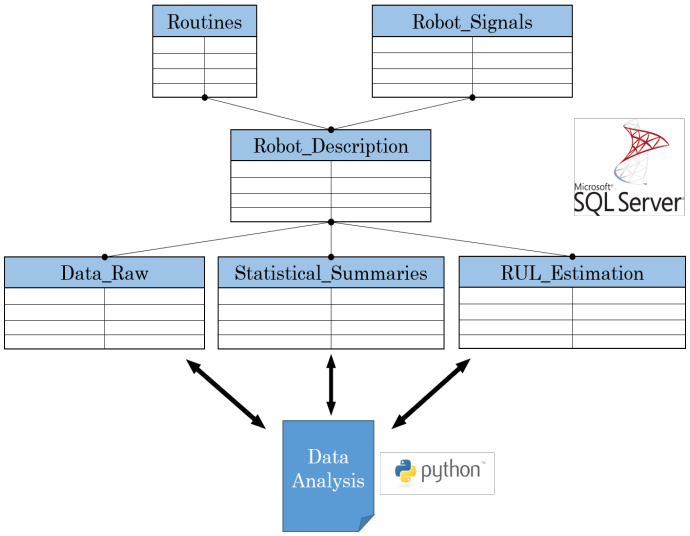

Figure 4.26: Diagram of the implemented database that stores the robot signals and metadata in the *data server*.

4.4.2 Implementation in an automotive body shop assembly line

The proposed network was implemented in an automotive manufacturing body shop assembly line. Manufacturing assembly lines are highly automated and hundreds of industrial robots work uninterruptedly separated in working cells. The PLCs in the control layer are able to manage several working cells simultaneously via INTERBUS or PROFINET protocols. A significant advantage of the solution is that the hardware required for the infrastructure already exists in any common automated assembly line. Therefore, the implementation is mainly based on software development to enhance the functionalities of the current infrastructure. In the presented use case, the only additional hardware asset added was a *data server*.

Infrastructure implementation

The first step is to code the signal recording and the TCP socket server in the robot controllers. Modern robot controllers integrate a TCP server to enable a socket-based signal acquisition. We collected the torque signals of the six joints in each robot. The signal acquisition rate is also configurable and it depends on the frequency in which we want to transmit the data.

The second step is to create a set of variables in the PLCs to inform the *data server* about the beginning and the end of the routines. These variables update their values exactly at the same time as the robot starts the routine, synchronizing in this way the data acquisition and creating comparable data batches.

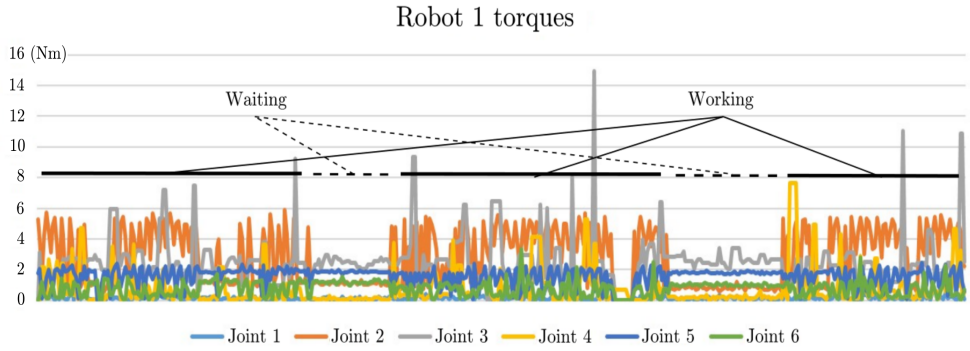

Figure 4.27: Continuous data acquisition of *Robot 1*.

Two main programs were implemented in the *data server*: one to read the variables of the PLCs and the other to handle the communication with the robot controllers. As mentioned above, the communication with the robot controller is performed via socket by implementing a TCP client in the server. The client connects to a remote TCP server (the robot controller) when the PLC notifies the start of a given routine.

When the data acquisition finishes, the received signals are merged with additional information coming form external sensors and databases. The language in which the models and the visualization of the results are implemented in the *Data storage and analysis layer*, depends on the software available in each company. However, the proposed architecture will remain invariant regardless of these differences.

We started by implementing the architecture in two robots inside the same working cell, before scaling up the solution to more cells and robots. When collecting the data, we checked that the TCP packets were not saturating the network and we ensured that the memory and the processor of the robot controllers where operating as usual. Thus, we ensured that the data acquisition did not have any negative impact in the production line before scaling up the architecture. We tested different transmission frequencies and none of them saturated the network.

4.4.3 Results

The data was collected in two ways. First without synchronizing the acquisition with the routines, collecting the data continuously without interruption. Afterwards, synchronizing the data collection with the PLCs. Figures 4.27 and 4.28 show the signals collected without synchronization. The signals correspond to two hours of data acquisition of two industrial robots (*Robot 1* and *Robot 2*) while working in several routines and waiting standby. The graphs show the torque of the six joints of each robot.

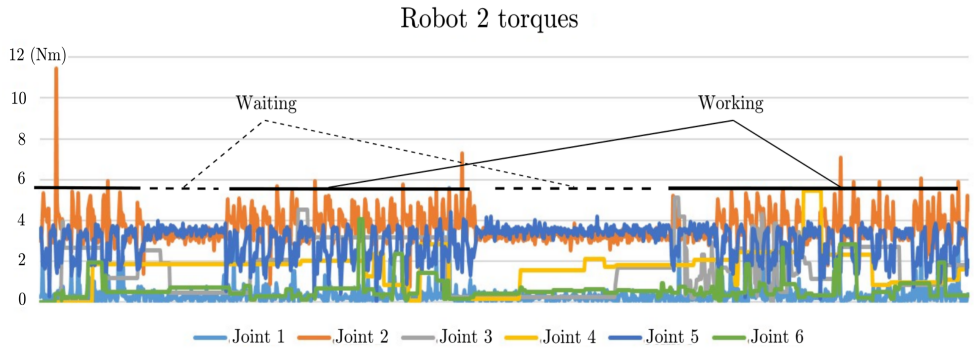

Figure 4.28: Continuous data acquisition of *Robot 2*.

Even though the robots execute different trajectories, both of them are ABB irb 6400r robots with a maximum payload of 200 Kg and they both have a 104 Kg spot welding gun attached to their flange. Note the difference in the behaviour of the two robots, not only between the working and waiting time, but also in the torque of each joint. As expected, the execution of different working regimes completely alters the behaviour of the joints and makes the generalization and comparison between these two robots unfeasible. In addition, by acquiring data in this way without synchronization, there is no clear distinction between the routines that each of them executes. The continuous data acquisition does not separate the different routines and therefore there is no way to compare them over time and detect deterioration or anomalies. In order to identify the wear of a robot, it is essential to be able to compare routines over time, and this is not possible if the routines cannot be separated.

In contrast, figures 4.29 and 4.30 show data acquired in two different moments (*T1* and *T2*) of the same robot (*Robot 2*) executing the same routine. These two graphs demonstrate the ability of our approach to automatically identify and separate data from specific routines. The torque data shown in 4.29 and 4.30 were acquired with the proposed architecture to demonstrate the possibility of achieving comparable data by using the *control layer*. The data acquisition is not programmed for any specific moment in time, but it starts automatically when the robot starts executing the specified routine. The proposed data acquisition procedure is an effective solution to the problem exposed in the previous paragraph with the continuous data acquisition.

The *control layer* effectively identifies the routine and the *data server* divides the signal streams in separated robot-routine binomials. As a result, the obtained signals are much more comparable over time and an eventual health degradation assessment is easier to address. One of the key benefits of this architecture is that data collection is performed at the same time in all the data sources. The result of this data acquisition

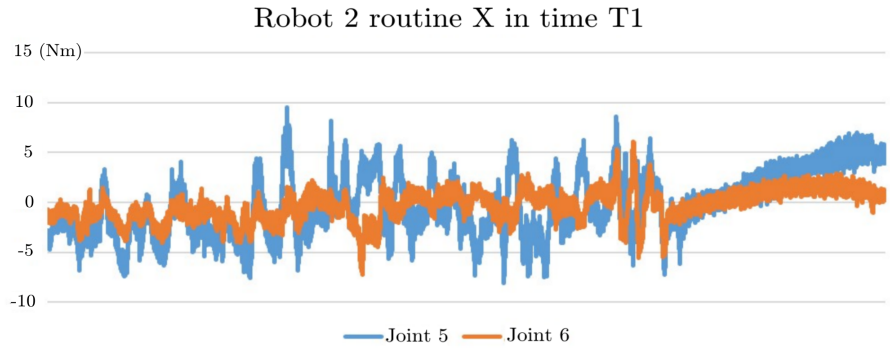

Figure 4.29: Synchronized data acquisition of *Robot 2* (joints 5 and 6) executing routine *X* in time *T1*.

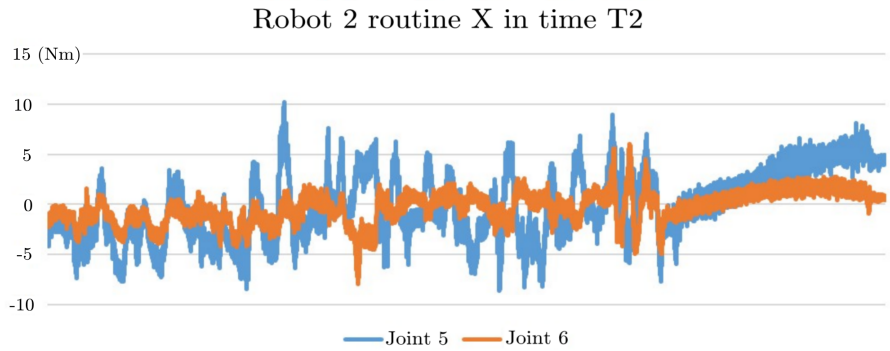

Figure 4.30: Synchronized data acquisition of *Robot 2* (joints 5 and 6) executing routine *X* in time *T2*.

procedure is a time series dataset that represents the behaviour of a given robot-routine binomial.

As explained above, it is hard to identify anomalies in the behaviour of a robot if there is no clear distinction between different routines and working conditions. Each robot requires a different effort in each joint. Thus, in order to compare real production line data of a given robot over time and predict possible failures, it is necessary to first distinguish between routines and then diagnose the robot's evolution.

Once we are able to isolate individual trajectories, we can begin calculating summary statistics of the trajectories. The objective of summary statistics is to condense the maximum amount of information of the trajectories in the smallest amount of data. These summaries will be used for long-term condition monitoring and predictive maintenance. Table 4.13 shows the summary statistics of the torque signal applied by the fifth motor of a monitored industrial robot in production. The summaries are stored along with the robot's ID number and the trajectory's ID. In

Robot_ID	Trajectory_ID	Average_Torque	Maximum_Torque	Variance_Torque
508	502	4.76	8.74	1.80
508	502	4.79	8.27	1.62
508	502	4.90	8.91	1.74
508	502	4.99	8.73	1.82
508	502	4.76	8.58	1.74
508	502	4.61	8.12	1.77
508	502	4.83	8.42	1.62

Table 4.13: Example of summary statistics of the acquired trajectories. Each row represents the statistical summary (median, average, maximum and variance) of the torque data applied by the same motor of a robot in production.

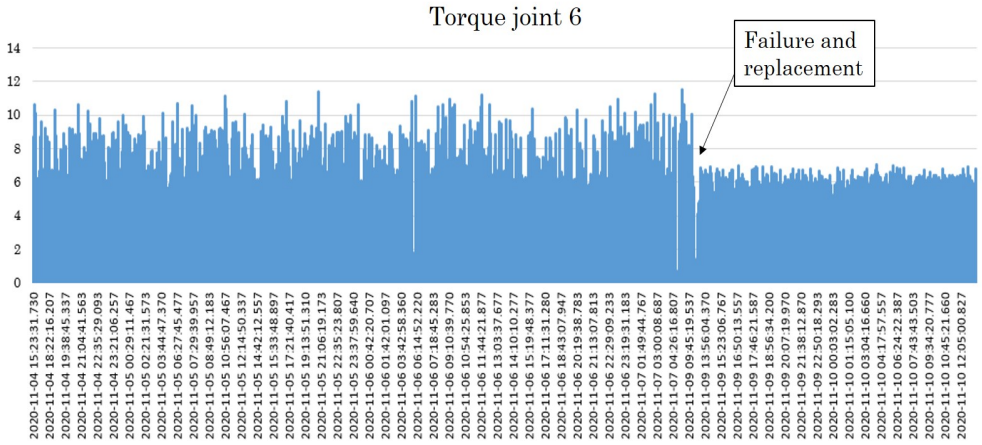

Figure 4.31: Synchronized acquired torque of the failing sixth joint.

this table we do not show all the columns of the dataset for readability and clearness reasons. The complete set of information that we summarize for each torque and joint angle signal is as follows: Date and time of the data acquisition, an id number of the robot, an id number of the motor, an id number of the trajectory, the median value, the average value, the maximum value, the 3rd quartile, the variance and the skewness. The decision of which statistical analysis to choose will be based on the data and the objective of the analysis. The effectiveness of predictive maintenance strategies for industrial robots will strongly rely on the robustness of these summaries.

We scaled the proposed architecture to twenty robots in the production line and started acquiring synchronized data. After a couple of weeks monitoring, one of the robots had a failure in the reducer of the sixth joint that stopped the production. The robot required a total replacement of the sixth joint. Figure 4.31 shows the data acquired some days before and after the replacement of the sixth joint.

By synchronizing the data acquisition, it is easily appreciable the change in the

torque applied by a robot joint before and after a joint failure. The torque was much higher before the joint replacement as a consequence of the unusual friction caused by the degraded reducer. After replacing the failing joint, the monitored torque signal stabilized and the peak values decreased significantly.

Figure 4.31 shows an example of the applicability of the presented solution to build a practical and reliable data acquisition infrastructure to detect and eventually predict robot joint failures. One-class classification models could be trained to model a healthy joint behavior after the replacement of the joint. In this way, the model would detect anomalies based on the torque applied by the joint and identify unusual torque increments for that particular robot-trajectory configuration.

Part V

Conclusions and future work

Chapter 5

Conclusions

This chapter summarizes the main conclusions of the dissertation, the contributions to knowledge and proposes recommendations for future work. In this chapter special attention will be given to the hypotheses exposed in chapter 2 in order to confirm or deny them. Overall, this thesis covers the gap between research done in laboratory and industry-oriented contributions for industrial robot predictive maintenance. There is a considerable gap between research in predictive maintenance for simple industrial assets (bearings, gearboxes, coils, etc.) and complex systems such as industrial robots. Moreover, the contributions focused on robot predictive maintenance, have been mainly implemented in laboratory-controlled conditions. This thesis, is in essence a step forward towards a reliable predictive maintenance solution for industrial robots in real world large scale industrial scenarios.

The following list enumerates the hypothesis exposed at the beginning of the thesis and responds to each one of them, based on the obtained results.

1. *Visual-based monitoring systems provide enough accuracy to detect deviations beyond the tolerance limits of industrial robots.*

   Chapter 4 section 4.1 showed that it is possible with nowadays vision techniques to have enough precision to detect deviations of the robot's end-effector below it's repeatability tolerances. The binary square fiducial markers used in this research work offer a robust and reliable measuring solution for assessing robot's end-effector deviations. Moreover, tracking the position of the robot's structure with fiducial markers can also identify the joint that is producing the deviation.

   However, it should be mentioned that although this solution has been successfully implemented in laboratory, the applicability of vision-based techniques in real industrial scenarios is more difficult due to factors such as air contamination by dust and general dirt. Vision-based techniques rely on the quality of the captured

images. Hence, the air quality and the required cleanliness is a crucial factor that could be difficult to achieve in real industrial scenarios.

2. *Torque sensors can effectively be used to detect medium and long term mechanical deterioration in industrial robot joints.*

   A torque monitoring approach can be used for industrial robot condition monitoring and predictive maintenance. Although the information of the torque is used in robots to detect collisions, excessive loads, etc. It can also be used to analyse mid and long term mechanical failures. The methodology and experimental implementation presented in chapter 4 section 4.2 gives a detailed description of how torque sensors can be used for that purpose. This sensors are not disturbed by external noise and the installation is made inside the robot's structure, which makes them suitable for a real production line environment. Moreover, they do not need the robot to be stopped or removed from the production line in order to record the data. The data acquisition can be done online while the robot works. Finally, torque sensors are not influenced by dirt or dust such as vision-based solutions and may therefore be more suitable for a large scale industrial implementation.

3. *An inefficient standby pose significantly decreases the remaining useful life of an industrial robot.*

   The motors of the joints are one of the most fragile parts of industrial robots. The motors can reach high temperatures and eventually wear out the permanent magnets of the breaks, as shown in chapter 4 section 4.2. Several factors influence the temperature of the joints: The ambient temperature, the load, an inefficient waiting position, the trajectory, the state of the lubricant, etc. Chapter 4 section 4.3 shows that robots with a mechanical failure in their 5th joint, tend to have a more horizontal standby position (9.17°on average). The position in which the robot waits in the production line is a fundamental factor which has received little attention from both researchers and practitioners. Optimizing the waiting position of industrial robots can increase their remaining useful life, especially the ones that spend most of their operational time waiting for the next product.

4. *Optimising an industrial robot's standby pose can significantly reduce its energy consumption in a production line.*

   The optimization of the standby pose can reduce significantly the electric consumption of the robot joints. Depending on the weight and the shape of the tool, and the pose of the robot, the electric consumption can be reduced to less than a half compared to a non-optimized standby pose. An optimal pose can be achieved for

any robot with any tool by using an optimization algorithm and measuring the torque or the electric current as explained in chapter 4 section 4.3.

5. *Common industrial assets offer enough technology to effectively assess the health status of industrial robots in real world production lines.*

   The communication between PLCs and industrial robot controllers can be synchronised to acquire data each time the robots execute previously defined trajectories. In this way, the data acquired is comparable over time and can be analysed to detect deviations caused by mechanical wear. Section 4.4 proposes a network architecture that can effectively detect medium and long term mechanical failures in real production line scenarios using common industrial assets.

Chapter 6

Contributions to knowledge

The following list enumerates the main contributions to knowledge of the thesis:

- Binary squared fiducial markers can detect deviations above the repeatability tolerance limits of an industrial robot.
- The methodology proposed in section 4.2 can detect medium-long term mechanical deterioration in an industrial robot joint, as long as the deterioration increments the torque needed in any joint of the robot.
- In order to build a machine learning model for fault prediction in industrial robots, torque sensors are be the most reliable data sources. As any relevant mechanical wear in a joint will cause an unusual increment in the torque of that joint.
- One of the most common failures in industrial robots of automotive plants is caused by overheating. The prolonged excessive heating of the fifth joint's motor demagnetizes the permanent magnets of the motor's brake. The demagnetization causes unusual friction in the brake and an increment in the torque applied by the joint. This is a cyclic process, as the increment in the torque needed to move the motor, causes more electric current to flow through the motor and thus increases the overheating in the joint.
- The result of the demagnetization is twofold. On the one hand, when the robot moves (brakes released) the brake exerts resistance to the movement of the motor, increasing the torque required to reach the desired position. On the other hand, when the robot stops (with the brakes activated) and if the demagnetization is severe enough, the permanent magnets do not apply sufficient force to hold the joint's position and the joint slowly moves towards the ground attracted by gravity.
- Robots in assembly lines may have very inefficient standby or waiting poses, which produce excessive overheating. The angle in which the fifth joint holds the tool

attached to the robot can be as determinant as the weight of the tool to cause an overheating in the motor of the fifth joint.

- Optimization algorithms such as genetic algorithms (section 4.3) can be used to optimize the standby pose of any robot with any tool attached to it. As long as the torque or the electric current of the joints are monitored.
- The inherent intelligence of robot controllers and their communication with common PLCs and data servers offer enough technology to build a network architecture capable of collecting synchronized and clean data for robot health status assessment in real world production lines.
- If an industrial robot suffers mechanical degradation and deviates from its normal behavior, motor torque signals will gradually increase. By synchronizing the data acquisition of the robot signals with the execution of the routines, it is possible to build a monitoring system that detects the deviation of those signals and infer a mechanical deterioration.

Chapter 7

Recommendations for Future Work

This section suggests possible future lines of work based on the results of the thesis. One of the greatest benefits of Big Data infrastructures and data analysis techniques is the possibility of extracting useful information in large networks and varied data sources such as those found on assembly lines. Extracting synchronized and structured data from many robots to feed machine learning algorithms, opens up a wide range of possibilities for the prescriptive maintenance of these assets.

Ideally, there should be no need for a specific routine such as the one proposed in section 4.2 to diagnose the health status of a robot. Based on a reliable data acquisition infrastructure, data analysis and machine learning models might be able to identify a deviation in the health status of a given robot and predict a failure regardless of it's current trajectory or tool. Therefore, further research is needed in order to fully automatize a predictive maintenance solution.

In this regards, future lines of work could be focused on building data based models by collecting structured data with the proposed network architecture e.g. If the acquired data is comparable, anomaly or novelty detection algorithms could be used to detect a deviation in the normal behaviour of a given robot. In addition, future work will also address the challenging task of determining the level of generalization that a predictive maintenance model for industrial robots should have and which algorithms are able to achieve robust models of such such a complex and non-linear behaviour.

Another interesting continuation of the presented thesis would be to create clusters of robots by grouping them according to their internal signals and metadata information such as the weight of the tool, the time spent in production, the robot type, etc. In this way, it might be possible to define clusters of robots by their normal or expected behaviour and identify robots that are operating outside the boundaries of what it is expected from them. This would permit to identify anomalous behaviour in robots

without prior additional information.

Finally, the monitoring of robot signals (position, speed and torque of the joints) can also be used to build the dynamic model of a given robot. These dynamic models are able to calculate the torque required by a robot given a certain tool and trajectory configuration. Hence, it would be possible to predict the effort that a robot would require even before installing it in the production line if the trajectory and tool are known. Moreover, with this methodology, it would also be possible to optimize the standby pose and the trajectory of industrial robots in a new production line from the design phase.

Part VI

Publications

Chapter 8

Publication 1: Towards manufacturing robotics accuracy degradation assessment: a vision-based data-driven implementation.

Robotics and Computer Integrated Manufacturing 67 (2021) 102029

Contents lists available at ScienceDirect

Robotics and Computer Integrated Manufacturing

journal homepage: www.elsevier.com/locate/rcim

Towards manufacturing robotics accuracy degradation assessment: A vision-based data-driven implementation

Unai Izagirre*, Imanol Andonegui, Luka Eciolaza, Urko Zurutuza

Electronics and Computer Science department, Mondragon Unibertsitatea, Arrasate - Mondragon, Spain

ARTICLE INFO

Keywords:
Robot health monitoring
Industrial robot
PHM
Machine learning
Augmented reality

ABSTRACT

In this manuscript we report on a vision-based data-driven methodology for industrial robot health assessment. We provide an experimental evidence of the usefulness of our methodology on a system comprised of a 6-axis industrial robot, two monocular cameras and five binary squared fiducial markers. The fiducial marker system permits to accurately track the deviation of the end-effector along a fixed non-trivial trajectory. Moreover, we monitor the trajectory deflection using three gradually increasing weights attached to the end-effector. When the robot is loaded with the maximum allowed payload, a deviation of 0.77mm is identified in the Z-coordinate of the end-effector. Tracing trajectory information, we train five supervised learning regression models. Such models are afterwards used to predict the deviation of the end-effector, using the pose estimation provided by the visual tracking system. As a result of this study, we show that this procedure is a stable, robust, rigorous and reliable tool for robot trajectory deviation estimation and it even allows to identify the mechanical element producing non-kinematic errors.

1. Introduction

Industrial robots are designed to be very robust and can withstand many years of uninterrupted operation. However, like any mechanical element working in contact with another mechanical element, an industrial robot will eventually deteriorate regardless of its design [1]. This deterioration process can last for years but once it begins to occur, it can quickly evolve to an irreversible failure. A large body of literature has been devoted to the development of Prognosis and Health Management (PHM) technologies of the individual components comprising industrial robots, such as gearboxes [2,3] or electric motors [4,5]. Samanta et al. [6] presented a system to monitor and predict machine conditions using soft computing techniques and a neuro-fuzzy system. They considered five different component faults to illustrate the effectiveness of the proposed solution: gear wear, gear tooth chipping, gear tooth crack, gear pitting and shaft misalignment. In contrast, the assessment of the health status at the system level has hitherto remained being an unexplored research challenge [7]. Noticeably, the modelling of a robot joint comprises still a hard endeavour. Considering the nonlinear behaviour of elastic-plastic friction interaction between rigid components, which are strongly dependent on inertial and acceleration dynamics, makes numerical exploration of health monitoring in robots extremely complicated, even when clustered computational resources are utilized [8]. In the light of this complexity, often the mathematical analyses used to estimate the degradation level of these components rely on a simplified dynamic modeling of the real problem, such as assuming constant speeds of operation [9], ignoring the temperature of the system [10], simplifying the effect of the friction [11], etc. All in all, these assumptions make the results of the models differ from reality. With this regards, there is a critical need to develop new methodologies to explore the deterioration of an industrial robot, considering the entire mechanical system, regardless of the mechanical status of a particular component comprising the robot [7]. This rapidly emerging research field can pave the way to enhance the precision and monitor the degradation of heavy load handling industrial robots, such as the ones used in the automotive and aerospace industry [7].

In recent years, there have been several approaches to address this problem. Physics-based simulation models and digital twins have been proposed in [12,13] for industrial robot predictive maintenance and remaining useful life (RUL) estimation. Luo et al. [14] proposed a hybrid approach based on a model-based digital twin and a data-based digital twin. They proved the feasibility of the hybrid digital twin approach in a cutting tool life prediction use case. Data-driven approaches have been increasingly used for condition monitoring and predictive maintenance of industrial robots. Kokkalis et al. [15] and Papanastasiou et al. [16] monitored the torque and the current in robot joints for

* Corresponding author.
E-mail address: uizagirre@mondragon.edu (U. Izagirre).

https://doi.org/10.1016/j.rcim.2020.102029
Received 29 October 2019; Received in revised form 7 July 2020; Accepted 7 July 2020
Available online 22 July 2020

collision detection and human-robot collaboration. Former studies used accelerometers to identify the degradation of an industrial robot [17–19]. In [20] a laser tracker was used to identify the pose of the robot end-effector and then control its deviation. The technique called *Visuo-Motor Control* was used in [21] to control an industrial robot by acting on robot's motors depending on the deviation of the end-effector. Instead of using a laser tracker, they used a camera-based vision system. In their work, as well as in the ones carried out by Quiao et al. in [22,23] the researchers used two cameras to obtain the coordinates of the end-effector.

Vision based technologies have been widely used to improve robotic systems in manufacturing processes. Recently, a vision-based methodology was proposed in [24] and implemented alongside machine learning classification models in [25] to handle randomly placed complex parts. Stereo cameras were used in [26] to correct the path of industrial robots in welding operations. Xu et al. [27] further improved the precision of image processing in seam tracking and carried out a systematic study of the application of computer vision technology in robotic GTAW and GMAW. Tsai et al. [28] constructed a vision-based path planning method for a golf club head robotic welding system.

The vision-based solutions for industrial robots proposed so far, have been mainly focused on product quality and process improvement. This manuscript aims to cover the gap in the implementation of vision-based techniques and machine learning models for industrial robot health assessment. In this work, we present a novel approach in which we study the feasibility of using fiducial marker based vision systems to assess the accuracy degradation and repeatability of an industrial robot at different loads. We trained five supervised learning regression models to predict the deviation of the robot's end-effector using the data provided by monocular cameras. After training the models, we tested their prediction accuracy using that data provided by both cameras.

The manuscript is structured as follows: in the next section we describe the used materials, the experimental setup and the procedure followed. Section 3 presents the obtained results and we conclude with a brief discussion and a summary of the contributions in Section 4. Finally, we identify the future lines of work in 5.

2. Experimental setup and procedure

2.1. Pose estimation using fiducial markers

Monitoring the trajectory deflection of an industrial manipulator requires combining the kinematics of the mechanical unit with the information acquired using external sensing devices, such as visual tracking systems comprised of a set of cameras and fiducial markers. Binary square fiducial markers have become a popular tool in numerous computer vision applications such as augmented reality, 3D reconstruction and robotics. In manufacturing, augmented reality techniques have been used to facilitate human-robot interaction [29] and robot path programming [30]. Augmented reality permits to consider the dynamic constraints of robotic systems and overcome traditional path programming drawbacks for unskilled workers[29].

Nevertheless, the advanteges of using fiducial markers as external surrogates for motion monitoring of the robot are manyfold; they allow estimating the position of a monocular camera with minimal cost, high robustness, and high speed, i.e., they bestow both accuracy against noise and robustness against outliers. Specifically, in this manuscript, we address the shortcomings of robot pose estimation by tracking calibrated ArUco markers [31,32] which dynamically trace the trajectory followed by a robot. An in depth explanation of the marker detection process used in our work can be found in [32]. In summary, marker detection process consists of four steps: Image segmentation, contour extraction and filtering, marker code extraction and subpixel corner refinement, respectively. In the first step, the marker detection algorithm uses temporal information to speed up the image segmentation process using a global thresholding method, preventing convolution operations required by e.g. the adaptative border detection used in [31]. Subsequently, a contour following algorithm is applied to the thresholded image. Formerly computed contours are then filtered by fitting them to a four corner convex polygon. Next, the algorithm binarizes these contours and determines whether the selected contours are valid markers or not. If the contours are indeed valid markers, the last step estimates the pose of each marker with subpixel accuracy. Once the markers are detected, the pose of each marker in the image is calculated.

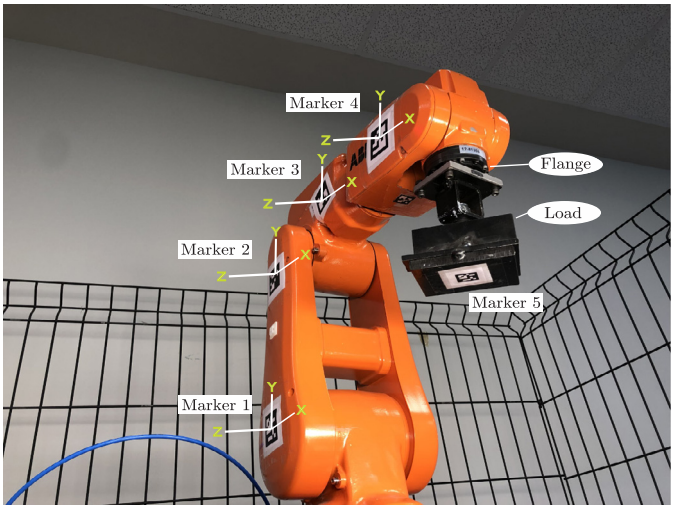

Fig. 1. Fiducial markers attached to the robot in the experimental setup.

2.2. Materials and setup

The experiments were carried out using a 6 Degrees of Freedom (DOF) industrial robotic manipulator ABB IRB 120, which maximum payload is limited to 3 Kg. Our robot has an slight looseness in the gear of the second joint, which is expected to cause a certain lack of precision. We placed fiducial markers at the rigid links of the robot, as shown in Fig. 1. To track the position of these fiducial markers and avoid occlusions during the robot trajectory we used two monocular cameras as it is shown in Fig. 2. The cameras were two *mvBlueCOUGAR-X* Gigabit Ethernet industrial cameras, model *102n* with 2MP resolution. We used 12mm focal length camera lenses which first and second order Brown-Conrady [33] radial and tangential distortion coefficients are

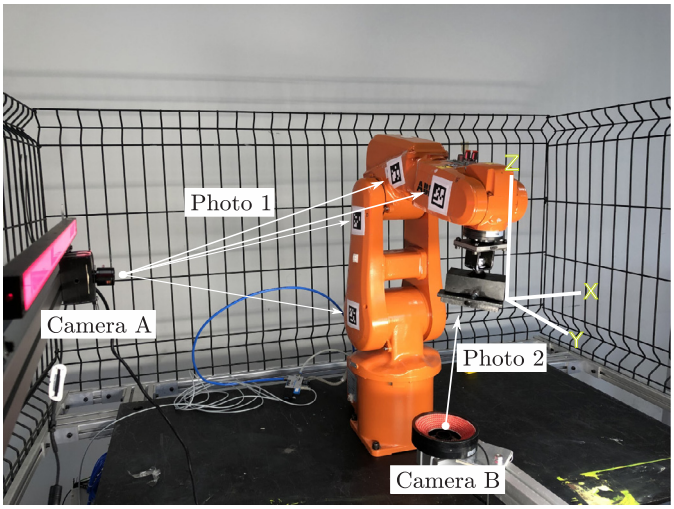

Fig. 2. Cameras *A* and *B* and the coordinate system of the end-effector.

-0.298340, 0.114099 and -1.054507e-05, -0.000599 respectively. These cameras are multiplatform and compatible with the OpenCV open-source library. Any industrial camera with similar characteristics is adequate for the described experiment, as the illumination condition are controlled. The images are taken when the robot is under stationary regime. Therefore, no special minimum frame-rate is required for the image acquisition.

The camera labelled as camera *A* (see Fig. 2) calculates the pose of these markers located on the side-viewed links of the manipulator, i.e. markers 1, 2, 3 and 4. While camera *B*, calculates the pose of the end-effector. An independent platform was build to isolate the cameras from the robot and prevent mechanical vibrations. A flat halogen red lamp illumination (model *LND-600A-DF*) and a non-collimated red diode bright field illumination (model *LDR2*) were used to optimize image acquisition on *A* and *B* cameras, respectively. In addition, we covered the entire experimental setup with a black opaque fabric to ensure that the lightning conditions remained unchanged throughout the whole experiment.

2.3. Experimental procedure

During the experimental data acquisition, the robot executes a closed non-trivial trajectory and meantime cameras *A* and *B* capture images of the markers at fixed time-stamps. The experimental procedure is schematically depicted in Fig. 3.

First, the robot executes a repetitive trajectory and time-stamped images of the markers are taken and stored. Each trajectory lasts 40 seconds. At the end of this trajectory, the robot returns to the starting point and one photo is taken with each camera. A photo to capture one side of the robot and the other to capture the end-effector. The first four markers will be used to monitor the position deviation from the first joint to the fourth. The fifth marker is used to detect the position of the end-effector. The kinematics of the end-effector are therefore calculated using the fiducial markers. The deviation of the robot corresponds to the relative changes in position and orientation of the kinematics acquired with the markers throughout the experiment. The images acquired using both cameras are stored until the end of the experiment. Subsequently, we calculate the position and orientation data of each marker shown in the set of images acquired during the data acquisition operation. When all the data about the position and orientation of each marker are obtained, we can proceed to the deviation analysis and the machine learning model creation, training and testing. We created the machine learning models and trained them to solve a supervised non-linear regression problem. The predictions of each model were later tested and compared to evaluate their accuracy.

The reason for training the models to solve a supervised non-linear regression problem, is that in real world scenarios, it is often difficult to obtain images of the robot's end-tool to compute its relative position. With this regards, we tested the accuracy of the models to identify the deviation of the end-effector using the camera located in one side of the robot. The hypothesis is that knowing the deviation of the end-effector using the fifth marker, and the pose of the robot using the rest of the markers, the deviation of the end-effector can be predicted using only the data of the pose of the first four markers. Without any need of the camera B. We used the estimated set of robot pose data to train five supervised learning regression models. These models then predict the robot's end-effector deviation using the information of the pose of the first 4 markers and we evaluate the accuracy of the predictions.

We conducted a total of three experiments following this same process. We increased the weight attached to the end-effector in each of the experiments to study the behaviour of the manipulator using different loads. The first experiment was carried out without any extra load, leaving the flange free. In the second and third experiments the load was 1.5 Kg and 3 Kg (the maximum payload), respectively. Each experiment saves 2000 images. After completing the experiments, we obtained three datasets with the positions (*X, Y* and *Z*) and rotations (R_x, R_y and R_z) of all these markers.

2.4. Software implementation

The software modules were all implemented in the same computer and the architecture of the software implementation is shown in Fig. 4. We used the open-source Robot Operating System (ROS) for the coordination between the robot trajectory execution and the image acquisition. The images were taken using the OpenCV [34] python library. After finishing the data acquisition, the coordinates of each marker in each image were obtained with the ArUco library and stored in csv datasets. The machine learning models were trained using these csv datasets without any preprocessing. The columns of the datasets consisted on six floating-point numbers for every fiducial marker. Three floating-points for the positions (*X, Y* and *Z*) and three floating-points for the rotations (R_x, R_y and R_z). Therefore, the total amount of columns in the datasets were 30 (6 for each of the 5 markers). The rows of the datasets (2000 for every experiment) were randomly split, selecting the 80% of the rows (1600) for training and the remaining 20% (400) for testing.

We trained five prediction models to estimate and compare their

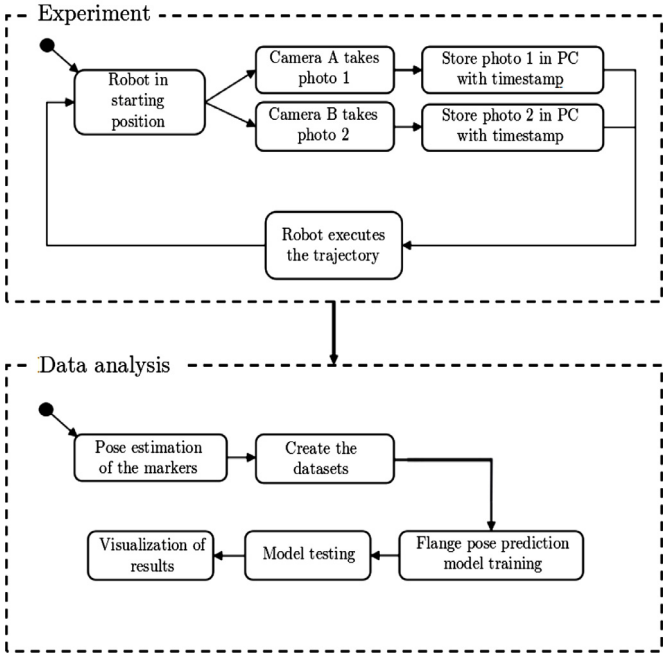

Fig. 3. Flow chart of the experimental procedure.

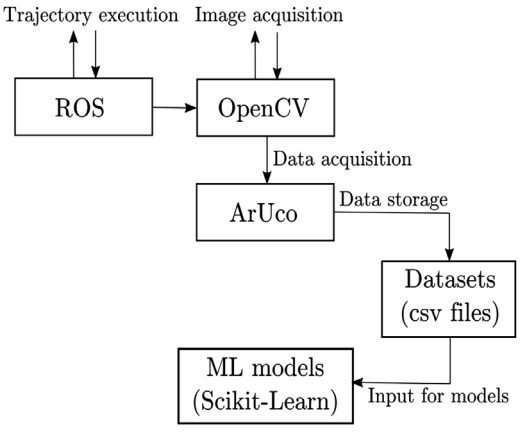

Fig. 4. Architecture of the implemented software modules.

accuracy. We implemented the models using Python and the Scikit-learn library [35]. The following list enumerates the implemented models and the main chosen hyperparameters:

- **Random Forest:** Number of trees = 1000; maximum depth = none; minimum samples to split = 2; split criterion = Mean Squared Error (MSE).
- **Support Vector Regression:** Kernel = rbf; Kernel coefficient (*gamma*) = *auto*; regularization parameter (*C*) = 1.0; epsilon = 0.1.
- **Lasso:** Alpha = 1.0; fit intercept = True; tolerance of the optimization = 0.0001.
- **Multi-Layer Perceptron:** Number of hidden layers = 1; nodes in hidden layer = 100; activation function of hidden layer = *relu*; learning rate = 0.001.
- **Bayesian Ridge:** Maximum iterations = 300; tolerance = 0.001.

We implemented a moving average model to predict the position of the end-effector in order to establish a baseline error. The moving average model was optimized by selecting the window size that maximized its prediction accuracy. The prediction accuracy of the optimized moving average was then used as a baseline performance to test the accuracy of the machine learning models. In this way, we were able to test the feasibility of the models for the presented use case.

The only hyperparameter that was optimized was the window size of the moving average model. The decision of not optimizing the rest of the hyperparameters was taken mainly to prove the applicability of supervised learning models, as the obtained result could only improve after hyperparameter optimization. We used the raw data of the coordinates to train the models without normalization.

3. Results

The analysed data contains the position in millimeters (*X, Y* and *Z*) and the rotation in radians (R_x, R_y and R_z) of every marker (see Fig. 1). Those values are obtained from the images and stored in the datasets. The final datasets are therefore comprised of 30 columns (6 coordinates for each marker) and 2000 rows for each experiment. Fig. 5 shows the dispersion of the coordinates of the end-effector using boxplots and scatter plots. Each dot in the scatter plot represents the actual position deviation (in *Z* and *Y* coordinates) of the end-effector. The coloring of the graphs represents the transient status of the experiments, from dark blue dots (the deviation of the flange when the experiment starts) to brown dots (the deviation of the flange when the experiment ends). The data shown in the first boxplot and scatter plot corresponds to the first experiment. The data of the second and third experiments is shown in the second and third boxplots and scatter plots respectively.

As it is shown in Fig. 5, the greatest dispersion occurs in the Z_{tool} coordinate (*Z* axis in the tool coordinate frame, Fig. 2) in the 3 cases. In the first two experiments the end-effector has an ascending tendency and in the third experiment, when the load equals the maximum payload, the end-effector descends in the negative *Z* direction. Note that the deviation in the Z coordinate increases significantly as weight is added to the flange. The robot deviated the most from its initial position (0.77mm) in the third experiment.

To foresee the source of the pose deviation in the *Z* coordinate, an analysis of the *R-squared* was conducted where $R \in [0, 1]$ and

$$R^2 = 1 - \frac{SS_{res}}{SS_{tot}}. \tag{1}$$

SS_{res} is given by

$$SS_{res} = \sum (f_i - \bar{y})^2 \tag{2}$$

where $\bar{y}$ is the mean of observed values associated to f_i predicted or modeled values. SS_{tot} is the total sum of squares and it is given by

$$SS_{tot} = \sum (y_i - \bar{y})^2. \tag{3}$$

The vertical displacement of the robot in the *Z* coordinate is controlled by joints 2 and 3, so the deviation must be originated in one of those two joints (or in both of them). To identify the origin of the deviation, the coordinates of the first four markers that are related to the robot's vertical movements have been compared with the flange's displacement in Z. The R_z, *X* and *Y* coordinates of the markers, as it can be seen in Fig. 1, are in charge of directing the movement of the flange in it's *Z* coordinate. In summary, the R-square coefficient between R_z, *X*

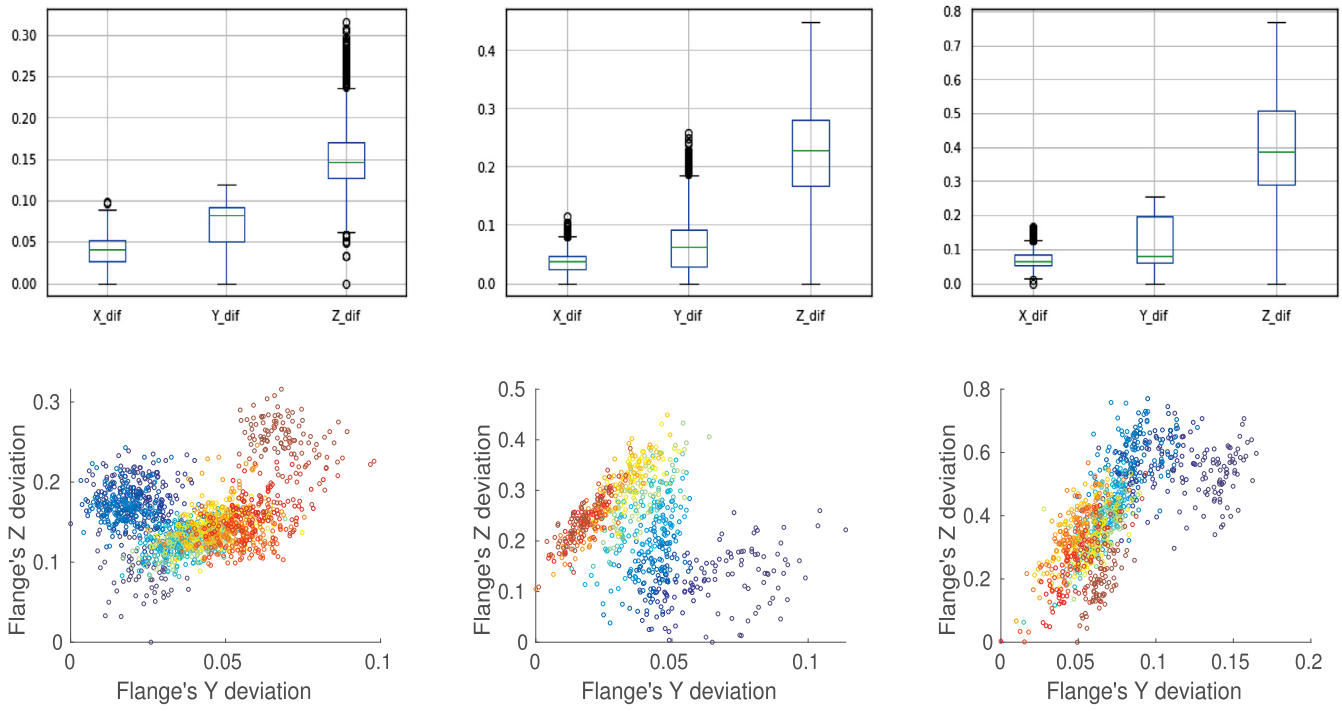

Fig. 5. Deviation in the flange of the robot in the *X, Y* and *Z* coordinates with 0Kg, 1.5Kg and 3Kg respectively.

Table 1
R-squared values between first 4 markers' R_z, Z and Y and flange's Z. (0Kg).

	Rz & flange Z	X & flange Z	Y & flange Z
Marker 1	0.037	0.002	0.003
Marker 2	**0.308**	**0.316**	**0.345**
Marker 3	0.038	0.037	0.117
Marker 4	0.009	0.108	0.030

Table 2
R-squared values between first 4 markers' R_z, Z and Y and flange's Z. (1,5Kg).

	Rz & flange Z	X & flange Z	Y & flange Z
Marker 1	0.053	0.226	0.264
Marker 2	0.010	0.248	**0.273**
Marker 3	0.135	0.110	0.263
Marker 4	**0.245**	**0.398**	0.234

Table 3
R-squared values between first 4 markers' R_z, Z and Y and flange's Z. (3Kg).

	Rz & flange Z	X & flange Z	Y & flange Z
Marker 1	0.028	0.001	0.061
Marker 2	**0.576**	**0.682**	**0.667**
Marker 3	0.142	0.504	0.376
Marker 4	0.538	0.623	0.368

and Y coordinates of the first four markers and the Z coordinate of the flange were calculated. The results are shown in Tables 1, 2 and 3.

In the first experiment, marker 2 obtains the highest *R-square* values (Table 1) with a significant difference. In the second experiment, markers 2 and 4 score the highest scores (Table 2). Finally, in the third experiment, marker 2 is again the marker with highest coefficient values (Table 3). This results show that markers 2 and 4 have the greatest relationship with the deviation of the flange. The marker 2 scores the most significant relationship with the flange compared to the rest of the markers specially when the flange is left free with no load attached to it or when the load is the maximum.

These results are in line with expectations, as markers 2 and 4 are the two most separate markers from the points where the vertical movement of the robot originates (joints 2 and 3) as can be seen in Fig. 1. Which means that, a rotation in joint 2 will be more noticeable in marker 2 than in marker 1, even though it affects both markers' pose.

As a result of the analysis, joint 2 was identified as the origin of the flange deviation. The reasons that led us to that conclusion were: first of all, if the deviation was originated in joint 3, there would be no correlation between marker 2 and the final deviation of the flange. This correlation would only be appreciable in the 4th marker, which is not the case. Second, if the source of the deviation were both joints (2 and 3) in a similar way, marker 4 would have a much higher correlation with the flange than marker 2, because the deviation of both joints could be appreciable in this 4th marker (the deviation of the 3rd joint plus the deviation propagated from the 2nd joint). Therefore, the fact that it is mainly the 2nd marker the one that scores the greatest R-squared coefficient values in most of the cases and with different loads, suggests that the source of the deviation in the Z coordinate of the flange is located in the 2nd joint.

After evaluating the relationship between the poses of the robot's side markers and the deviation of the flange, six regression models were trained following a supervised learning process to predict the position of the flange in the Z coordinate. We trained the models using the information of the pose of the four markers (the position and the rotation in X, Y and Z) as the predictor variables and the position in the Z coordinate of the flange as the target variable. Which resulted in a total of 24 floating-point predictor variables (6 coordinates for each of the 4 markers) and a single floating-point target variable.

In Fig. 6 we show a comparison of the actual position of the flange in the Z coordinate and the position predicted by the models that obtained the highest accuracy (bayesian ridge in the first experiment and random forest in the second and third).

To evaluate the prediction accuracy of the models, the Mean Absolute Error (MAE) and the Root Mean Squared Error (RMSE) were calculated. MAE and RMSE are both widely used metrics for error measuring in statistics. MAE is given by

$$MAE = \frac{\sum_{i=1}^{n} |y_i - x_i|}{n} \tag{4}$$

and RMSE by

$$RMSE = \sqrt{\frac{\sum_{i=1}^{n} (y_i - x_i)^2}{n}} \tag{5}$$

where y_i is the set of predicted values and x_i is the set of real values.

To see whether our models capture the behaviour of the system or not, we established a baseline prediction by calculating the moving average of the real data. That is, we calculated the RMSE and MAE errors we would obtain if we used the moving average value to predict the position of the flange in the Z coordinate. As previously mentioned, we optimized the window size of the moving average model to chose the window with the highest prediction accuracy for every experiment. We then compared the results with the rest of the models. In Fig. 7 we show the learning curve of the moving average obtained by reducing the RMSE error as the window size increases (second experiment). When the window size is about 40, the RMSE error stops decreasing and the model does not score better results. This value obtained by optimizing the windows size is then compared with the results of the rest of the models. The comparison is shown in tables 4, 5 and 6.

The effectiveness and feasibility of some of the implemented models can be seen both in the graphs and in the improvement of the error with respect to the baseline error in the tables. The Random Forest, Support Vector Regression and Bayesian Ridge models obtain the best results and the error of the moving average is improved in the three cases. Multi-Layer Perceptron obtains the worst results. The authors believe

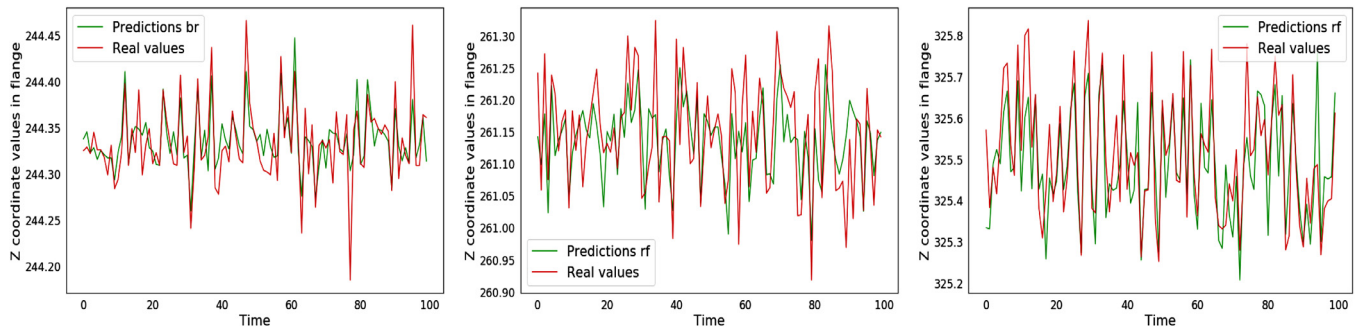

Fig. 6. Predictions of the flange's Z coordinate position and real values with 0, 1.5 and 3kg of load respectively.

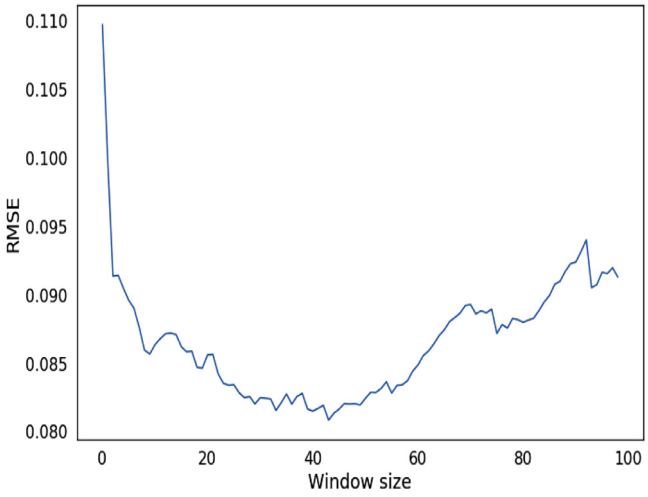

Fig. 7. Learning curve of the moving average windows size in the experiment with 1,5Kg of load.

Table 4
Error of the trained models with no extra load.

	RMSE	MAE
Moving Average	0.04162	0.03094
Random forest	**0.02540**	0.02152
SVR	0.04148	0.03477
LASSO	0.03946	0.02883
Multi-layer perceptron	0.15250	0.12415
Bayesian ridge	0.02763	**0.02140**

Table 5
Error of the trained models with 1,5Kg.

	RMSE	MAE
Moving Average	0.08142	0.064390
Random forest	**0.06557**	**0.02152**
SVR	0.07154	0.05670
LASSO	0.08391	0.06806
Multi-layer perceptron	0.17636	0.13704
Bayesian ridge	0.06648	0.05297

Table 6
Error of the trained models with 3Kg.

	RMSE	MAE
Moving Average	0.16102	0.13129
Random forest	0.09765	**0.02152**
SVR	0.10546	0.08506
LASSO	0.15757	0.12729
Multi-layer perceptron	0.28744	0.23893
Bayesian ridge	**0.08845**	0.07093

that the volume of the data (less than five thousands rows) might not be enough to properly train a neural network model.

4. Conclusions

The aim of this work is twofold. First, is to experimentally test the feasibility of vision-based data driven techniques to analyse the health status of an industrial robot. The second objective is to train a regression model to predict the deviation of the end-effector. The main idea of this second objective is to predict the deviation of the end-effector using only the deviation data provided by one camera (A).

The results demonstrate that binary square fiducial markers can reliably be used for the above mentioned purpose. This technique offers a more economical solution than others such as laser tracker pose estimation. In our case, we verified that, the Z coordinate of the flange is the one that deviates the most and that this deviation increases as the load reaches the maximum payload of the manipulator.

The described procedure can also be used to detect the joint that is producing the deviation. Although the proposed procedure is able to effectively locate the faulty joint, further investigation will be required in order to elaborate a root cause analysis of the failure causing the deviation.

Finally, the feasibility of using supervised learning models to detect deviations in the end-effector with data captured from one side of the robot is tested. The results are promising, as several models are able to improve the baseline error of the moving average in all the experiments. The results are even more relevant if we take into account that we did not optimize the hyperparameters of the models. The proposed approach could also be used in future works for RUL estimation. The authors believe that the combination of the presented approach with other sources of information such as the electrical current or the torque of the motors, could significantly help in assessing the health status and deterioration of an industrial robot.

5. Future work

The integration of the proposed solution with already existing health assessment solutions is an interesting future line of work. The integration of multiple health assessment approaches could be used to develop reliable root cause analysis and RUL estimation solutions for industrial robots.

The implementation of the proposed solution in a real production line environment is another identified future line of work. Vision-based techniques strongly depend on lighting and dirt conditions. However, these conditions are much more difficult to control in real production lines than in research labs. Therefore, further work is required to build a more robust solution capable of working in real industrial conditions.

A limitation of the presented work is that the deviation of the flange is not analysed in the entire trajectory. Augmented reality techniques such as the one used in this work permit to track the position of the markers in movement with live video recordings. Thus, a deviation in the dynamic behavior of the end-effector could be detected using the marker detection with live video recordings. However, the accuracy required to detect the deviation of an industrial robot is harder to achieve when it is moving than when it is stopped. Hence, further research is required to extrapolate the proposed solution to full trajectory tracking.

CRediT authorship contribution statement

Unai Izagirre: Writing - original draft, Data curation, Formal analysis, Project administration. **Imanol Andonegui:** Writing - original draft, Data curation, Writing - review & editing, Project administration. **Luka Eciolaza:** Formal analysis, Writing - review & editing, Project administration. **Urko Zurutuza:** Formal analysis, Writing - original draft, Writing - review & editing, Project administration.

Declaration of Competing Interest

The authors declare that they have no known competing financial interests or personal relationships that could have appeared to influence the work reported in this paper.

References

[1] B. Bhushan, Introduction to tribology, John Wiley & Sons, 2013.
[2] I. Bravo-Imaz, H.D. Ardakani, Z. Liu, A. García-Arribas, A. Arnaiz, J. Lee, Motor current signature analysis for gearbox condition monitoring under transient speeds

using wavelet analysis and dual-level time synchronous averaging, Mech Syst Signal Process 94 (2017) 73–84.
[3] J.P. Salameh, S. Cauet, E. Etien, A. Sakout, L. Rambault, Gearbox condition monitoring in wind turbines: areview, Mech Syst Signal Process 111 (2018) 251–264.
[4] M. Cheng, J. Hang, J. Zhang, Overview of fault diagnosis theory and method for permanent magnet machine, Chinese Journal of Electrical Engineering 1 (1) (2015) 21–36.
[5] M. Riera-Guasp, J.A. Antonino-Daviu, G.-A. Capolino, Advances in electrical machine, power electronic, and drive condition monitoring and fault detection: state of the art, IEEE Trans. Ind. Electron. 62 (3) (2014) 1746–1759.
[6] B. Samanta, C. Nataraj, Prognostics of machine condition using soft computing, Robot Comput Integr Manuf 24 (6) (2008) 816–823.
[7] G. Qiao, B.A. Weiss, Advancing measurement science to assess monitoring, diagnostics, and prognostics for manufacturing robotics, International journal of prognostics and health management 7 (Spec Iss on Smart Manufacturing PHM) (2016).
[8] A.C. Bittencourt, S. Gunnarsson, Static friction in a robot jointmodeling and identification of load and temperature effects, J Dyn Syst Meas Control 134 (5) (2012) 051013.
[9] A. Carvalho Bittencourt, Modeling and Diagnosis of Friction and Wear in Industrial Robots, Linköping University Electronic Press, 2014 Ph.D. thesis.
[10] L. Simoni, M. Beschi, G. Legnani, A. Visioli, Friction modeling with temperature effects for industrial robot manipulators, Proceedings of the Intelligent Robots and Systems (IROS), 2015 IEEE/RSJ International Conference on, IEEE, 2015, pp. 3524–3529.
[11] A.C. Bittencourt, E. Wernholt, S. Sander-Tavallaey, T. Brogårdh, An extended friction model to capture load and temperature effects in robot joints, Proceedings of the 2010 IEEE/RSJ International Conference on Intelligent Robots and Systems, IEEE, 2010, pp. 6161–6167.
[12] P. Aivaliotis, K. Georgoulias, G. Chryssolouris, The use of digital twin for predictive maintenance in manufacturing, Int. J. Computer Integr. Manuf. 32 (11) (2019) 1067–1080.
[13] P. Aivaliotis, K. Georgoulias, Z. Arkouli, S. Makris, Methodology for enabling digital twin using advanced physics-based modelling in predictive maintenance, Procedia CIRP 81 (2019) 417–422.
[14] W. Luo, T. Hu, Y. Ye, C. Zhang, Y. Wei, A hybrid predictive maintenance approach for cnc machine tool driven by digital twin, Robot Comput Integr Manuf 65 (2020) 101974.
[15] K. Kokkalis, G. Michalos, P. Aivaliotis, S. Makris, An approach for implementing power and force limiting in sensorless industrial robots, Procedia CIRP 76 (2018) 138–143.
[16] S. Papanastasiou, N. Kousi, P. Karagiannis, C. Gkournelos, A. Papavasileiou, K. Dimoulas, K. Baris, S. Koukas, G. Michalos, S. Makris, Towards seamless human robot collaboration: integrating multimodal interaction, The International Journal of Advanced Manufacturing Technology 105 (9) (2019) 3881–3897.
[17] C. Rodriguez-Donate, L. Morales-Velazquez, R.A. Osornio-Rios, G. Herrera-Ruiz, R.d.J. Romero-Troncoso, FPGA-based fused smart sensor for dynamic and vibration parameter extraction in industrial robot links, Sensors 10 (4) (2010) 4114–4129.
[18] A.A. Jaber, Design of an intelligent embedded system for condition monitoring of an industrial robot, Springer, 2016.
[19] M. Karlsson, F. Hörnqvist, Robot condition monitoring and production simulation, PhD dissertation, Luleå tekniska universitet, 2018.
[20] Y. Zeng, W. Tian, D. Li, X. He, W. Liao, An error-similarity-based robot positional accuracy improvement method for a robotic drilling and riveting system, The International Journal of Advanced Manufacturing Technology 88 (9–12) (2017) 2745–2755.
[21] J.A. Walter, K. Schulten, Implementation of self-organizing neural networks for visuo-motor control of an industrial robot, IEEE Trans. Neural Networks 4 (1) (1993) 86–96.
[22] G. Qiao, B.A. Weiss, Quick health assessment for industrial robot health degradation and the supporting advanced sensing development, J. Manuf. Syst. 48 (2018) 51–59.
[23] G. Qiao, B.A. Weiss, Monitoring, Diagnostics, and Prognostics for Robot Tool Center Accuracy Degradation, Proceedings of the 13th International Manufacturing Science and Engineering Conference, ASME, 2018.
[24] P. Tsarouchi, G. Michalos, S. Makris, G. Chryssolouris, Vision system for robotic handling of randomly placed objects, Procedia CIRP 9 (2013) 61–66.
[25] P. Aivaliotis, A. Zampetis, G. Michalos, S. Makris, A machine learning approach for visual recognition of complex parts in robotic manipulation, Procedia Manuf. 11 (2017) 423–430.
[26] G. Michalos, S. Makris, A. Eytan, S. Matthaiakis, G. Chryssolouris, Robot path correction using stereo vision system, Procedia Cirp 3 (2012) 352–357.
[27] Y. Xu, G. Fang, N. Lv, S. Chen, J.J. Zou, Computer vision technology for seam tracking in robotic gtaw and gmaw, Robot Comput Integr Manuf 32 (2015) 25–36.
[28] M.J. Tsai, H.-W. Lee, N.-J. Ann, Machine vision based path planning for a robotic golf club head welding system, Robot Comput Integr Manuf 27 (4) (2011) 843–849.
[29] C. Chen, Y. Pan, D. Li, S. Zhang, Z. Zhao, J. Hong, A virtual-physical collision detection interface for ar-based interactive teaching of robot, Robot Comput Integr Manuf 64 (2020) 101948.
[30] H. Fang, S. Ong, A. Nee, Interactive robot trajectory planning and simulation using augmented reality, Robot Comput Integr Manuf 28 (2) (2012) 227–237.
[31] S. Garrido-Jurado, R. Munoz-Salinas, F.J. Madrid-Cuevas, R. Medina-Carnicer, Generation of fiducial marker dictionaries using mixed integer linear programming, Pattern Recognit 51 (2016) 481–491.
[32] F.J. Romero-Ramirez, R. Muñoz-Salinas, R. Medina-Carnicer, Speeded up detection of squared fiducial markers, Image Vis Comput 78 (2018) 38–47.
[33] A.E. Conrady, Decentred lens-systems, Mon Not R Astron Soc 79 (5) (1919) 384–390.
[34] G. Bradski, The OpenCV Library, Dr. Dobb's Journal of Software Tools (2000) 2236121.
[35] F. Pedregosa, G. Varoquaux, A. Gramfort, V. Michel, B. Thirion, O. Grisel, M. Blondel, P. Prettenhofer, R. Weiss, V. Dubourg, J. Vanderplas, A. Passos, D. Cournapeau, M. Brucher, M. Perrot, E. Duchesnay, Scikit-learn: machine learning in python, Journal of Machine Learning Research 12 (2011) 2825–2830.

Chapter 9

Publication 2: A Methodology and Experimental Implementation for Industrial Robot Health Assessment via Torque Signature Analysis

applied sciences

MDPI

Article

A Methodology and Experimental Implementation for Industrial Robot Health Assessment via Torque Signature Analysis

Unai Izagirre *, Imanol Andonegui, Aritz Egea and Urko Zurutuza

Electronics and Computer Science Department, Mondragon Unibertsitatea, 20500 Arrasate, Spain; iandonegui@mondragon.edu (I.A.); aegea@mondragon.edu (A.E.); uzurutuza@mondragon.edu (U.Z.)

* Correspondence: uizagirre@mondragon.edu

Received: 21 September 2020; Accepted: 3 November 2020; Published: 6 November 2020

Abstract: This manuscript focuses on methodological and technological advances in the field of health assessment and predictive maintenance for industrial robots. We propose a non-intrusive methodology for industrial robot joint health assessment. Torque sensor data is used to create a digital signature given a defined trajectory and load combination. The signature of each individual robot is later used to diagnose mechanical deterioration. We prove the robustness and reliability of the methodology in a real industrial use case scenario. Then, an in depth mechanical inspection is carried out in order to identify the root cause of the failure diagnosed in this article. The proposed methodology is useful for medium and long term health assessment for industrial robots working in assembly lines, where years of almost uninterrupted work can cause irreversible damage.

Keywords: PHM; industrial robots; Industry 4.0; predictive maintenance

1. Introduction

In recent decades, research in industrial robots focused mainly on improving manufacturing processes, optimizing trajectories, improving accuracy, etc. However, predictive maintenance and health assessment of robots, has not received as much attention [1,2]. From a maintenance point of view, industrial robots are a complex kinematic chain comprised of several mechanical components that have been extensively studied individually: Motors, speed reducers, gears and bearings just to cite some. Notwithstanding, the union of all these components in a single system and its maintenance as a whole, significantly increases the complexity of failure prediction. In general, health assessment techniques for machinery can be classified in two main groups: physical model-based and data-driven [3]. The former uses deterministic mathematical models to describe the expected behavior of a given system and compares this expected behavior with the real behavior. The latter, analyses data captured with sensors and applies statistical and machine learning methods to detect patterns and predict behavior.

Model-based approaches have been widely used to detect failures in industrial components [4–6]. Unfortunately, it is often difficult to implement an analytical model that accurately describes the behavior of such complex systems. In order to build an analytical model of an industrial robot, there are some approximations and assumptions that have to be made such as constant speeds, temperature of the lubricant, loads, etc. [7]. These necessary approximations distance the model from the real behavior of the system, thus data-driven approaches can be more accurate for industrial robot health assessment [1]. In addition, the expansion of the Industrial Internet of Things (IIoT) and Big Data technology in the era of smart manufacturing [8] is pushing the way towards the implementation of reliable data analysis solutions for predictive maintenance.

Data-based monitoring and IoT solutions are rapidly emerging and transforming the manufacturing industry into an industrial Big Data environment [9]. Several research groups have addressed the issue of monitoring the mechanical condition of machine-tools and industrial robots with data-driven approaches [10–13]. Mourtzis et al. [14] developed a holistic framework for milling and CNC machine tool modelling using the OPC-UA communication standard. They implemented a data acquisition device in order to integrate machine-tools without connectivity in their solution. Vogl et al. [15] proposed a multi-sensor system for machine tool axes monitoring and degradation assessment. A.A. Jaber [2] developed an embedded system for industrial robot condition monitoring using accelerometers at the flange of the robot. He detected a mechanical failure in the gears of the robot joints and emphasized the need for more research in the field of robot predictive maintenance. The drawback of using this approach for robots in a real assembly line is that it is hard to isolate external vibrations from vibration caused by the robot's failure. To overcome this issue, acoustic emission sensors were used in [16] to detect a faulty rolling bearing on a welding robot joint. An important issue to take into account with both accelerometers and acoustic emission sensors, is that they are intrusive in the sense that they have to be attached to the structure of the robot. This can be a drawback in real assembly lines because a sudden detachment of one of these sensors could cause either a stop in the production line, or a defect in manufactured products. Lubricant or wear debris analysis is also commonly used for industrial robot joint health assessment. It consist on analysing the wear particles inside the oil that lubricates the joints. As illustrated in [17], any mechanical element working in contact with another mechanical element will deteriorate and degrade regardless of the design. A disadvantage of analysing wear debris in the lubricant is that it needs advanced laboratory equipment and it is highly time consuming. In addition, this method also needs the robot to be completely stationary [18].

According to the author's knowledge, there is only one article that suggests using torque data of industrial robot joints to assess their health status. Bittencourt et al. studied in [12] the feasibility of using torque data for industrial robot and repetitive machinery condition monitoring. However, they did not measure the torque with sensors. Instead, they calculated the torque by estimating it from the electric current. The electric current in the motors is directly proportional to the torque required by each joint. The higher the torque, the more electric current each joint will require. In their study, Bittencourt et al. used kernel density estimates and the Kullback-Leibler distance to detect deviations in the repetitivity of an industrial robot joint's torque [12]. They considered both real data from accelerated wear tests and simulated data. Industrial robots are presently manufactured with a torque sensor installed in each joint and therefore, no additional torque sensor needs to be installed. Moreover, torque data is also useful to monitor and control the energy consumption of the robots. A deteriorated robot joint should require higher torque to accomplish a specific task compared to a healthy robot joint. However, the feasibility of torque sensors to detect medium and long-term mechanical deterioration in industrial robot joints has not been proven and it remains unclear.

The novelty of the paper resides in three main contributions. First, we show the effectiveness of joint torque monitoring to detect motor brake failures inside robot joints. We perform an in depth mechanical inspection to find the root cause of a frequent failure of high payload industrial robots. Second, we emphasize the influence of the standby pose of industrial robots in the reduction of their RUL by analysing a dataset with more than 600 robots. Last but not least, we present and validate a methodology for industrial robot health assessment using torque sensors. The proposed methodology is based on the conclusions extracted from the experiments and the mechanical inspection carried out. The methodology proposed in this paper is applicable to any kind of 6 Degree-of-freedom (DOF) robot with any kind of load. The data is acquired in a non-intrusive way, as torque sensors are located inside the structure of the manipulator.

The manuscript is structured as follows: Section 2 describes the experiment carried out, as well as the obtained results. In Section 3 we perform an in depth root cause analysis of the mechanical fault detected in the experiment. Section 4 analyses a possible cause of the reduction of the remaining useful life of the robots and suggests preventive measures to enlarge their RUL. In Section 5 we propose

a methodology to monitor the health status of industrial robots based on the experiments explained in previous sections, and finally Section 6 sums up the main conclusions and future lines.

2. Experimental Design and Implementation

We designed an experiment to compare the torque applied by a faulty robot joint and a healthy one. If the mechanical wear has a significant effect in the effort of the joint, our hypothesis is that the faulty joint would require higher torque than a healthy joint to execute a given trajectory. Therefore, the methods selected to identify a faulty joint should focus on measuring the increment of the torque applied in the robot joints, whether they are statistical methods or machine learning models. Figure 1 describes the process of the experimental procedure carried out. First, a faulty robot wrist was removed from an automotive assembly line after years of uninterrupted work. The faulty robot caused a sudden stop in the production line and it was replaced by a new one. The experiment was performed using a 6 DOF industrial robot (ABB IRB 6400r), two robot wrists (the faulty wrist and the new one), two loads representing the 15% and 90% of the maximum payload of the robot and four torque sensors, two sensors for each wrist, located in the 5th and 6th joints. These sensors are factory built-in torque sensors and the robotic systems uses them in the control feedback-loop. The ABB IRB 6400r is a widely used industrial robot in the automotive industry with a maximum payload of 200 Kg.

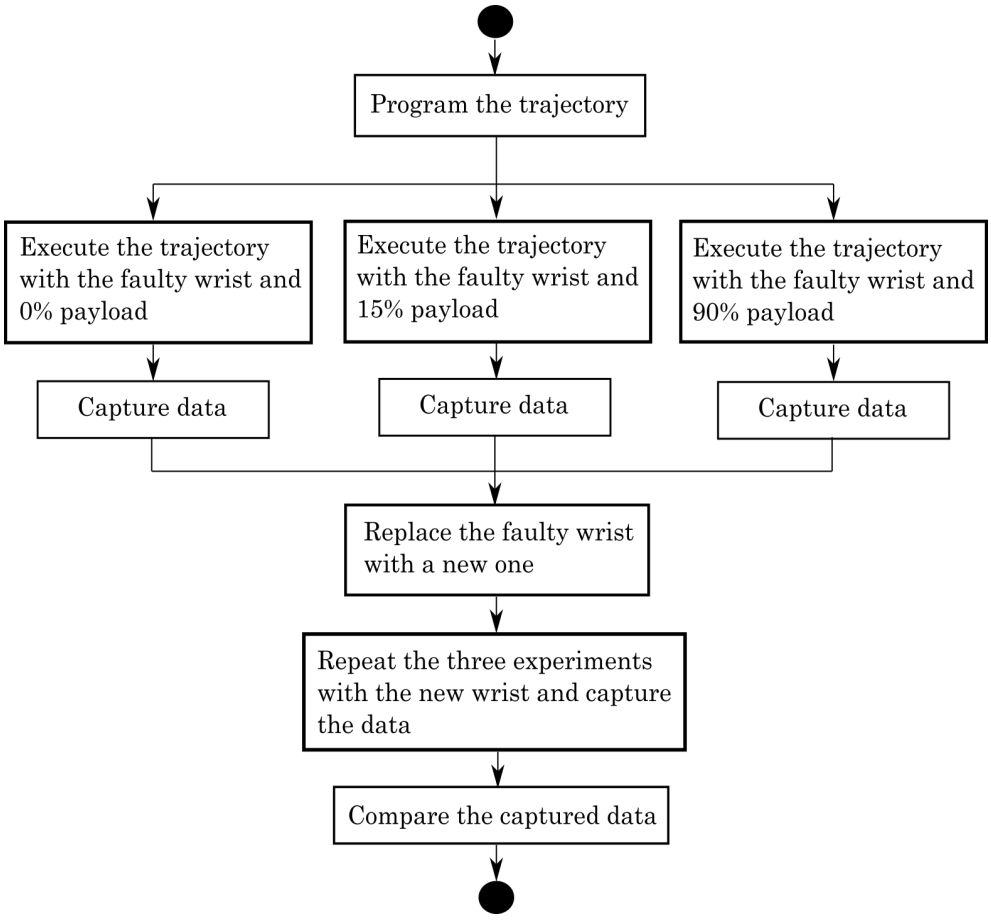

Figure 1. Flowchart of the experimental procedure carried out.

A non-trivial fixed trajectory was programmed in order to excite the robot joints. First of all, the faulty wrist was installed in the ABB robot in a laboratory facility, out of the production line. Then, the programmed trajectory was executed three times with three different loads each time. The loads represented the 0%, 15% and 90% of the maximum payload of the robot. We executed the trajectories and collected the torque data with a sampling rate of 100 ms. Afterwards, the faulty wrist

was removed and the new one installed in the same ABB robot. The trajectory was repeated again three times with the same three different loads in each repetition. Therefore we collected the data of the torque applied in the 5th and 6th joints throughout the six trajectory executions (three with the faulty wrist and tree with the new wrist).

After completing all these trajectories, torque signals were acquired and stored in csv files following the format specified in Table 1. The signals were stored as floating point numbers and using the standard unit (Nm) for the torque. We used the TCP/IP communication protocol to connect with the robot controller and capture the torque signals, which is an Industry 4.0 communication standard. The TCP/IP protocol is suitable for Industry 4.0 and Big Data scenarios, as it is able to interconnect large number of devices [19]. Some researchers have used the OPC-UA communication protocol [9] which is built on top of TCP/IP for data acquisition in industrial scenarios. The data shown in Figures 2 and 3 disclose an evident increment in the torque of the faulty wrist's 5th joint. This increment is clearly appreciable in all the three experiments and throughout the execution of the whole trajectory, therefore the effort required by the motor of the 5th joint was higher than expected with any of the three loads and in any robot pose or movement. In contrast, the torque of the 6th joint does not change significantly in any experiment.

Table 1. Example of the torque data captured by one robot in one experiment e.g., The column name *Torque_joint_5_A* refers to the torque acquired in the 5th joint of robot *A* (faulty robot).

Observation	Time (s)	Torque_Joint_5_A (Nm)	Torque_Joint_6_A (Nm)
1	0	0.819	−1.045
2	0.100	4.08	2.109
3	0.200	9.007	4.323
4	0.300	10.118	6.137
...	...	...	...

The increment in the torque is measured by first calculating the absolute value of the acquired signals. The absolute value of the torque in each joint is then integrated to calculate the total amount of torque applied throughout the whole trajectory in all the experiments. Once the total applied torque is calculated, the percentage of increase between the two wrists is calculated. Tables 2 and 3 show the results of the 5th and 6th joints respectively.

Table 2. Total torque of the 5th joint of the new and faulty wrists. *Load 1*, *Load 2* and *Load 3* represent the 0%, 15% and 90% of the maximum payload respectively.

	New (Nm)	Faulty (Nm)	Increase
Load 1	19,567	42,830	118.88%
Load 2	21,224	46,451	118.86%
Load 3	62,235	124,703	100.37%

Table 3. Total torque of the 6th joint of the new and faulty wrists. *Load 1*, *Load 2* and *Load 3* represent the 0%, 15% and 90% of the maximum payload respectively.

	New (Nm)	Faulty (Nm)	Increase
Load 1	17,910	19,039	6.31%
Load 2	20,852	19,982	−4.17%
Load 3	28,671	28,970	1.04%

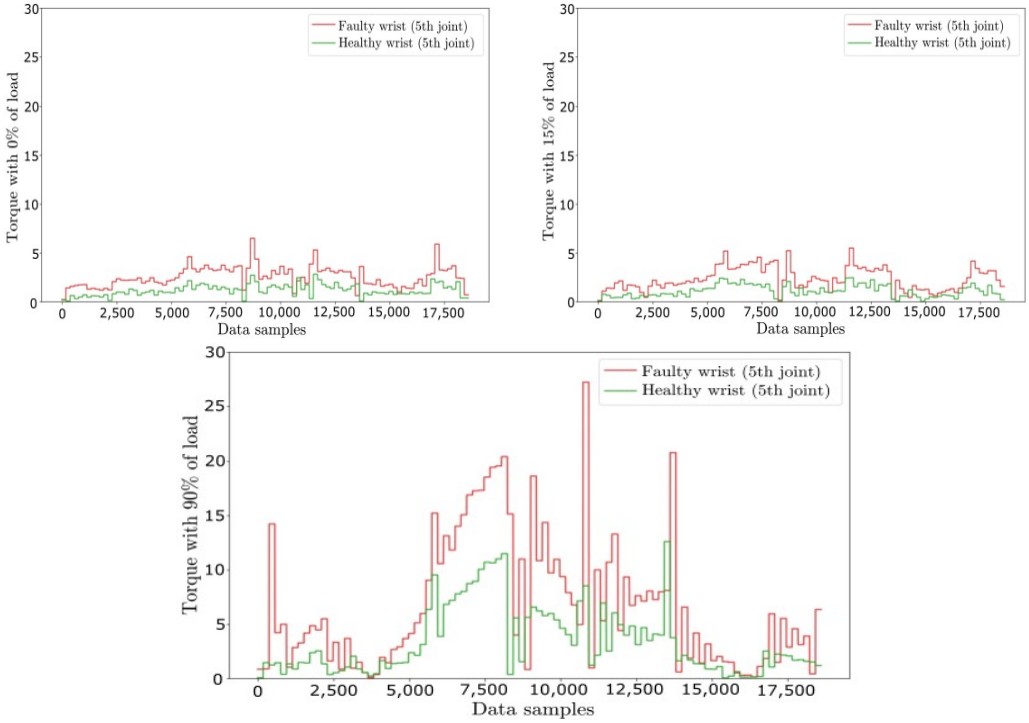

Figure 2. Torque values of the 5th joint in a faulty wrist and in a healthy wrist with different loads and same trajectory.

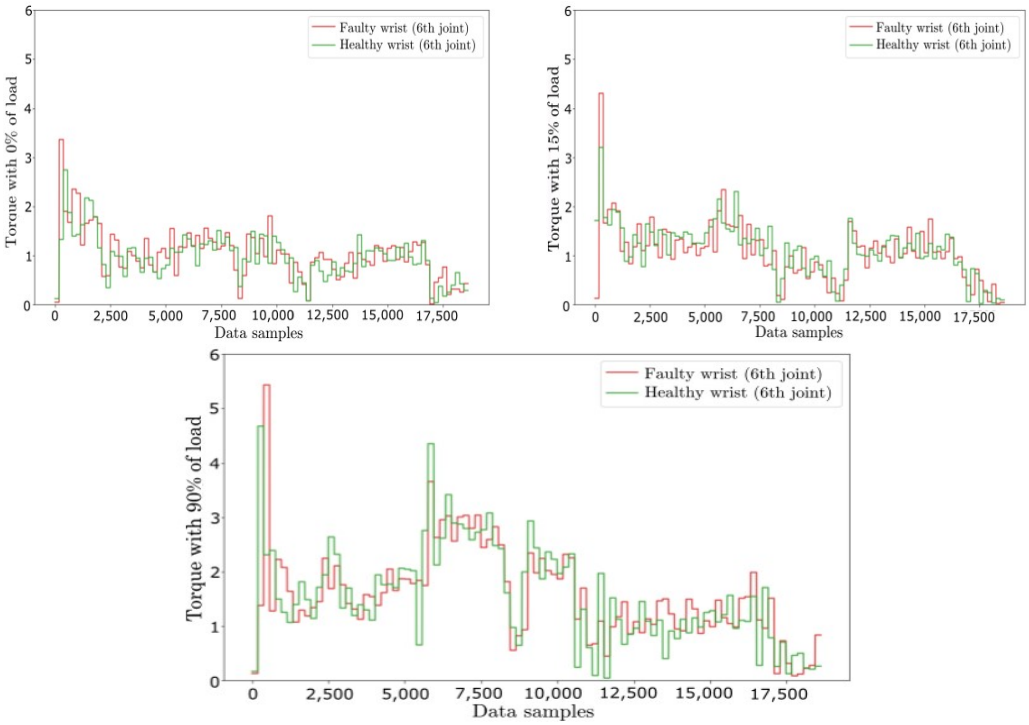

Figure 3. Torque values of the 6th joint in a faulty wrist and in a healthy wrist with different loads and same trajectory.

The increment in the torque is homogeneous, i.e., The torque increases in the whole trajectory and not only in certain movements or positions. The fact that the torque increases in the whole trajectory and not only in certain poses, reveals that the deterioration affects to the entire movement of the joint. The results also show that at the time of the failure, the electric consumption of joint 5 in the faulty wrist was at least twice as high as expected for a healthy joint.

Although the acquired data effectively detects the wear in the joint, the detected increment is not enough on its own to deduce a root cause of the fault. Thence, we conducted a root cause analysis with an in-depth mechanical inspection in order to identify the cause.

3. Root Cause Analysis of the Faulty Joint

3.1. Mechanical Inspection

The first step of the mechanical inspection consisted on disassembling the faulty wrist. The 5th joint of the wrist is composed of an electric motor and a speed reducer. First, we inspected the gears of the speed reducer, shown in Figure 4. We did not find any evidence of wear or pitting in the surface of the gears and there was no apparent damage in the gears that could cause the significant increment detected in the torque. The lubricant oil of the reducer was extracted and analysed in the process of disassembling the faulty wrist. We confirmed that the lubricant was within the quality tolerance limits as no metallic debris was found in the oil.

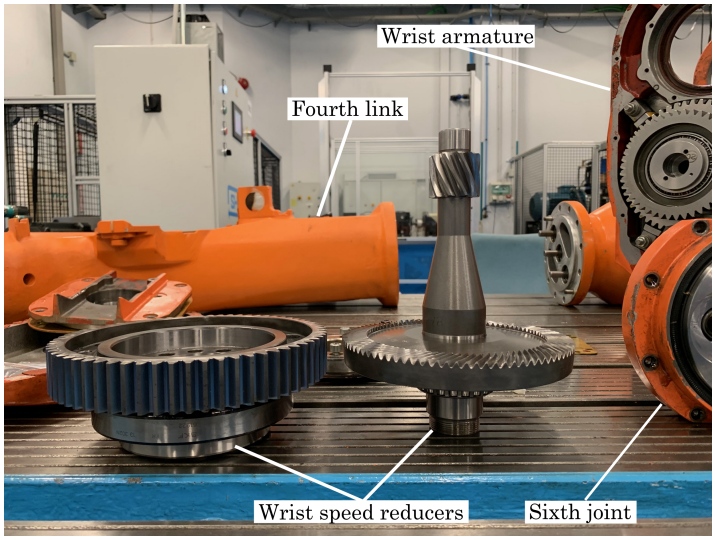

Figure 4. Mechanical inspection of the gears, bearings and motors of the wrist.

Afterwards, we examined the motor of the 5th joint. An increment such as the one detected in the experiment could be caused due to a significant decrease in the motor's coil resistance. We measured the resistance of the coil using an ohmmeter and compared it with the resistance of the coil of a new motor. The resistance values in both coils were identical. Hence, the motor's coil was dismissed as the cause of the joint fault.

3.2. Analysis of the Motor Brake

After analysing the condition of the speed reducer and the motor, we inspected the brake of the motor. The brake of the 5th joint is a permanent magnet brake that stops the motor when the robot is shut down or when an emergency stop is required. As illustrated in the schematic of Figure 5 this kind of brakes have three main parts: a metallic armature, a field coil and a neodymium (NdFeB) permanent magnet. The brake works in the following way: when the robot shuts down or makes an emergency stop, there is no voltage applied to the coil and the permanent magnet attracts the armature, stopping the rotation of the motor. In contrast, if the robot controller applies 24V to the field coil of the brake, it produces a magnetic field compensating the magnetic field created by the permanent magnet and the motor is released.

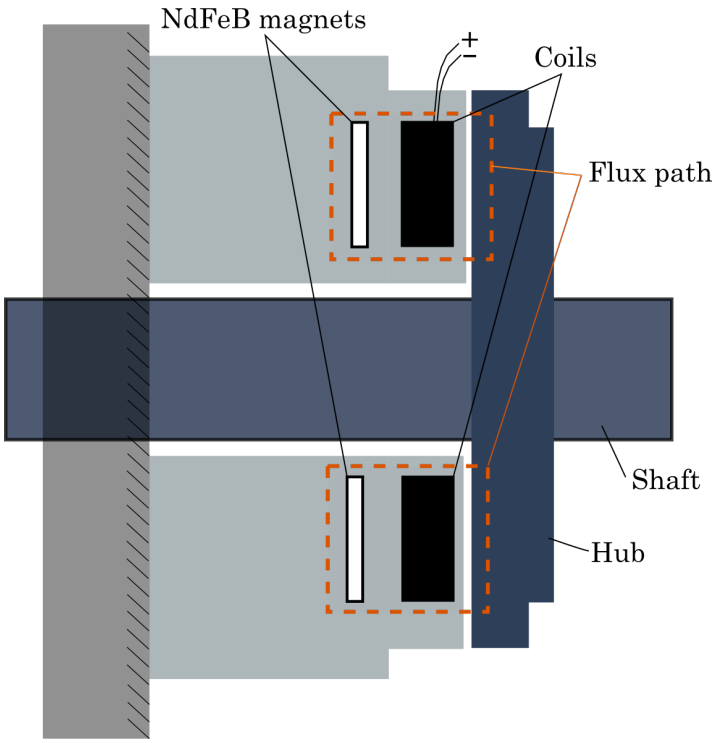

Figure 5. Schematic of the motor brake.

We measured the resistance of the brake's coil and compared it with the resistance of a completely new coil. In both cases the values reached 15.4 Ω. Therefore, the coil of the brake could not be the cause of the detected torque increment.

Finally, we inspected the permanent magnets of the brake. The permanent magnets used in this brake are squared NdFeB magnets. We noticed a slight deformation in the corners of the magnets, as some magnetic particles were detached from them. We found the particles filling the space where the magnets are located. Figure 6 shows the permanent magnets inside the brake of the faulty joint compared to a completely new brake. In addition, Figure 6 shows that the colouring of the brake's armature was changed. These kind of stainless steel armatures, have a metallic light silver colour when manufactured. However, the inspected brake had a reddish coloring as a consequence of oxidation.

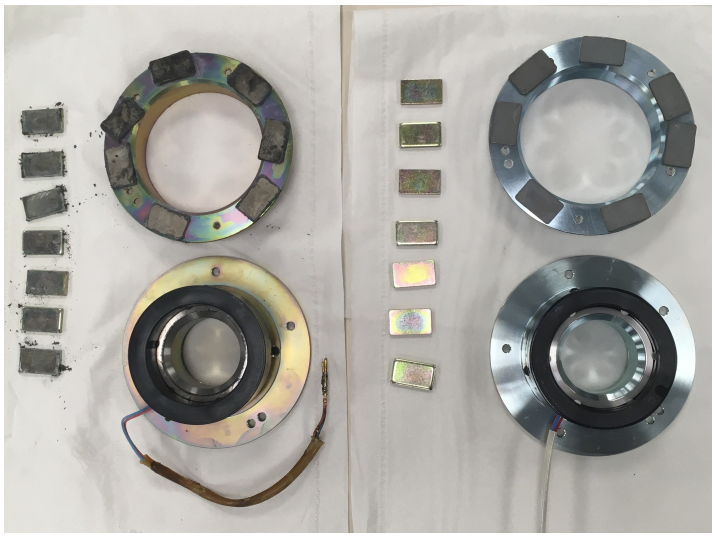

Figure 6. The motor brake of the faulty joint and its permanent magnets (**left**) compared to a completely new motor brake (**right**).

We performed two tests to diagnose the health status of the permanent magnets. The first test consisted on measuring the M(H) hysteresis curve of the magnets. Then, we magnetized the permanent magnets and measured again the M(H) hysteresis curve after the magnetization. The results of the tests are shown in Figure 7.

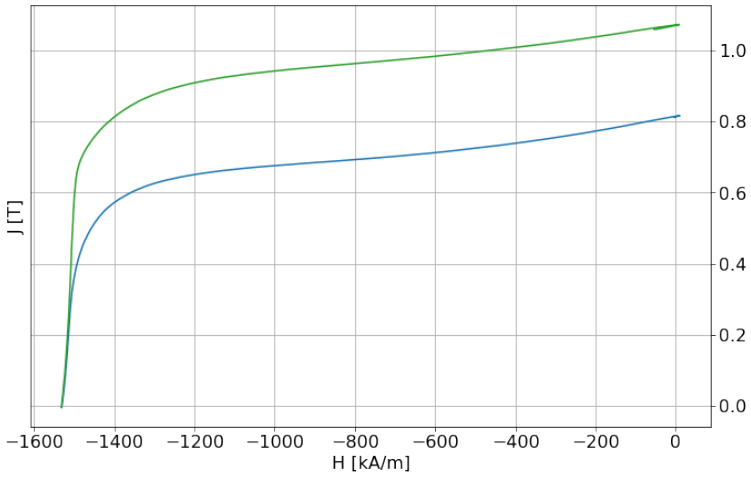

Figure 7. Magnetic hysteresis curve of the motor brake's permanent magnet before (blue) and after (green) magnetization.

There is a 24% loss from 0.814 T before magnetization to 1.071 T after the magnetization. This significant magnetic field loss has a direct impact in the malfunction of the motor's brake. As a consequence, the brake constantly resists the movement of the motor. This produces the torque increment in the 5th joint throughout the whole trajectory identified in Section 2.

The second test consisted on measuring the magnetic hysteresis curve at different temperatures. Figure 8 shows the different M (H) curves at 26, 80, 100 and 120 °C and Table 4 shows the magnetic properties of the permanent magnet at these temperature regimes. Br (T) is the residual induction or flux density, that is the magnetic induction corresponding to zero magnetizing force in a magnetic material after saturation. Hci (kA/m) is the intrinsic coercive force of a material and indicates its resistance to demagnetization.

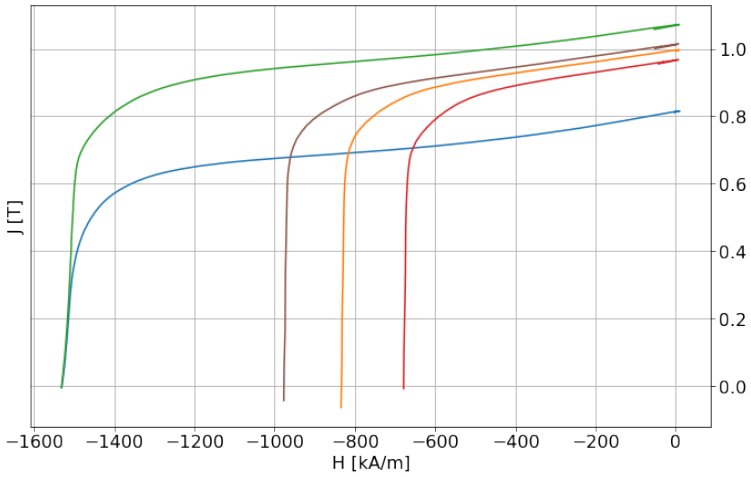

Figure 8. Magnetic hysteresis curve of the permanent magnet at 26 (green), 80 (brown), 100 (orange) and 120 °C (red).

Table 4. Magnetic properties of the permanent magnet at the measured temperatures.

T (°C)	Br (T)	Hci (kA/m)
26	1.071	1531
80	1.013	976.9
100	0.9957	833.4
120	0.9668	678.5

There are two additional considerations that have to be taken into account. The technical specifications of the 5th joint's motor indicates that the surface temperature of the motor can reach up to 140 °C. Therefore, the temperatures inside the motor brake could be even higher than the temperatures reached in the test. Moreover, in the recently published work by M. Haavisto [20] the time dependent demagnetization of NdFeB permanent magnets is extensively investigated. She experimentally proved that this type of magnets can be demagnetized if exposed to higher than 80 °C for a long period of time. This conclusion is especially relevant for industrial robots working in assembly lines for years uninterruptedly.

These results of the tests, the mechanical inspection carried out, the state of the motor brake, as well as the previously mentioned PhD dissertation [20], give us enough evidence to conclude that the temperatures inside the motor of the 5th joint of the robot, reached high enough temperatures for sufficient time to produce a magnetization loss in the permanent magnets of the motor brake. This caused the failure in the wrist and the increased torque values shown in Section 2.

4. The Influence of the Standby Pose in Robot Failures

In real automotive manufacturing production lines, there is substantial difference in the waiting and working time of the robots depending on their process and location. Some of them execute trajectories almost uninterruptedly, while others spend most of the time waiting. The most active robots work approximately 85% of the total operative time and the most inactive robots only around 20%.

In the previous section, we identified the root cause of the wrist failure in the demagnetization of the motor magnets. This demagnetisation, as well as the oxidation of the brake, is produced by a relatively high temperature prolonged over long periods of time. In this section, we analyse two factors that strongly influence the overheating in industrial robot wrists: the pose in which the robots wait for the next product and the load they carry.

We collected a dataset with more than 600 robots of a real manufacturing assembly line to analyze the influence of the load and the waiting pose in robot wrist failures. The information stored in the dataset was structured in three columns: the mechanical failures of the 5th joint in the last 15 years (57 failures in total), the load of the robots and the orientation of their 5th joint. The orientation of the 5th joint represents the verticality of the joint. As illustrated in Figure 9 if the joint is completely vertical to the ground, the orientation will have a value of 0 and if the joint is completely horizontal to the ground, the value of the orientation will be 90. Therefore, when we talk about the orientation, we are refering to the verticality of the 5th joint when the robot waits stationary for the next product.

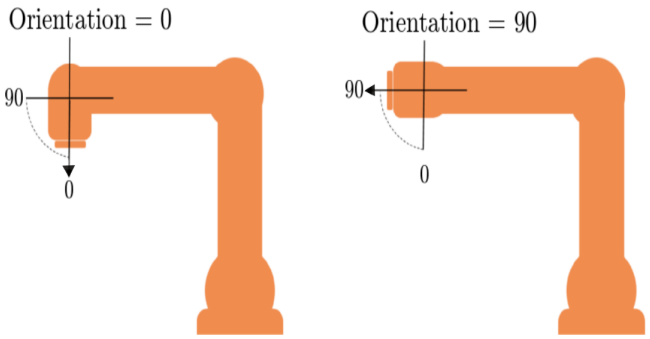

Figure 9. Orientation value in the dataset represents the *verticality* or *horizontality* of the 5th joint.

Figures 10 and 11 show the difference in distribution in the load and standby orientation of the 5th joint of more than 600 industrial robots. The boxplots are grouped by robots that never had a mechanical failure in that joint (0) and robots that did fail (1). These boxplots show that robots that had a failure in the 5th joint tend to work with higher loads and hold the load in a more horizontal pose. The differences in the load and orientation are shown in Table 5. There is a difference of 29.71 Kg in the mean of the load between the robots that have failed and the robots that have not failed yet. The mean of the standby orientation of the 5th joint is 9.17 ° closer to the parallel of the ground for robots that have failed.

These results show that both the carried load and the orientation of the 5th joint while waiting have a significant impact in the RUL of industrial robot wrists. The fifth joint of the robot requires more effort to hold a heavier load and to hold a given load in a more horizontal orientation. Thus, this effort results in a higher torque that the motor must apply, which increases the current in the motor coil and the temperature of the motor.

Table 5. Standby orientation and load means with recorded historical failures and without failures.

	Orientation (°)	Load (Kg)
With failure	71.39	148.5
Without failure	62.22	118.79

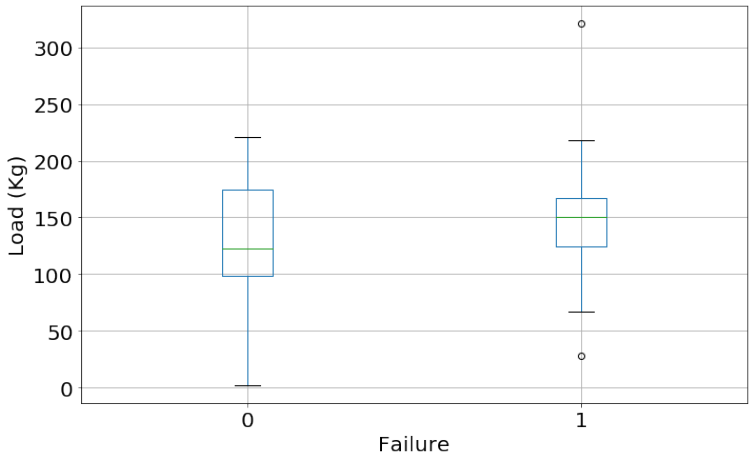

Figure 10. Mean load of robots without recorded failures (0) and with failures (1).

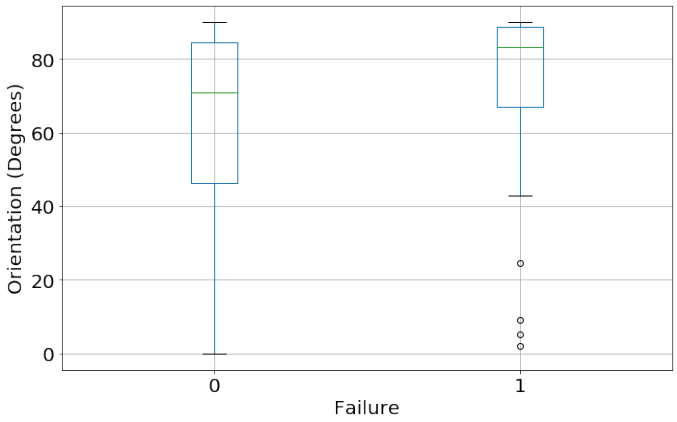

Figure 11. Mean standby orientation no recorded failures (0) and with failures (1).

5. The Health Assessment Program Methodology

Based on the results of the previous sections, we propose a methodology for diagnosing the health status of industrial robot joints with torque signature analysis. The diagram representing the methodology can be seen in Figure 12. The main idea behind the proposed methodology is that a joint that suffers a mechanical degradation will require higher torque to execute a certain trajectory than a healthy one. As the time goes by, the mechanical elements attached to the motor (i.e., The brake and the reducer) will inevitably suffer mechanical deterioration. This will require higher effort to execute the same trajectory. To illustrate the methodology, let's say that a robot R_1 executes a certain program P_1 and needs to apply torque T_1 in a joint to complete the trajectory. If there is any mechanical deterioration, the system will be less efficient, but the robot controller will make sure that this deterioration does not affect the accuracy of the robot. Even if the accuracy remains invariant, to finish the same program P_1 the required torque now (T_2) will be higher than before ($T_2 > T_1$).

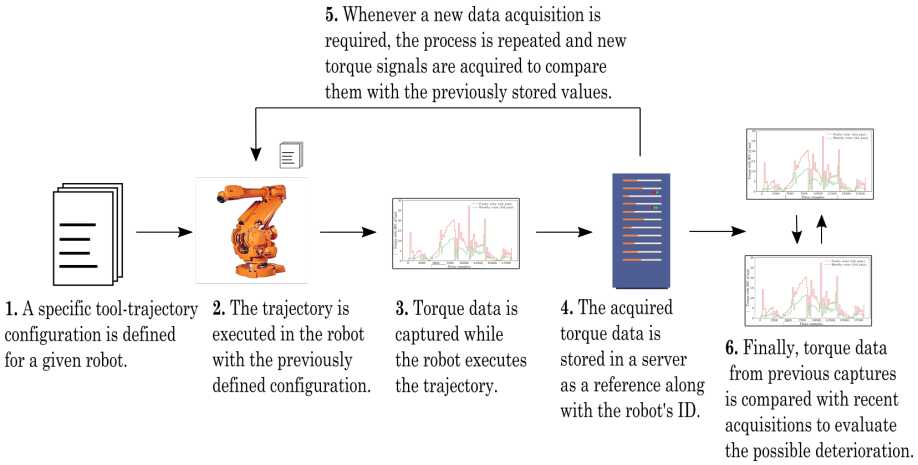

Figure 12. Diagram of the proposed methodology. First, the trajectory and tool are defined. Then, the program is executed and torque data is acquired. The recorded data is stored in a server as a reference along with the robot's ID. The process is periodically repeated and the new signals are compared with previously recorded ones to diagnose a possible deterioration.

We therefore propose to use a specific trajectory-tool combination in the robots of the production line to assess their current health status. As described in the diagram of Figure 12 robots will execute a predefined non-trivial trajectory with a known load and they will require a certain amount of torque in each joint to complete this trajectory. To acquire torque data in all the joints, the trajectory must use the whole set of joints comprising the robot manipulator. We will call *Health Assessment Program* (*HAP*) to that predefined trajectory-load combination. These two specifications will always have to

remain unchanged in order to make a fair comparison of the results. However, an advantage of the methodology is that the precise shape, center of mass and inertia of the load are not required to be known or modeled.

The first step is to execute the trajectory with the robot attaching the corresponding load. The torque of each joint will be recorded during the the whole process, producing a digital *signature* of the torque of each joint. This initial torque data or *signature* will be used as a reference for that particular robot. This initial data will be stored with an identification number of the robot. Whenever we want to analyse the mechanical deterioration of the joints of that robot, we will run the *HAP* again and compare the previously stored values with the recently acquired ones. If there is no change in the torque values, we can conclude that there is no significant mechanical deterioration in the joints yet. In contrast, if there is some increase in the torque of a certain joint, it will mean that the motor of that joint is requiring more effort than expected.

The proposed methodology is applicable to any joint or industrial robot. In addition programming the *HAP* as an additional trajectory to the usual routine of the robots is enough. It is not necessary to take the robot off the production line to diagnose it. Which is a significant advantage compared to existing condition monitoring techniques.

6. Discussion and Conclusions

We reported a methodology for industrial robot health assessment. The methodology was validated experimentally comparing the torque of two robot wrists. These results show that torque sensors provide reliable information to detect mechanical deterioration of an industrial robot's joint. We carried out the comparisons with different loads and the increment in the torque was clearly appreciable with the three tested loads. Therefore, the methodology is proved to be useful with any load configuration. The recorded torque data shows an homogeneous increase in the faulty wrist. The source of the malfunction was located in the permanent magnets of the motor brakes with an in depth mechanical inspection. We measured the magnetic field of the permanent magnets and the hysteresis curves showed a 24% of magnetic field loss in the permanent magnets of the faulty joint. The effect of this magnetic field loss can be effectively detected with the proposed methodology.

A direct conclusion of the work is that the electrical consumption of the faulty joint was approximately twice that of a healthy joint. Therefore, even if a robot does not show any apparent malfunction it might still be working in conditions which are far from ideal due to mechanical deterioration and fatigue. The proposed method could help manufacturers to monitor not only the mechanical condition of the robot joints but also the electrical over-consumption i.e., Detecting the most energy-consuming robots or work cells. Controlling the energy consumption of robots is a fundamental factor to achieve sustainable factories and to reduce pollution.

Another significant advantage of the methodology is that torque measurement is done inside the robot's physical structure. As we mentioned in the introduction, if a sensor or a wire installed in the outside part of the robot's structure detaches and falls into the production line, it could cause significant damage to the product being manufactured or even stop the production line. Therefore, since torque sensors are inside the robot's physical structure, this possible inconvenience is dismissed. Last but not least, the methodology is applicable to any industrial robot, as long as the acquired data is compared with robots of the same model. Hence, our approach does not depend on the robot manufacturer or the robot type. It only depends on the programmed trajectory and the carried load, which are both configurable by researchers and practitioners.

A limitation of the presented work is that the detection of torque deviation depends on a pre-defined tool and trajectory configuration. Therefore, if either of these two characteristics change, torque signals would also inevitably change and the data regarding the monitored robot should be readjusted. Another limitation of the presented work is that the execution of the *Health Assessment Program* requires the robot to momentarily stop its normal production behavior to execute a pre-defined trajectory and acquire the correct torque signals.

An identified future line of work is to implement machine-learning models to detect anomalies in the torque of robot joints with different tool and trajectory configurations. Although our approach requires a specific trajectory and tool configuration for the data to be comparable, a machine-learning model might be flexible enough to detect deviations with different trajectory and tool configurations and extrapolate the behavior learned in one use case to the rest. Another interesting future line of work would be to use the proposed methodology to train predictive models to estimate the RUL of industrial robots in real production line conditions. Our methodology effectively detects deviations from the normal behavior of robot joints in real world scenarios, but further research is needed to accurately assess the RUL of the monitored robotic systems. Finally, torque data monitoring could also be used to find an optimal standby pose of industrial robots in order to minimize the effort of the joints. Based on the observed influence of the waiting pose in the wrist failures (Section 4). An optimal standby pose for a given robot model and tool, could minimize the effort and thus torque and temperature of the joints, increasing their RUL and optimizing the energy consumption.

Author Contributions: Conceptualization, U.I., I.A. and U.Z.; methodology, U.I. and I.A.; software, U.I. and A.E.; validation, I.A., A.E. and U.Z.; formal analysis, U.I. and A.E.; investigation, U.I.; resources, I.A. and U.Z.; data curation, U.I.; writing—original draft preparation, U.I.; writing—review and editing, U.I., I.A. and U.Z.; visualization, U.I. and A.E.; supervision, I.A. and U.Z.; project administration, I.A. and U.Z.; funding acquisition, I.A. and U.Z. All authors have read and agreed to the published version of the manuscript.

Funding: Unai Izagirre, Imanol Andonegui and Urko Zurutuza are part of the Intelligent Systems for Industrial Systems research group of Mondragon Unibertsitatea (IT886-16), supported by the Department of Education, Universities and Research of the Basque Country.

Conflicts of Interest: The authors declare no conflict of interest. The funders had no role in the design of the study; in the collection, analyses, or interpretation of data; in the writing of the manuscript, or in the decision to publish the results.

References

1. Qiao, G.; Weiss, B.A. Advancing measurement science to assess monitoring, diagnostics, and prognostics for manufacturing robotics. *Int. J. Progn. Health Manag.* **2016**, *7*. [CrossRef]
2. Jaber, A.A. *Design of an Intelligent Embedded System for Condition Monitoring of an Industrial Robot*; Springer: Berlin/Heidelberg, Germany, 2016.
3. Peng, Y.; Dong, M.; Zuo, M.J. Current status of machine prognostics in condition-based maintenance: A review. *Int. J. Adv. Manuf. Technol.* **2010**, *50*, 297–313. [CrossRef]
4. Qin, Y. A new family of model-based impulsive wavelets and their sparse representation for rolling bearing fault diagnosis. *IEEE Trans. Ind. Electron.* **2017**, *65*, 2716–2726. [CrossRef]
5. Blancke, O.; Tahan, A.; Komljenovic, D.; Amyot, N.; Hudon, C.; Lévesque, M. A hydrogenerator model-based failure detection framework to support asset management. In Proceedings of the 2016 IEEE International Conference on Prognostics and Health Management (ICPHM), Ottawa, ON, Canada, 20–22 June 2016; pp. 1–6.
6. Dalla Vedova, M.D.; Germanà, A.; Berri, P.C.; Maggiore, P. Model-Based Fault Detection and Identification for Prognostics of Electromechanical Actuators Using Genetic Algorithms. *Aerospace* **2019**, *6*, 94. [CrossRef]
7. Bittencourt, A.C. Modeling and Diagnosis of Friction and Wear in Industrial Robots. Ph.D. Thesis, Linköping University Electronic Press, Linköping, Sweden, 2014.
8. Tao, F.; Qi, Q.; Liu, A.; Kusiak, A. Data-driven smart manufacturing. *J. Manuf. Syst.* **2018**, *48*, 157–169. [CrossRef]
9. Mourtzis, D.; Vlachou, E.; Milas, N. Industrial Big Data as a result of IoT adoption in manufacturing. *Procedia CIRP* **2016**, *55*, 290–295. [CrossRef]
10. Sun, X.; Jia, X. A fault diagnosis method of industrial robot rolling bearing based on data driven and random intuitive fuzzy decision. *IEEE Access* **2019**, *7*, 148764–148770. [CrossRef]
11. Borgi, T.; Hidri, A.; Neef, B.; Naceur, M.S. Data analytics for predictive maintenance of industrial robots. In Proceedings of the 2017 International Conference on Advanced Systems and Electric Technologies (IC_ASET), Hammamet, Tunisia, 14–17 January 2017; pp. 412–417.

12. Bittencourt, A.C.; Saarinen, K.; Sander-Tavallaey, S.; Gunnarsson, S.; Norrlöf, M. A data-driven approach to diagnostics of repetitive processes in the distribution domain—Applications to gearbox diagnostics in industrial robots and rotating machines. *Mechatronics* **2014**, *24*, 1032–1041. [CrossRef]
13. Vallachira, S.; Orkisz, M.; Norrlöf, M.; Butail, S. Data-driven gearbox failure detection in industrial robots. *IEEE Trans. Ind. Inform.* **2019**, *16*, 193–201. [CrossRef]
14. Mourtzis, D.; Milas, N.; Athinaios, N. Towards machine shop 4.0: a general machine model for CNC machine-tools through OPC-UA. *Procedia CIRP* **2018**, *78*, 301–306. [CrossRef]
15. Vogl, G.W.; Calamari, M.; Ye, S.; Donmez, M.A. A sensor-based method for diagnostics of geometric performance of machine tool linear axes. *Procedia Manuf.* **2016**, *5*, 621–633. [CrossRef]
16. Liu, X.; Wu, X.; Liu, C.; Liu, T. Research on condition monitoring of speed reducer of industrial robot with acoustic emission. *Trans. Can. Soc. Mech. Eng.* **2016**, *40*, 1041–1049. [CrossRef]
17. Bhushan, B. *Introduction to Tribology*; John Wiley & Sons: Hoboken, NJ, USA, 2013.
18. Ebersbach, S.; Peng, Z.; Kessissoglou, N. The investigation of the condition and faults of a spur gearbox using vibration and wear debris analysis techniques. *Wear* **2006**, *260*, 16–24. [CrossRef]
19. Wang, L.; Wang, G. Big data in cyber-physical systems, digital manufacturing and industry 4.0. *Int. J. Eng. Manuf. (IJEM)* **2016**, *6*, 1–8.
20. Haavisto, M. Studies on the Time-Dependent Demagnetization of Sintered NdFeB Permanent Magnets. 2013. Available online: https://trepo.tuni.fi/handle/10024/115203 (accessed on 13 April 2020).

Chapter 10

Publication 3: Torque-based methodology and experimental implementation for industrial robot standby pose optimization

The International Journal of Advanced Manufacturing Technology (2020) 111:2065–2072
https://doi.org/10.1007/s00170-020-06234-5

ORIGINAL ARTICLE

Torque-based methodology and experimental implementation for industrial robot standby pose optimization

Unai Izagirre[1] · Gautier Arcin[2] · Imanol Andonegui[1] · Luka Eciolaza[1] · Urko Zurutuza[1]

Received: 16 April 2020 / Accepted: 9 October 2020 / Published online: 22 October 2020

Abstract

This manuscript reports on a novel methodology and experimental implementation for industrial robot standby pose optimization. First, we analyze the influence of the standby pose of robots in the reduction of their useful life by conducting a preliminary study in an automotive assembly line. Afterwards, we propose a novel methodology to optimize the standby pose of industrial robots by minimizing the torque applied in the joints. The results show that the methodology can reduce by 31.37% the average torque applied by a 200-kg-payload, 6 degree-of-freedom industrial robot in normal production conditions. In addition, we demonstrate that the methodology is robot model and tool invariant, by implementing the presented solution in a Kuka KR3 and two ABB IRB 6400r robots with different tools. The benefits of optimizing the standby pose of industrial robots in manufacturing assembly lines are twofold. First, it reduces the stress and temperature of the joints, increasing the remaining useful life. Second, it offers the possibility of substantially reducing the energy consumption of the production line, as the time spent by industrial robots in a standby pose can reach up to 80% of their total operational time.

Keywords Pose optimization · PHM · Industrial robots · Genetic algorithms · Sustainable manufacturing

1 Introduction

Industrial robots have been used for decades in the manufacturing industry. The efficiency and accuracy of these complex systems have improved substantially and their high repeatability and robustness are enabling the automatization of more industrial processes year by year. However, like any other machine, industrial robots are prone to failure regardless of their robustness. These failures usually occur after years of normal operational behavior and are difficult to predict due to the complexity and non-linearity inherent in robotic systems. The complexity of industrial robots and the low frequency of failures make it difficult to precisely address the root cause of a certain failure and to establish standards for robot condition monitoring. However, there are some known factors that negatively affect the Remaining Useful Life (RUL) of industrial robots.

The overheating of robot joints is one of the most common sources of failure. A relatively high temperature in the motor of a joint over a long period can produce a motor brake failure. Thus, controlling the temperature of the joints is a key maintenance measure for industrial robots, especially for those subjected to very demanding working regimes.

There are three main methods to reduce the temperature of industrial robot joints: decreasing the weight of the tool, optimizing the trajectory (e.g., reducing the speed), or optimizing the standby pose. In this article, we will focus on the third method. The standby pose is the stationary pose of the robots when they wait for the next product in an assembly line. While the robots wait, the motors inside the joints apply torque to hold the tool in the pose they are programmed to. Depending on the pose and the tool, the amount of torque applied by each joint will be different. Minimizing the total torque applied in a standby pose reduces both the temperature of its joints and the total electric consumption.

Sustainability has not been considered in the optimization of industrial processes until very recently. However, in

✉ Unai Izagirre
uizagirre@mondragon.edu

[1] Electronics and Computer Science department, Mondragon Unibertsitatea, Mondragón, Spain

[2] Système Robotiques et Interactifs, UPSSITECH, Toulouse, France

the last few years, there is an increasing urge to reduce the electric consumption in factories and turn the industry into a more sustainable sector. In this context, the optimization of robot trajectories to reduce the energy consumption is a growing research field. Paes et al. [9] presented a systematic methodology for an energy-optimal path planning in an ABB industrial robot. They also addressed the need for further research to integrate the standby pose of the robots in the optimization procedure. Brossog et al. [1] proposed a dynamic model for a 6 degree-of-freedom (DoF) industrial robot working in an assembly line and analyzed its power consumption as well as its dynamic behavior. They also surveyed in Brossog et al. [2] the state of the art in industrial robot energy consumption and concluded that most of the contributions propose predictions based on simulation models. Gadaleta et al. [4] conducted an in-depth review of the state-of-the-art concerning eco-design and eco-programming methods in industrial robots. However, according to the authors' knowledge, all the contributions that minimize energy consumption in robotic systems focus on trajectory optimization.

Unfortunately, the reality of manufacturing assembly lines is not as flexible as research laboratories. In real assembly lines, every robot has to execute a defined trajectory in its working cell. Therefore, the constraints of the work carried out in each station might not always permit optimizing the trajectory to its maximum extent. In addition, even though industrial robots spend a substantial portion of the total operational time waiting stationary in the work cell and consuming energy meanwhile, the standby pose optimization has not received much attention from researchers or practitioners. Recent contributions analyze the impact of the pose in the stiffness of the robotic system. Xiong et al. [12] proposed a stiffness-based pose optimization of an industrial robot for five-axis milling. Lin et al. [5] presented a robot pose optimization methodology based on robotic performance indexes. Torque fluctuation minimization and force balancing have also been extensively addressed. Zhang and Chen [14] minimized the torque fluctuation using a simple PD controller and a mass redistribution scheme by optimizing the design variables of the feedback control gains and the dimensions of links. Ouyang and Zhang [8] adjusted the kinematic parameters (AKP) to minimize the torque fluctuation and the joint forces. They demonstrated that the *AKP* was ently better than other force balancing methods such as the *counterweights*. However, regarding failure prediction and RUL estimation, there is no research contribution that studies the influence of the standby pose in industrial robot failures.

In this manuscript, we implement genetic algorithms to optimize the pose of industrial robots by acquiring online internal torque data. Genetic algorithms have been widely used for the optimization of industrial processes. These algorithms are simple to implement and efficient for multivariate optimization problems. Fleming and Chipperfield [3] extensively studied the applicability of genetic algorithms in engineering, specially in job shop scheduling, robotics, and aerodynamics. Mitra and Gopinath [7] implemented a multiobjective genetic algorithm for an industrial grinding operation. Man et al. [6] focused in the applicability of genetic algorithms for control and signal processing. Yıldız [13] proved the effectiveness of genetic algorithms for the optimization of milling operations. Recently, Wang et al. [11] optimized the torque of a robot joint using genetic algorithms in the context of building a cost-effective haptic system, comprising a haptic environment and its corresponding robot.

As mentioned above, although the optimization of robot trajectories is a growing research field, the standby pose of industrial robots in real production environments has been largely omitted by researchers and practitioners. The lack of studies that reflect the impact of the standby pose in reducing the RUL of industrial robots might be a plausible cause for this gap. Therefore, the objective of our work is, on the one hand, to emphasize the importance of the standby pose in the reduction of the RUL and, on the other hand, to offer a practical pose optimization solution that can be applied regardless of the robot model or the attached tool in real-world scenarios. Apart from decreasing the RUL, optimizing the standby pose of heavy payload industrial robots could significantly reduce the overall energy consumption of highly automated assembly lines, e.g., in the automotive or aeronautical industry.

In Section 2, we motivate our contribution by explaining the importance of optimizing the standby pose of industrial robots in manufacturing assembly lines. Section 3 describes the infrastructure of the experiment and the implemented optimization algorithm. We present the results of the experiment in Section 4; and in Section 5, we show the actual torque optimization potential in a real automotive manufacturing assembly line. Finally, Section 6 summarizes the conclusions and proposes future lines of work.

2 Motivation

The optimization of the standby or waiting pose consists of finding the optimal stationary pose in which the robots wait for the next product in an assembly line. The optimal pose depends on the robot model and the attached tool. In our case, we will use the torque applied in each joint of the robot to measure the effort of the joints. The objective of the optimization algorithm will therefore be to minimize the total torque applied in the joints when the robots are stationary. In real manufacturing assembly lines, industrial

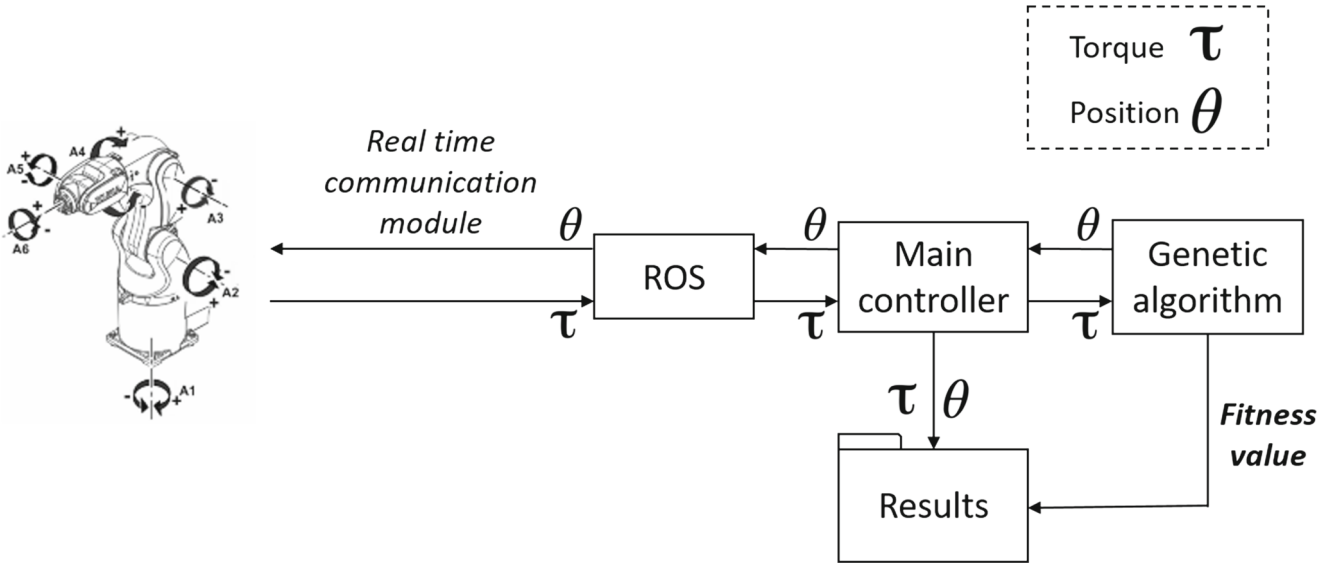

Fig. 1 Diagram of the data acquisition modules

robots spend between 20 and 80% of the total operational time waiting in a stationary or standby pose for the next product, depending on their work regime. However, both researchers and practitioners have paid little attention to the efficiency of the standby pose of industrial robots and much more to the efficiency of the trajectories. In this section, as well as in Section 5, we will emphasize the importance of optimizing the robot pose in real industrial environments.

There are two main reasons to optimize the standby pose of industrial robots. First, there is a significant electric consumption saving potential. As a consequence of the climate crisis, there is an increasing need to reduce energy consumption in industry. As the use of robots in manufacturing production lines increases, it is necessary to develop and implement methods that minimize the electrical consumption of these systems. By minimizing joint torque, the motors inside the joints require less electric current to hold a stationary pose. As a result, the total electric consumption of assembly lines could be significantly reduced, especially in highly automated factories, e.g., automotive body shop assembly lines.

The second reason is to increment the useful life of industrial robots. If the effort of a joint is reduced, the electric current of its motor and thus its temperature will also decrease. The temperature directly affects the useful life of the components inside the joints, such as the permanent magnets of the brakes and the wires of the coils (Fig. 1).

We conducted a preliminary study by collecting the historical failure data of 621 industrial robots in a real automotive production line to illustrate the importance of the standby pose in robot failures. The data collected consists of the pose of robot joints while being stationary and information about whether the robot had a failure in a particular joint or not. In Table 1, we show the difference in the mean standby orientation of the fifth joint of all the robots. The data in the first row corresponds to robots that have failed in the fifth joint and the second row corresponds to robots that have never failed. We measured the orientation in degrees, which ranges between 0° and 90°. Figure 2 shows and schematic of an industrial robot wrist (5th and 6th joints) and a representation of the angles used in the study. As shown in the figure, 0° represents absolute verticality to the ground in the 5th joint and 90° represents total horizontality to the ground.

Table 1 Standby orientation mean with recorded historical failures and without failures

	Orientation of the 5th joint (°)
With failure	71.39
Without failure	62.22

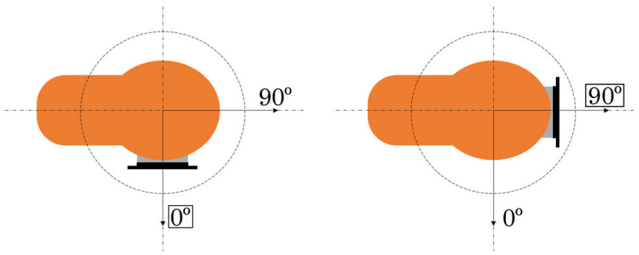

Fig. 2 Schematic of the 5th and 6th joints (wrist) of a robot and the corresponding degrees used to represent the verticality and horizontality of the 5th joint

These preliminary results show that robots waiting in a standby pose closer to the horizontal plane with reference to the ground tend to fail more frequently in the 5th joint than robots whose stationary pose is closer to the vertical plane.

3 Experimental implementation

We optimized the standby pose of a Kuka KR3 robot and implemented The Robot Operating System (ROS) [10] as a communication and control interface between the robot and a laboratory computer. We used real-time communication with a frequency of 12 ms in order to ensure a reliable data acquisition process. The genetic algorithm was developed from scratch with the Python programming language. The architecture of the data acquisition process is shown in Fig. 1.

The experimental process starts by defining a set of 40 random joint angles (the initial population) in the Genetic algorithm module. These angles are sent to the main controller, which moves the robot to the first random pose and waits until the movement has finished. When the robot reaches the desired pose, the controller waits approximately half a second for the robot to stabilize, and then it captures the torque of all the six joints for another half a second. We calculate the median of the captured torques in each joint to eliminate non-Gaussian noises, frequent in non-linear and dynamic industrial machinery. These torque values are stored in a file alongside the angles of the joints and the scored fitness value. The fitness value is calculated based on the total torque applied to hold the current pose. The more torque is applied, the higher the fitness score. Therefore, the genetic algorithm selects the angles with the lowest fitness score. In each epoch or iteration, the best 20 individuals (poses) are selected as the parents of the next generation. The next generation is created by crossover, mixing the genes (joint angles) of the selected parents. A mutation ranging between 0 and 0.05 radians is randomly introduced in every 1 out of 4 new individuals to maintain genetic diversity and avoid local minima. Following this process iteratively, each generation of individuals reduces the torque applied by the robot compared to the previous generation until the algorithm converges in an optimal solution.

Our methodology allows easily applying physical constraints to the search space of the genetic algorithm. The constraints are implemented for two main reasons: to avoid the collisions between the robot and nearby physical obstacles and to avoid singularity poses. The algorithm rejects the angles that are in conflict with the physical constraints, i.e., every new generation of poses that the algorithm creates is checked to ensure that the new individuals satisfy the specified constraints. The constraints are defined by calculating the forward kinematics equations of the industrial robot with every new generation of individuals.

Although we decided to minimize the total torque of the robot, it is also possible to minimize the torque of a certain joint or group of joints, or even to implement a multiobjective optimization algorithm with multiple

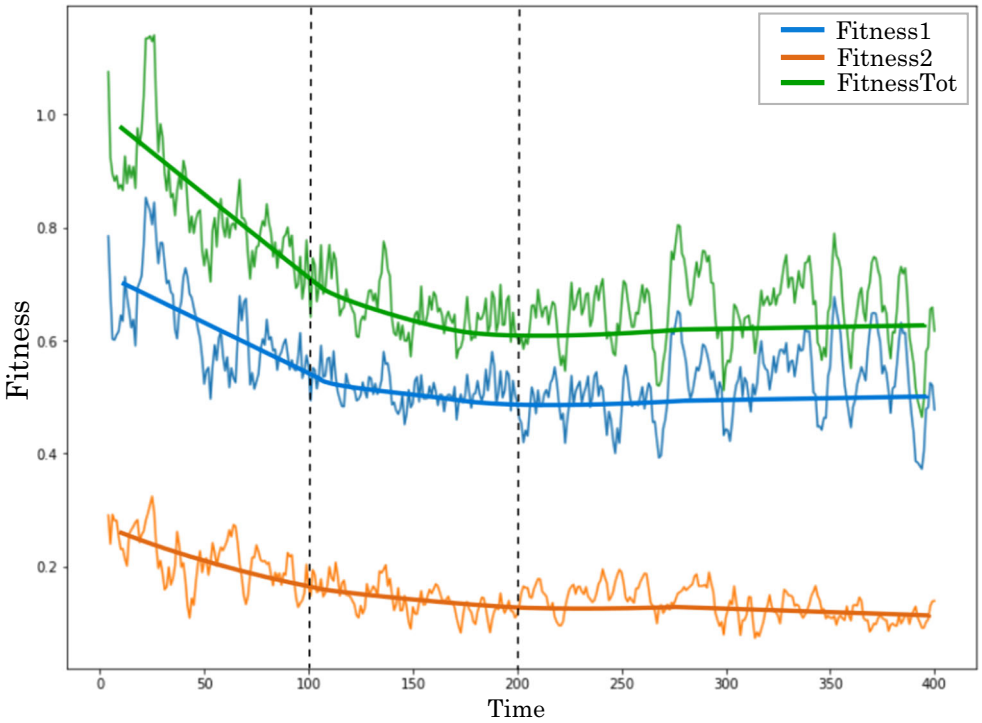

Fig. 3 Fitness function value of joints 1, 2, and 3 (blue); joints 4, 5, and 6 (orange); and the sum of the two fitness values (green)

objectives to optimize, e.g., to maximize the torque of a joint while minimizing the torque of another one. In our case, we developed a multiobjective minimization algorithm to minimize both the sum of the torques in joints 1, 2, and 3 and the sum of the torques in joints 4, 5, and 6 separately.

4 Results

Each of the two optimization objectives, i.e., sum of torques in joints 1, 2, and 3, and sum of torques in joints 4, 5, and 6, had its own fitness function. Figure 3 shows the fitness function of the two optimization objectives (Fitness1 and Fitness2) throughout the whole optimization process, as well as the sum of these two fitness functions (FitnessTot).

The genetic algorithm minimizes faster the fitness functions in the first 100 iterations than in the rest of the process. Afterwards, from iteration 100 to iteration 200, the fitness functions are minimized slower reaching a convergence point. Finally, the genetic algorithm reaches an optimal solution and converges approximately in the 200th iteration. Figure 4 shows the angles of each joint in radians while the optimization algorithm was executing. The lines in the figure represent the joint angles in each iteration, until the algorithm eventually finds the optimal standby pose.

The optimal standby pose in which the robot applies the minimum torque to hold the pose is shown in Fig. 5. The achieved pose is logically coherent, as the robot reaches a pose of equilibrium. The center of gravity of the whole systems stays as close as possible to the base of the robot. Therefore, the motors of the joints require the minimum amount of effort to hold the optimized pose.

Fig. 5 The optimal standby pose obtained by minimizing the total torque applied by the joints with the multiobjective genetic algorithm

The methodology is applicable to any robot and tool configuration. Every robot and tool will have its own optimal pose depending on the dimensions and center of gravity of the whole system. The algorithm will find the minimum torque-demanding pose regardless of the attached tool and without any additional code modification. To demonstrate the applicability of the methodology in

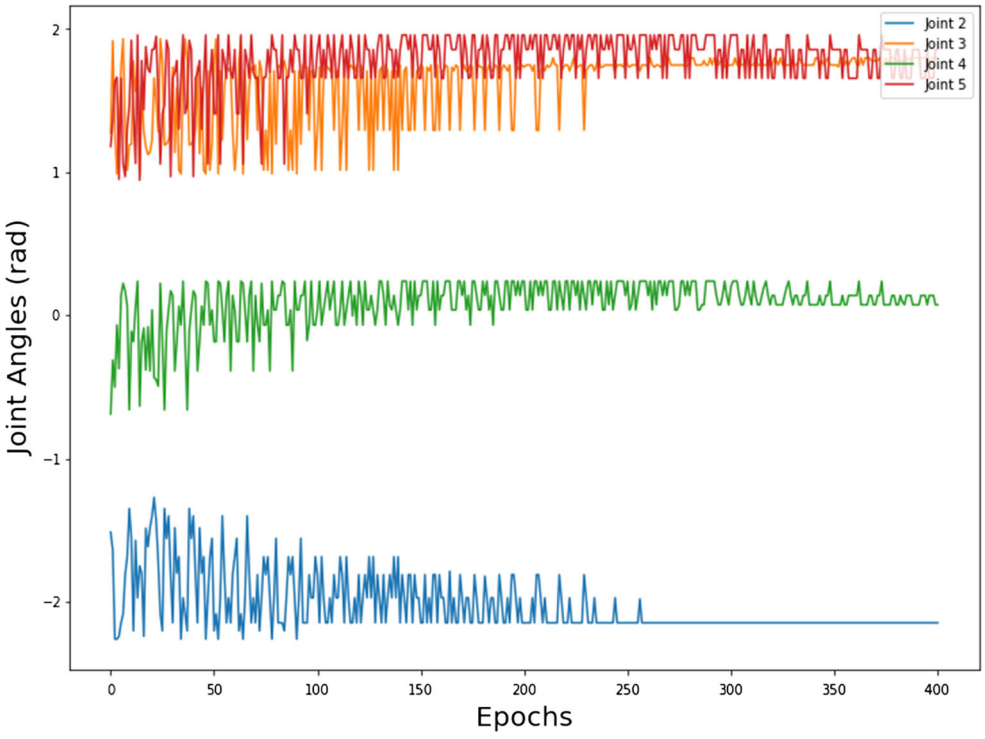

Fig. 4 The angle value (rad) of each joint while the optimization algorithm was in execution. The angles of joints 1 and 6 were removed from the figure for clarity

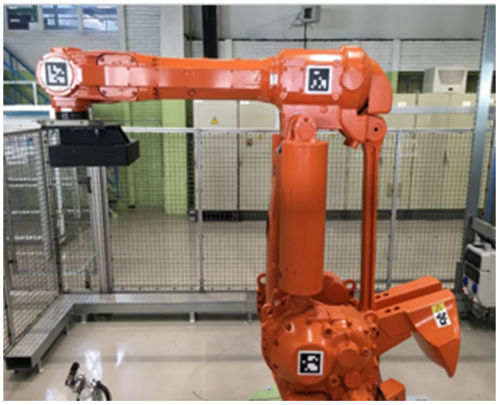

Fig. 6 Standard pose

Fig. 8 Optimized pose

different robots, we optimized the standby pose of a large ABB IRB 6400r industrial robot, following the same process described in this manuscript.

The optimization potential is more appreciable with large industrial robots, as they carry very heavy loads in assembly lines. Figures 6, 7, and 8 show the robot with a load of 140 kg in the default standby pose, in an extended pose, and in the optimized pose respectively. The total torque applied in these three poses is shown in Table 2. The robot applies 3.27 times more torque in the extended pose than in the optimal pose. This increment in the torque is a key factor for robot maintenance as pointed out in Section 2, especially for highly critical robots such as those located in assembly line bottlenecks.

5 Implementation in a manufacturing assembly line

We implemented the methodology in a real automotive manufacturing assembly line to measure the real optimization potential on industrial production working conditions. We selected a robot that had a particularly high failure frequency compared to the rest of the robots. In addition, the workstation of this robot was identical to an adjacent station. Which means that the work of this particular station was duplicated in another contiguous station and the robots of both stations executed the same work in parallel. These conditions allowed us to optimize the waiting pose of one robot and compare its torque minimization with respect to the robot that executed the same work in the contiguous station.

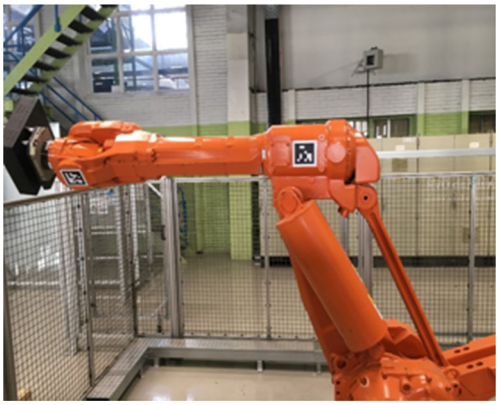

Fig. 7 Extended pose

The selected robot had a spot welding gun attached to the flange and carried a total load of 165.7 kg. We optimized the standby pose of the robot by implementing the presented methodology. The pose in which the robot waits for the next product was therefore modified to minimize the total torque applied in the joints. The period of time that robots spend waiting for the next product on automotive assembly lines depends on many factors: the state of the assembly line, the production rate, the trajectories that the robots have to execute, their location on the line, etc. Hence, the influence of the standby pose optimization on the energy efficiency and the increase of the robot's RUL will also depend on all these factors that determine its working regime.

Once we optimized the pose, we monitored the torque of all the joints in both robots (the optimized robot and its homologous in the contiguous workstation). The monitoring was carried out over approximately 2 h in normal production conditions. Figure 9 shows the total torque applied (the

Table 2 Torque required by an ABB IRB 6400r robot with a load of 140 kg in three different poses

Pose	Applied torque (Nm)
Standard	7.764
Extended	17.413
Optimized	5.333

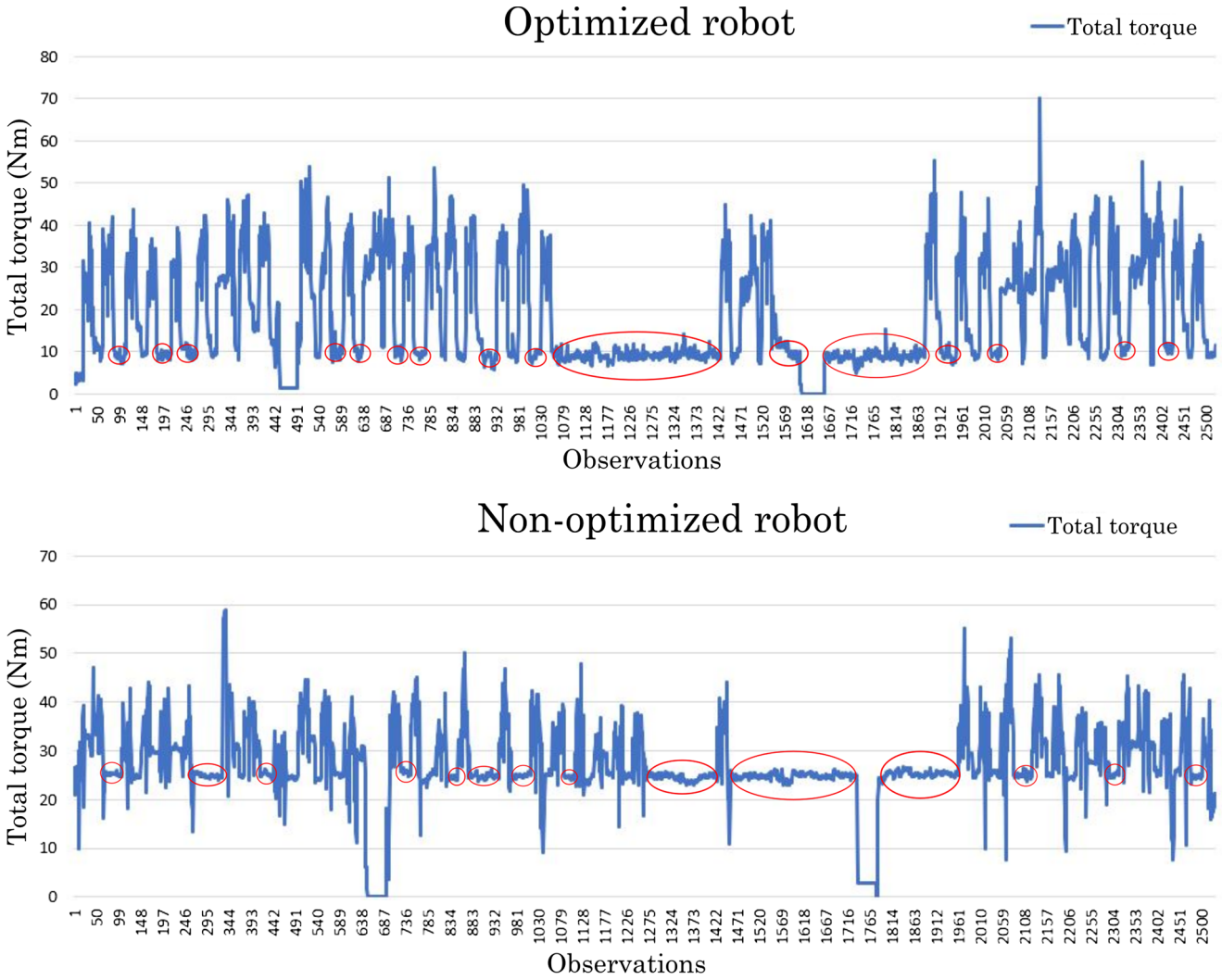

Fig. 9 Total torque of the optimized and non-optimized robots respectively. The red circles identify examples of periods of time in which the robots wait in their standby pose

sum of the torque of the 6 joints) by the optimized and non-optimized robots.

The torque minimization potential is significant as shown in the figures. The circles indicate specific periods of time in which the robots wait in a standby pose. The standby pose highly influences the median and mean values of the total torque in industrial robots. The median and mean values of the total torque in the optimized robot were 11.28 Nm and 18.56 Nm respectively. In contrast, the median and mean values of the non-optimized robot were 25.38 Nm and 27.06 Nm, respectively, which implies a 31.37% reduction of the average total torque applied by the optimized robot in normal production conditions. It is evident from these results that the optimization of the standby pose can significantly affect the total torque applied by industrial robots in real-world scenarios and therefore requires special attention from maintenance personnel.

6 Conclusions and future work

Although academic research has given little attention to the pose in which industrial robots wait, the standby pose directly influences the RUL and the electric consumption of these machines. We implemented a genetic algorithm to minimize the total torque of three different industrial robots. The results demonstrate that the difference in the total torque applied by a non-optimized standby pose can be up to 3.26 times higher than an optimized standby pose in a heavy payload industrial robot. The methodology is implemented to optimize the pose of an ABB IRB 6400r in real production conditions and its total applied torque is reduced by a 31.37%. A remarkable advantage of the methodology is its flexibility. It is robot model and tool invariant and the optimization is applicable to individual joints as well as to the entire robotic system. In addition,

the genetic algorithm permits to add constraints in its search space to avoid nearby obstacles. This might be especially useful for real-world scenarios, where industrial robots work in very limited workstations.

Further research is needed to accurately quantify the impact of a non-optimized standby pose in the RUL of industrial robots. A long-term study on the influence of the standby pose in the reduction of their RUL could path the way toward an effective predictive maintenance strategy for these complex systems. In future work, the possibility of modifying the trajectory or the standby pose of a robot to minimize the effort of a particular joint that is showing signs of imminent failure might prove important. If the effort on a failing joint can be reduced by minimizing the applied torque, maintenance personnel may have more time to plan interventions and reduce the impact on production. Finally, it would also be an interesting topic for future studies to propose a multiobjective optimization algorithm that would not only consider the total applied torque, but also the final state and location of the robots in the assembly line to facilitate a more efficient production time.

Acknowledgments This work has been developed by the Intelligent Systems for Industrial Systems group supported by the Department of Education, Language Policy and Culture of the Basque Government.

Funding It has been partially funded by the Basque Government.

References

1. Brossog M, Kohl J, Merhof J, Spreng S, Franke J et al (2014) Energy consumption and dynamic behavior analysis of a six-axis industrial robot in an assembly system. Procedia Cirp 23:131–136
2. Brossog M, Bornschlegl M, Franke J et al (2015) Reducing the energy consumption of industrial robots in manufacturing systems. Int J Adv Manuf Technol 78(5-8):1315–1328
3. Fleming P, Chipperfield A (1997) Genetic algorithms in engineering systems, vol 55. IET, London
4. Gadaleta M, Pellicciari M, Berselli G (2019) Optimization of the energy consumption of industrial robots for automatic code generation. Robot Comput Integr Manuf 57:452–464
5. Lin Y, Zhao H, Ding H (2017) Posture optimization methodology of 6r industrial robots for machining using performance evaluation indexes. Robot Comput Integr Manuf 48:59–72
6. Man KF, Tang KS, Kwong S (2012) Genetic algorithms for control and signal processing. Springer Science & Business Media, New York
7. Mitra K, Gopinath R (2004) Multiobjective optimization of an industrial grinding operation using elitist nondominated sorting genetic algorithm. Chem Eng Sci 59(2):385–396
8. Ouyang P, Zhang W (2005) Force balancing of robotic mechanisms based on adjustment of kinematic parameters
9. Paes K, Dewulf W, Vander Elst K, Kellens K, Slaets P (2014) Energy efficient trajectories for an industrial abb robot. Procedia Cirp 15:105–110
10. Quigley M, Conley K, Gerkey B, Faust J, Foote T, Leibs J, Wheeler R, Ng AY (2009) Ros: an open-source robot operating system. In: ICRA workshop on open source software, Kobe, Japan, vol 3, p 5
11. Wang F, Qian Z, Lin Y, Zhang W (2020) Design and rapid construction of a cost-effective virtual haptic device. IEEE/ASME Trans Mechatron
12. Xiong G, Ding Y, Zhu L (2019) Stiffness-based pose optimization of an industrial robot for five-axis milling. Robot Comput Integr Manuf 55:19–28
13. Yıldız AR (2009) A novel hybrid immune algorithm for global optimization in design and manufacturing. Robot Comput Integr Manuf 25(2):261–270
14. Zhang W, Chen X (2001) Mechatronics design for a programmable closed-loop mechanism. Proc Inst Mech Eng C 215(3):365–375

Chapter 11

Publication 4: A practical and synchronized data acquisition network architecture for industrial robot predictive maintenance in manufacturing assembly lines

A practical and synchronized data acquisition network architecture for industrial robot predictive maintenance in manufacturing assembly lines

***Abstract*—This manuscript presents a network architecture and a methodology for industrial robot data acquisition. We propose a non-intrusive and scalable robot signal extraction architecture, easily applicable in real manufacturing assembly lines. All the infrastructure needed for the implementation of the architecture is comprised of traditional well-known industrial assets. We synchronize the data acquisition with the execution of robot routines using common Programmable Logic Controllers (PLC) to obtain comparable data batches. A network architecture that acquires comparable and structured data over time, is a crucial step to advance towards an effective predictive maintenance of these complex systems, in terms of effectively detecting time dependent degradation. We implement the architecture in a real automotive manufacturing assembly line and show the potential of the solution to detect robot joint failures in real world scenarios.**

***Index Terms*—Cyber-Physical Systems, Industry 4.0, Predictive Maintenance, Industrial robots, IIoT**

I. Introduction

THE world's most industrialized economies are currently undergoing the so called fourth industrial revolution or Industry 4.0. This revolution covers a wide variety of technological developments such as: the digitalization of factories, the implementation of Big Data and advanced analytics solutions, the Internet of Things (IoT), the development and integration of new Cyber-Physical Systems (CPS), Smart cities, predictive maintenance policies, etc. In this manuscript, we will be focusing on two areas of Industry 4.0 in manufacturing: the evolution of CPS and data-based predictive maintenance.

Before we dig deeper into the issue, it is necessary to clarify the distinction between Industry 4.0 and CPS. CPS refers to a physical system controlled by communication networks and software. In the manufacturing industry, all the physical processes of the assembly line such as industrial robots, welding machines, cooling systems, etc. are controlled by industrial communication networks, centralized servers and Programmable Logic Controllers (PLC). Industry 4.0 in contrast, covers the evolution of traditional cyber-physical systems, as well as recently introduced concepts such as the implementation of Industrial Internet of Things (IIoT), Big Data infrastructures, machine learning models, etc. Thus, the evolution of CPS is a part of the whole framework of Industry 4.0.

In this context, traditional CPS are evolving to overcome new industrial challenges related to heterogeneous data acquisition and manipulation. This evolution can be separated into two fundamental categories [1]: system infrastructure and data analysis. The former refers to the network infrastructure itself and it's evolution, whereas the latter focuses on the analysis of the data, including statistical analysis or the training and testing of machine learning models.

The network architecture proposed in this article, is framed in the evolution of traditional cyber-physical systems within the Industry 4.0 paradigm and it is focused on the system infrastructure. The data acquisition methods, as well as the transformation and integration of heterogeneous data are three identified research challenges [2]. Traditional CPS were designed and implemented way before the concept of Industry 4.0 was introduced and these challenges arose as a consequence. Thus, to effectively implement data analysis in real industrial environments, it is necessary to first design and implement data acquisition, transformation and integration mechanisms that are coherent with the global framework of Industry 4.0.

Even though industry is making efforts to adapt to this new reality, the Prognosis and Health Management (PHM) of complex machinery is a challenging task and very few cases do in fact succeed in real life [3]. One of the main reasons behind this difficulty is that real machines are exposed to much more conditions than tested in laboratory. Even if we have a fleet of similar machines as it is the case of industrial robots, each individual will evolve and degrade differently, due to its unique work regime and environment.

In the last few years, several contributions have proposed condition monitoring and predictive maintenance solutions for industrial robots based on both analytical models [4], [5] and data-driven [6], [7], [8], [9] approaches. Nevertheless, the maintenance of industrial robots in manufacturing plants is yet either corrective (after a failure) or preventive (periodic joint lubricant checks for wear debris detection). In fact, there is no consensus about which is the most reliable methodology for industrial robot condition monitoring and predictive maintenance at production line scale. In other words, there is no clear approach or methodology to implement a predictive maintenance solution for a fleet of industrial robots in a real manufacturing assembly line.

On the one hand, the intelligence inherent in industrial robots can be very useful to overcome CPS challenges, as it offers the possibility of monitoring data in a synchronized, clean and structured way. On the other hand, the evolution of CPS and the implementation of Industry 4.0 technologies can help to advance towards an effective predictive maintenance policy for industrial robots. Therefore, the network architecture that we propose emphasizes the importance of the integration between the evolution of CPS and industrial robot maintenance strategies. Taking in this way a step forward towards a pragmatic predictive maintenance policy for industrial robots

in real industrial environments.

Bittencourt et al. [10] monitored a robot joint in a real accelerated wear test. They validated a methodology to detect a deviation in the monitored torque, caused by an increased friction in the joint. Their methodology assumes that the monitored data batches collected under a repetitive behavior are directly comparable when there is no fault and will vary otherwise. Therefore, in order to extrapolate the methodology to a real world scenario, it is essential to collect the data synchronously so that the batches are comparable.

The novelty of our manuscript resides on the description of a network architecture and methodology required as a preliminary step to carry out a reliable and practical PHM for a fleet of industrial robots in a real industrial environment. The proposed solution is especially useful for highly automated assembly lines.

The article is structured as follows: section II analyses the characteristics of complex industrial system condition monitoring. Section III describes the main differential characteristics of industrial robots and their advantages and disadvantages. In section IV we propose an architecture for an effective and synchronized data acquisition of a fleet of industrial robots and we describe the methodology in section V. Afterwards, we implement the proposed solution in a real automotive manufacturing assembly line and present the results in VI. Finally in section VII we summarize the main conclusions and define future lines of work.

II. Complex industrial system condition monitoring

Complex industrial systems work with critical processes and the failure of one of these systems often results in a significant economic loss for companies. Maintenance personnel carry out regular preventive maintenance tasks to keep these systems in the best possible condition and avoid eventual failures. As a consequence, complex industrial systems do not fail so often and there is not much representative data of failure states, which makes the training of data-driven models for health monitoring even more challenging.

Although these factors hinder the implementation of data-driven predictive models, the following contributions demonstrate the applicability of machine learning algorithms for PHM in complex industrial PHM use cases. Leahy et al. [11], [12] diagnosed wind turbine faults using machine learning models. Widodo et al. [13] implemented a support vector machine (SVM) and a relevance vector machine (RVM) for battery health prognostics. Pecht [14] defined a road-map for implementing PHM in electronic systems and emphasized the inaccuracy of traditional failure prediction models based on constant failure rates.

The absence of faulty operating conditions does not allow to train models with a supervised learning approach, where a percentage of the data is classified as *healthy* and the rest as *faulty*. As pointed out by Michau et al. in [15], unsupervised one-class classification can effectively deal with the diversity of the operating conditions of complex industrial systems. They proposed to first learn the healthy state of complex machinery using unsupervised models and then calculate the difference between the healthy and the current monitored state to detect deviations and possible failures. This approach only uses data of the healthy status of a machine to train the models, assuming the lack of faulty data that characterizes complex industrial systems.

In some cases like in assembly line industrial robots, the large number of assets form fleets. A factory-scale PHM solution should be able to extrapolate the healthy conditions learned in certain robots to create a generalized solution for the rest of the fleet's individuals. Collecting data from a fleet of complex systems, as in the case of industrial robots, can help to analyse and compare a wide variety of conditions that would be very difficult to cover with only a few individuals. However, in order to collect representative data of a fleet of robots, it is necessary to first design and implement a reliable network architecture that supports this data acquisition.

III. Predictive maintenance for industrial robots

Contributions on the predictive maintenance of industrial robots have been mainly focused on the selection of auspicious sensors and methodologies that address the PHM of individual industrial robots. Quiao et al. [16] warns about the importance of approaching the predictive maintenance of robotic systems from a holistic point of view, as a whole system and not by analysing their components individually. The interaction between the components within the robot, makes the behaviour of the system as a whole, distinct from that of the components monitored separately e.g. the behaviour and the environment of an electric motor is different when it is working attached to the ground, isolated and at constant speeds or moving inside a robot joint, with changing accelerations, loads, temperatures, torques, etc.

Some of the characteristics that differentiate industrial robots from other industrial systems are beneficial to build data-based predictive maintenance solutions. On the one hand, robotic systems permit to record structured data by monitoring internal signals. Which is a great inherent advantage over less sensorized industrial systems. Nowadays robot controllers are able to record information of the joints using factory built-in sensors and send the data through socket communication to an external server.

In addition, in highly automated assembly lines, industrial robot fleets can reach up to several hundred individuals and each one of them is a potential source of information. As mentioned before, the knowledge extracted in a given robot might be extrapolated to the rest of the fleet. Moreover, as all the robots working in a manufacturing production line are connected to a control network, it is possible to use this network to automatize and synchronize the data acquisition of an entire robot fleet in manufacturing production lines.

On the other hand, the main drawback for implementing data-based predictive maintenance solutions for industrial robots, is the complexity of the system. Robotic systems are highly configurable, both in terms of the trajectories they execute and the wide variety of tools they can use. Hence, while the behaviour of a robot with a certain path and tool may

be representative of impending failure, the same behaviour in another robot with another path and tool may be representative of a healthy state.

IV. Data acquisition network architecture

The network architecture is shown in figure 1. We divided it in five layers: data acquisition, control, external sensors, robot metadata, data storage and analysis and visualization layers. The implementation of the architecture does not require additional infrastructure than the usual found in a conventional automated production line as we explain in section VI.

A. Data acquisition layer

The data acquisition layer is the subnet that records the data from the robots and stores it in the data server. Nowadays robot controllers can send internal signals through TCP socket communication to an external receiver. This feature has to be enabled in the controller by specifying the internal signals to collect e.g. speed, resolver angle, torque, etc.

The signals can be acquired on demand. When the socket communication is enabled in the robot controllers, the data can be transmitted continuously or on demand when an external agent establishes connection. In our case, the *data server* decides when to start and end the acquisition and from which robot.

B. Control layer

Depending on the work they have to perform, the PLCs know which routine is each robot executing and when. This is crucial to synchronize the data acquisition and it is the core of our proposal.

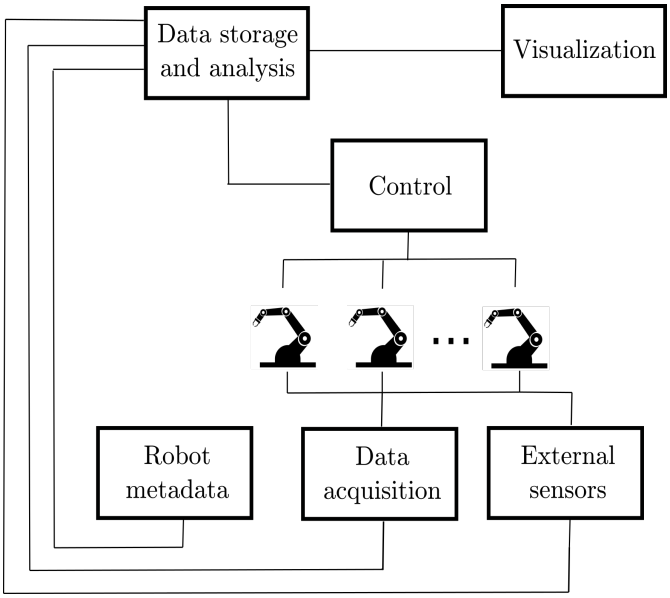

Fig. 1: The data acquisition network architecture. The control layer is used to synchronize the acquisition of robot signals with additional external sensors, as well as with the executed routines.

The difference between collecting data continuously and on demand is essential when the purpose of the data collection is to build predictive models. Specially for industrial robots, as their behaviour changes drastically depending on the routine they are executing. If the data acquisition process is done in a way in which every stream of data has a certain robot and routine assigned to it, the data will be comparable and representative of that particular robot and routine binomial.

Therefore, this architecture enables the data recording either continuously or discontinuously and synchronized. Each of these forms has its benefits. On the one hand, if the data is collected continuously, it describes the entire operational behavior of the robot. Including all the routines and the periods in which the robot waits standstill for the execution of the next routine. Depending on the robot, this standstill waiting time can be even longer than the actual execution of it's routines.

On the other hand, if the data is discontinuously and synchronously collected, the acquisition is only be performed when the robots execute certain routines. As a result, there is no recording while the robot waits standstill, but the data from a certain routine is directly comparable over time. This ability to compare the data of a robot-routine binomial over time is the key enabler for detecting anomalies and predicting medium and long-term wear. Therefore, the implementation of a data acquisition network architecture that supports both continuous and synchronized data extraction is a necessary preliminary step for building feasible predictive models.

C. External sensors layer

The signals collected from the data acquisition layer consist of internal robot signals. However, if there is more information to be recorded with additional external sensors, the data captured with the external sensors will be transmitted trough this layer. Examples of additional external sensors could be acoustic emission sensors, oil debris sensors, thermal images, etc.

A powerful benefit of the proposed architecture is that even if the external sensors are not intelligent enough to capture data on demand, the server will know which information stream coming from the external sensors merges with the internal robot signals of the data acquisition layer. The merging is possible by using the timer of the control layer to save the data that is acquired online with the external sensors. In this way, the control layer establishes the exact period of time when the data acquisition has to be performed in both layers. This synchronization is possible by using the PLCs of the control layer.

D. Robot metadata layer

The robot's metadata is used to classify the data acquired in the rest of the layers. The metadata contains information of the tool that each robot is holding and its weight, their maximum payload, the standby or waiting pose of each robot, the history of faults and its frequency, etc. The signals recorded in a faulty state of a given robot can be very similar to those recorded in the healthy state of another one. Therefore, By adding the metadata, it is possible to compare the acquired data between

robots that have similar working regimes and therefore detect anomalies in robots that should be behaving in the same way.

E. Data storage and analysis layer

The *data storage and analysis* layer consists of a server responsible for storing and analysing the data acquired from the *data acquisition*, *additional sensors* and *robot metadata* layers. The server communicates with the PLCs to decide when to start collecting the data in each robot and merges the acquired signals with the appropriate additional information. As mentioned in the *control layer* section, although we propose to collect the data on demand, it is also possible to monitor and store the data continuously e.g. if we want to store the behaviour of a robot uninterruptedly both when it executes routines and when it waits in a standby pose. The diagram of the database that stores robot signals and robot metadata is shown in figure 2. Where each table stores the following information:

- *Routines:* Defines which routine is recorded in each robot.
- *Robot_Signals:* Defines which signals are recorded in each robot (resolver angle, speed or torque).
- *Robot_Description:* Stores the metadata of each robot (ID number, IP address, model, location in line, load, date of last failure, attached tool, etc.)
- *Data_Raw:* Stores the data that comes directly from the *Data acquisition layer*. We do not clean or process the data before storing it in this table.
- *Statistical_Summaries:* After processing the data stored in the *Data_Raw* table, we store the results of the statistical analysis and summaries of each routine in this table. Each line of the table saves an statistical descriptive summary of all the acquired raw data.
- *RUL_Estimation:* Finally, once the data analysis is carried out, the results of the Remaining Useful Life (RUL) are calculated using the current health status of each robot and it's historical failure records. This table stores a RUL estimation for each robot based on the results of the data analysis.

In our case, the data analysis is implemented in the same server where the data is stored. However, it is also possible to separate these functionalities in two different servers, one for data storage and the other one for the data analysis and model implementation, as long as the communication between each other is guaranteed.

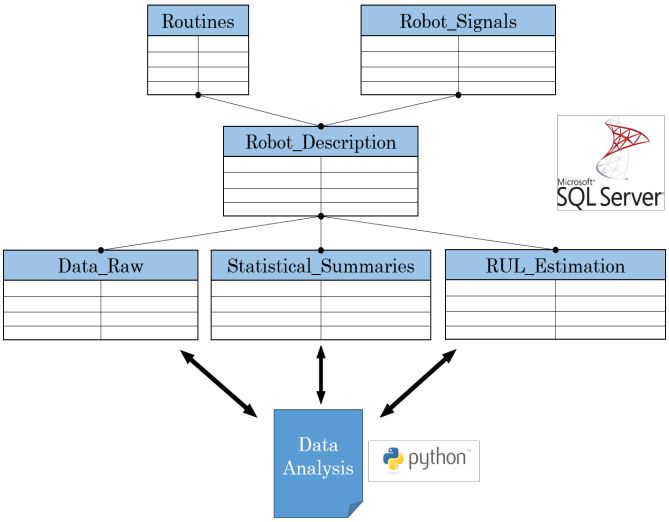

Fig. 2: Diagram of the implemented database that stores the robot signals and metadata in the *data server*.

F. Visualization layer

The visualization layer consists in data visualization software and infrastructure. It visualizes the results extracted from the analysis and the predictions calculated with the models. Our architecture permits to analyse and visualize robot data at two independent levels: at an individual scale with predictive maintenance models and RUL estimation for individual robots, and at a general scale with a global visualization of the robot fleet.

V. Data acquisition process

The data acquisition process is illustrated in figure 3. The process starts in the *data server*, by selecting the robot and routine to be monitored. The server checks in the corresponding PLC the status of the robot (*Robot-1* in the sequence diagram) and it waits until the PLC confirms that the routine has started (*routine X* in the sequence diagram).

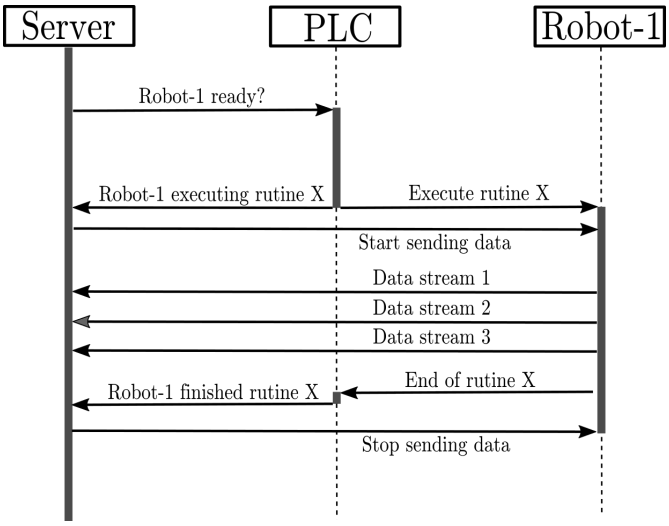

Fig. 3: Sequence diagram of the data acquisition process.

The PLC sends a signal to the robot to start the routine and simultaneously confirms the start to the *data server*. When the server receives the confirmation signal from the PLC, it opens the TCP/IP socket communication with the robot controller and starts receiving the robot signals. The signals that the controller captures and sends have to be previously coded in the controller, as well as the transmission frequency (ranging from $1\,\mathrm{ms}$ to 100 or $500\,\mathrm{ms}$). When the robot finishes the routine, it sends a message to the PLC and the PLC sends another one to the server to stop the data acquisition. Finally the server closes the socket communication with the robot controller, finishing the data acquisition process.

In the TCP/IP socket communication, the robot controller acts as a TCP server while the *data server* acts as a TCP client. The controller opens the communication port and waits until the server connects to receive the data. The server, connects to the robots when the PLC confirms that the robot has started to execute a certain routine, as explained above. In this way, the server assigns a signal stream to an specific robot-routine combination, clearly separating between different working regimes. A remarkeble benefit of this architecture is that the signal acquisition is carried out in a network separated from the control layer. The collected signals do not pass through the PLCs in their way to the *data server* and therefore, there is no risk of saturating the control network or the PLCs. After storing the signals in the *data server*, additional information from external data sources (external sensors or databases) can be added to the collected signal streams. The synchronization with the PLCs allows collecting data from external sensors at the same time of the execution of the routine.

VI. Implementation in an automotive body shop assembly line

We implemented the network architecture in an automotive manufacturing body shop assembly line. Manufacturing assembly lines are highly automated and hundreds of industrial robots work uninterruptedly separated in working cells. The PLCs in the control layer are able to manage several working cells simultaneously via INTERBUS or PROFINET protocols. The hardware required for the proposed infrastructure already exists in any common automated assembly line. Therefore, the implementation is mainly based on software development to enhance the functionalities of the current infrastructure. In our case, the only additional hardware asset we added was the *data server*.

A. Infrastructure implementation

The first step is to code the signal recording and the TCP socket server in the robot controllers. Modern robot controllers integrate a TCP server to enable a socket-based signal acquisition. We collected the torque signals of the six joints in each robot. The signal acquisition rate is also configurable and it depends on the frequency in which we want to transmit the data.

The second step is to create a set of variables in the PLCs to inform the *data server* about the beginning and the end of the routines. These variables update their values exactly at the same time as the robot starts the routine, synchronizing in this way the data acquisition and creating comparable data batches.

We implemented two main programs in the *data server*: one to read the variables of the PLCs and the other to handle the communication with the robot controllers. As mentioned above, the communication with the robot controller is performed via socket by implementing a TCP client in the server. The client connects to a remote TCP server (the robot controller) when the PLC notifies the start of a given routine.

When the data acquisition finishes, the received signals are merged with additional information coming form external sensors and databases. The language in which the models and the visualization of the results are implemented in the *Data storage and analysis layer*, depends on the software available in each company. However, the proposed architecture will remain invariant regardless of these differences.

We started by implementing the architecture in two robots inside the same working cell, before scaling up the solution to more cells and robots. When collecting the data, we checked that the TCP packets were not saturating the network and we ensured that the memory and the processor of the robot controllers where operating as usual. Thus, we ensured that the data acquisition did not have any negative impact in the production line before scaling up the architecture. We tested different transmission frequencies and none of them saturated the network.

B. Results

We collected the data in two ways. First without synchronizing it with the routines, collecting the data continuously without interruption. Afterwards, synchronizing the data collection with the PLCs. In figures 4 and 5 we show the collected signals without synchronization. The signals correspond to two hours of data acquisition of two industrial robots (*Robot 1* and *Robot 2*) while working in several routines and waiting standby. The graphs show the torque of the six joints of each robot.

Even though the robots execute different trajectories, both of them are ABB irb 6400r robots with a maximum payload of $200\,\mathrm{Kg}$ and they both have a $104\,\mathrm{Kg}$ spot welding gun attached to their flange. Note the difference in the behaviour of the two robots, not only between the working and waiting time, but also in the torque of each joint. The execution of different working regimes completely alters the behaviour of the joints and makes the generalization and comparison between these two robots unfeasible. In addition, by acquiring data in this way without synchronization, there is no clear distinction between the routines that each of them executes. The continuous data acquisition does not separate the different routines and therefore there is no way to compare them over time and detect deterioration or anomalies. In order to identify the wear of a robot, it is essential to be able to compare routines over time, and this is not possible if the routines cannot be separated.

In contrast, figures 6 and 7 show data acquired in two different moments (*T1* and *T2*) of the same robot (*Robot 2*) executing the same routine. These two graphs demonstrate the

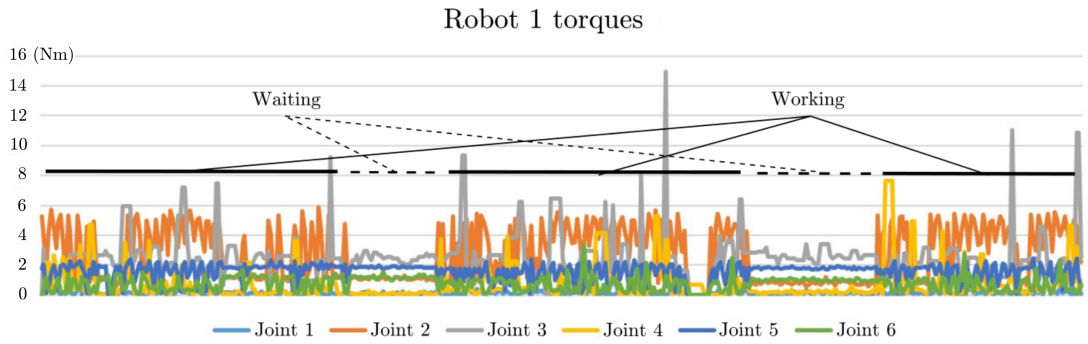

Fig. 4: Continuous data acquisition of *Robot 1*.

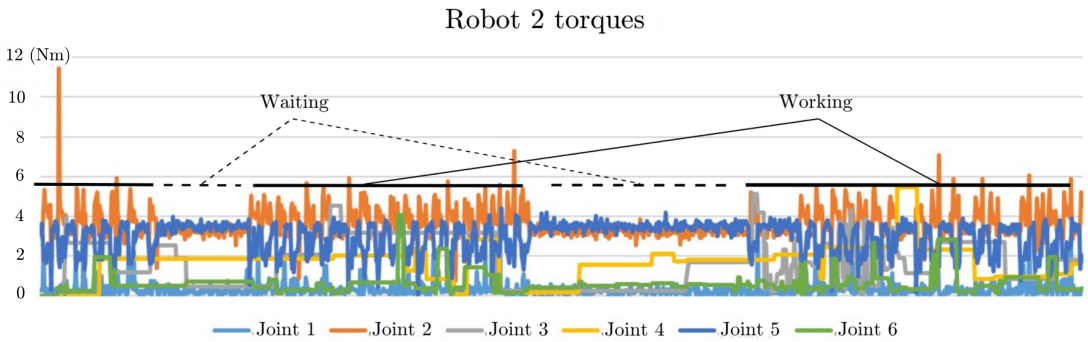

Fig. 5: Continuous data acquisition of *Robot 2*.

Robot_ID	Motor_ID	Trajectory_ID	Median_Torque	Average_Torque	Maximum_Torque	Variance_Torque
508	5	502	4.76	4.34	8.74	1.80
508	5	502	4.79	4.43	8.27	1.62
508	5	502	4.90	4.54	8.91	1.74
508	5	502	4.99	4.61	8.73	1.82
508	5	502	4.76	4.52	8.58	1.74
508	5	502	4.61	4.28	8.12	1.77
508	5	502	4.83	4.62	8.42	1.62

TABLE I: Example of summary statistics of the acquired trajectories. Each row represents the statistical summary (median, average, maximum and variance) of the torque data applied by the same motor of a robot in production.

ability of our approach to automatically identify and separate data from specific routines. The torque data shown in 6 and 7 were acquired with the proposed architecture to demonstrate the possibility of achieving comparable data by using the *control layer*. The data acquisition is not programmed for any specific moment in time, but it starts automatically when the robot starts executing the specified routine. The proposed data acquisition procedure is an effective solution to the problem exposed in the previous paragraph with the continuous data acquisition.

The *control layer* effectively identifies the routine and the *data server* divides the signal streams in separated robot-routine binomials. As a result, the obtained signals are much more comparable over time and an eventual health degradation assessment is easier to address. One of the key benefits of this architecture is that data collection is performed at the same time in all the data sources. The result of this data acquisition procedure is a time series dataset that represents the behaviour of a given robot-routine binomial.

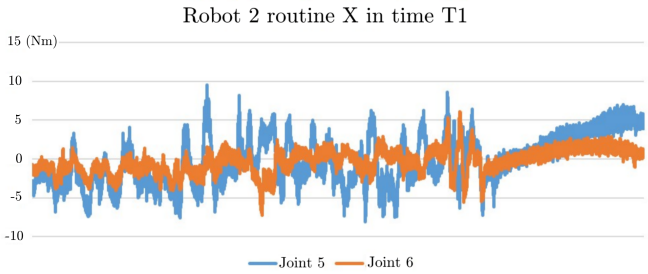

Fig. 6: Synchronized data acquisition of *Robot 2* (joints 5 and 6) executing routine *X* in time *T1*.

As explained above, it is hard to identify anomalies in the behaviour of a robot if there is no clear distinction between different routines and working conditions. Each robot requires

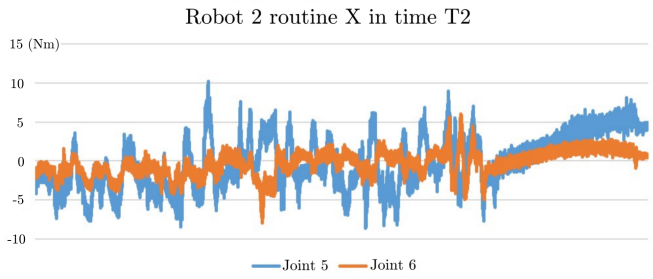

Fig. 7: Synchronized data acquisition of *Robot 2* (joints 5 and 6) executing routine *X* in time *T2*.

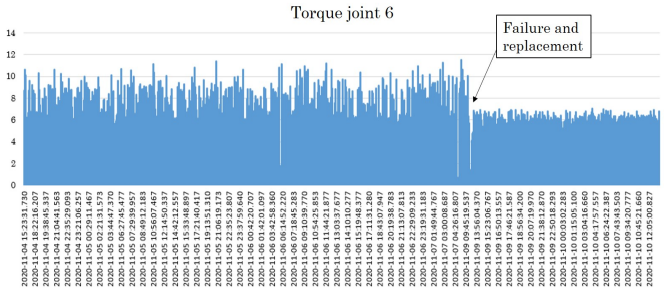

Fig. 8: Synchronized acquired torque of the failing sixth joint.

a different effort in each joint. Thus, in order to compare real production line data of a given robot over time and predict possible failures, it is necessary to first distinguish between routines and then diagnose the robot's evolution.

Once we are able to isolate individual trajectories, we can begin calculating summary statistics of the trajectories. The objective of summary statistics is to condense the maximum amount of information of the trajectories in the smallest amount of data. These summaries will be used for long-term condition monitoring and predictive maintenance. Table I shows the summary statistics of the torque signal applied by the fifth motor of a monitored industrial robot in production. The summaries are stored along with the robot's ID number and the trajectory's ID. In this table we do not show all the columns of the dataset for readability and clearness reasons. The complete set of information that we summarize for each torque and joint angle signal is as follows: Date and time of the data acquisition, an id number of the robot, an id number of the motor, an id number of the trajectory, the median value, the average value, the maximum value, the 3rd quartile, the variance and the skewness. The decision of which statistical analysis to choose will be based on the data and the objective of the analysis. The effectiveness of predictive maintenance strategies for industrial robots will strongly rely on the robustness of these summaries.

We scaled the proposed architecture to twenty robots in the production line and started acquiring synchronized data. After a couple of weeks monitoring, one of the robots had a failure in the reducer of the sixth joint that stopped the production. The robot required a total replacement of the sixth joint. Figure 8 shows the data acquired some days before and after the replacement of the sixth joint.

By synchronizing the data acquisition, it is easily appreciable the change in the torque applied by a robot joint before and after a joint failure. The torque was much higher before the joint replacement as a consequence of the unusual friction caused by the degraded reducer. After replacing the failing joint, the monitored torque signal stabilized and the peak values decreased significantly.

Figure 8 shows an example of the applicability of the presented solution to build a practical and reliable data acquisition infrastructure to detect and eventually predict robot joint failures. As described in section II, one-class classification models could be trained to model a healthy joint behavior after the replacement of the joint. In this way, the model would be trained to detect anomalies based on the torque applied by the joint and identify unusual torque increments for that particular robot-trajectory configuration.

VII. Conclusions and Future Work

The purpose of this work is to present a network architecture capable of collecting data from industrial robots in a robust, reliable and clean way, in order to implement predictive maintenance models afterwards. The architecture only uses well known industrial assets and thus it requires no extra infrastructure investment for an automated manufacturing assembly line. Based on PLC and robot controller programming, industrial robots can benefit from the intelligence of their own controllers to send structured signal data to an external server. The proposed solution also takes into account additional external sensors or databases that could be included in the network to extend the information of the monitored robots.

The main benefit of this architecture is that the synchronization of the data acquisition separates the information obtained by each robot in each routine automatically. This permits to compare the behaviour of a robot in the same routine over time and predict possible failures in an easier way than by capturing continuous data without synchronization. In this way, the final goal of building predictive maintenance models for complex industrial systems like industrial robots becomes more realistic.

After implementing the architecture, the next step is to further analyse the data collected under different working regimes. The eventual robot failures will also be very valuable in order to train and test predictive maintenance models. The training and testing of these models is independent from the data acquisition layer. Hence, the proposed architecture will remain unchanged regardless of the data analysis strategy carried out. Future lines of work will focus on building machine learning models capable of modelling healthy robot behaviour using the proposed architecture e.g. If the acquired data is comparable, anomaly or novelty detection algorithms could be used to detect a deviation in the normal behaviour of a given robot. Future work will also address the challenging task of determining the level of generalization that a predictive maintenance model for industrial robots should have and which algorithms are able to robustly model such a complex and non-linear behaviour.

REFERENCES

[1] L. D. Xu and L. Duan, "Big data for cyber physical systems in industry 4.0: a survey," *Enterprise Information Systems*, vol. 13, no. 2, pp. 148–169, 2019.

[2] M. Khan, X. Wu, X. Xu, and W. Dou, "Big data challenges and opportunities in the hype of industry 4.0," in *2017 IEEE International Conference on Communications (ICC)*. IEEE, 2017, pp. 1–6.

[3] J. Lee, H.-A. Kao, S. Yang *et al.*, "Service innovation and smart analytics for industry 4.0 and big data environment," *Procedia Cirp*, vol. 16, no. 1, pp. 3–8, 2014.

[4] I. Trendafilova and H. Van Brussel, "Non-linear dynamics tools for the motion analysis and condition monitoring of robot joints," *Mechanical Systems and Signal Processing*, vol. 15, no. 6, pp. 1141–1164, 2001.

[5] A. Carvalho Bittencourt, "Modeling and diagnosis of friction and wear in industrial robots," Ph.D. dissertation, Linköping University Electronic Press, 2014.

[6] A. A. Jaber, *Design of an intelligent embedded system for condition monitoring of an industrial robot*. Springer, 2016.

[7] X. Liu, X. Wu, C. Liu, and T. Liu, "Research on condition monitoring of speed reducer of industrial robot with acoustic emission," *Transactions of the Canadian Society for Mechanical Engineering*, vol. 40, no. 5, pp. 1041–1049, 2016.

[8] A. C. Bittencourt, K. Saarinen, S. Sander-Tavallaey, S. Gunnarsson, and M. Norrlöf, "A data-driven approach to diagnostics of repetitive processes in the distribution domain–applications to gearbox diagnostics in industrial robots and rotating machines," *Mechatronics*, vol. 24, no. 8, pp. 1032–1041, 2014.

[9] U. Izagirre, I. Andonegui, A. Egea, and U. Zurutuza, "A methodology and experimental implementation for industrial robot health assessment via torque signature analysis," 2020.

[10] A. C. Bittencourt, K. Saarinen, and S. Sander-Tavallaey, "A data-driven method for monitoring systems that operate repetitively-applications to wear monitoring in an industrial robot joint," *IFAC Proceedings Volumes*, vol. 45, no. 20, pp. 198–203, 2012.

[11] K. Leahy, R. L. Hu, I. C. Konstantakopoulos, C. J. Spanos, and A. M. Agogino, "Diagnosing wind turbine faults using machine learning techniques applied to operational data," in *2016 IEEE International Conference on Prognostics and Health Management (ICPHM)*. IEEE, 2016, pp. 1–8.

[12] K. Leahy, R. L. Hu, I. C. Konstantakopoulos, C. J. Spanos, A. M. Agogino, and D. T. O'Sullivan, "Diagnosing and predicting wind turbine faults from scada data using support vector machines," *International Journal of Prognostics and Health Management*, vol. 9, no. 1, pp. 1–11, 2018.

[13] A. Widodo, M.-C. Shim, W. Caesarendra, and B.-S. Yang, "Intelligent prognostics for battery health monitoring based on sample entropy," *Expert Systems with Applications*, vol. 38, no. 9, pp. 11 763–11 769, 2011.

[14] M. G. Pecht, "A prognostics and health management roadmap for information and electronics-rich systems," *IEICE ESS Fundamentals Review*, vol. 3, no. 4, pp. 4_25–4_32, 2010.

[15] G. Michau, Y. Hu, T. Palmé, and O. Fink, "Feature learning for fault detection in high-dimensional condition monitoring signals," *Proceedings of the Institution of Mechanical Engineers, Part O: Journal of Risk and Reliability*, p. 1748006X19868335, 2019.

[16] G. Qiao and B. A. Weiss, "Advancing measurement science to assess monitoring, diagnostics, and prognostics for manufacturing robotics," *International journal of prognostics and health management*, vol. 7, no. Spec Iss on Smart Manufacturing PHM, 2016.

Bibliography

[1] Fazel Ansari, Robert Glawar, and Wilfried Sihn. Prescriptive maintenance of cpps by integrating multimodal data with dynamic bayesian networks. In *Machine Learning for Cyber Physical Systems*, pages 1–8. Springer, 2020.

[2] Pramod Bangalore and Lina Bertling Tjernberg. An artificial neural network approach for early fault detection of gearbox bearings. *IEEE Transactions on Smart Grid*, 6(2):980–987, 2015.

[3] Tarak Benkedjouh, Kamal Medjaher, Noureddine Zerhouni, and Saïd Rechak. Health assessment and life prediction of cutting tools based on support vector regression. *Journal of Intelligent Manufacturing*, 26(2):213–223, 2015.

[4] Maurizio Bevilacqua and Marcello Braglia. The analytic hierarchy process applied to maintenance strategy selection. *Reliability Engineering & System Safety*, 70(1):71–83, 2000.

[5] Bharat Bhushan. *Introduction to tribology*. John Wiley & Sons, 2013.

[6] André Carvalho Bittencourt, Kari Saarinen, Shiva Sander-Tavallaey, Svante Gunnarsson, and Mikael Norrlöf. A data-driven approach to diagnostics of repetitive processes in the distribution domain–applications to gearbox diagnostics in industrial robots and rotating machines. *Mechatronics*, 24(8):1032–1041, 2014.

[7] Erik Leandro Bonaldi, Levy Ely de Lacerda de Oliveira, Jonas Guedes Borges da Silva, Germano Lambert-Torresm, and Luiz Eduardo Borges da Silva. Predictive maintenance by electrical signature analysis to induction motors. In *Induction Motors-Modelling and Control*. IntechOpen, 2012.

[8] Salah Bouhouche, Laib Laksir Yazid, Sissaoui Hocine, and Jürgen Bast. Evaluation using online support-vector-machines and fuzzy reasoning. application to

condition monitoring of speeds rolling process. *Control Engineering Practice*, 18(9):1060–1068, 2010.

[9] André Carvalho Bittencourt. *Modeling and Diagnosis of Friction and Wear in Industrial Robots*. PhD thesis, Linköping University Electronic Press, 2014.

[10] Varun Chandola, Arindam Banerjee, and Vipin Kumar. Anomaly detection: A survey. *ACM computing surveys (CSUR)*, 41(3):1–58, 2009.

[11] Zhe Cheng and Niaoqing Hu. Quantitative damage detection for planetary gear sets based on physical models. *Chinese Journal of Mechanical Engineering*, 25 (1):190–196, 2012.

[12] Danny I Cho and Mahmut Parlar. A survey of maintenance models for multi-unit systems. *European journal of operational research*, 51(1):1–23, 1991.

[13] Balbir S Dhillon. *Engineering maintenance: a modern approach*. cRc press, 2002.

[14] José A Caldeira Duarte, João C Taborda A Craveiro, and Tomás Pedro Trigo. Optimization of the preventive maintenance plan of a series components system. *International Journal of Pressure Vessels and Piping*, 83(4):244–248, 2006.

[15] S Ebersbach, Z Peng, and NJ Kessissoglou. The investigation of the condition and faults of a spur gearbox using vibration and wear debris analysis techniques. *Wear*, 260(1-2):16–24, 2006.

[16] Erika Echavarria, Tetsuo Tomiyama, and Gerard JW van Bussel. Fault diagnosis approach based on a model-based reasoner and a functional designer for a wind turbine. an approach towards self-maintenance. In *Journal of Physics: Conference Series*, volume 75, page 012078. IOP Publishing, 2007.

[17] Erika Echavarria, Tetsuo Tomiyama, H Huberts, and G Van Bussel. Fault diagnosis system for an offshore wind turbine using qualitative physics. In *Proc. EWEC*. Citeseer, 2008.

[18] Yanhui Feng, Yingning Qiu, Christopher J Crabtree, Hui Long, and Peter J Tavner. Monitoring wind turbine gearboxes. *Wind Energy*, 16(5):728–740, 2013.

[19] Diego FernáNdez-Francos, David MartíNez-Rego, Oscar Fontenla-Romero, and Amparo Alonso-Betanzos. Automatic bearing fault diagnosis based on one-class ν-svm. *Computers & Industrial Engineering*, 64(1):357–365, 2013.

[20] Diego Galar and Mirka Kans. The impact of maintenance 4.0 and big data analytics within strategic asset management. In *Maintenance Performance and Measurement and Management 2016 (MPMM 2016). November 28, Luleå, Sweden*, pages 96–104. Luleå tekniska universitet, 2017.

[21] Mari Cruz Garcia, Miguel A Sanz-Bobi, and Javier Del Pico. Simap: Intelligent system for predictive maintenance: Application to the health condition monitoring of a windturbine gearbox. *Computers in Industry*, 57(6):552–568, 2006.

[22] Brian P Graney and Ken Starry. Rolling element bearing analysis. *Materials Evaluation*, 70(1), 2012.

[23] Liang Guo, Hongli Gao, Haifeng Huang, Xiang He, and ShiChao Li. Multifeatures fusion and nonlinear dimension reduction for intelligent bearing condition monitoring. *Shock and Vibration*, 2016, 2016.

[24] Minna Haavisto. Studies on the time-dependent demagnetization of sintered ndfeb permanent magnets. 2013.

[25] Hashem M Hashemian. State-of-the-art predictive maintenance techniques. *IEEE Transactions on Instrumentation and measurement*, 60(1):226–236, 2010.

[26] Qingbo He, Fanrang Kong, and Ruqiang Yan. Subspace-based gearbox condition monitoring by kernel principal component analysis. *Mechanical Systems and Signal Processing*, 21(4):1755–1772, 2007.

[27] RBW Heng and Mohd Jailani Mohd Nor. Statistical analysis of sound and vibration signals for monitoring rolling element bearing condition. *Applied Acoustics*, 53(1-3):211–226, 1998.

[28] Alaa Abdulhady Jaber. *Design of an intelligent embedded system for condition monitoring of an industrial robot*. Springer, 2016.

[29] Gregory J Kacprzynski, Michael Gumina, Michael J Roemer, Daniel E Caguiat, Thomas R Galie, and Jack J McGroarty. A prognostic modeling approach for predicting recurring maintenance for shipboard propulsion systems. In *ASME Turbo Expo 2001: Power for Land, Sea, and Air*. American Society of Mechanical Engineers Digital Collection, 2001.

[30] Matthias KARNER, Robert GLAWAR, Wilfried SIHN, and Kurt MATYAS. Integrating machine tool condition monitoring and production scheduling in

metal forming. *Proceedings of MOTSP 2o18 (in Press), Primosten, Croatia*, 2018.

[31] Nguyen LD Khoa, Bang Zhang, Yang Wang, Fang Chen, and Samir Mustapha. Robust dimensionality reduction and damage detection approaches in structural health monitoring. *Structural Health Monitoring*, 13(4):406–417, 2014.

[32] Jeffery L Kohler, Joseph Sottile, and Frederick C Trutt. Alternatives for assessing the electrical integrity of induction motors. *IEEE Transactions on Industry Applications*, 28(5):1109–1117, 1992.

[33] Andrew Kusiak and Wenyan Li. The prediction and diagnosis of wind turbine faults. *Renewable Energy*, 36(1):16–23, 2011.

[34] Mark A Latino, Robert J Latino, and Kenneth C Latino. *Root cause analysis: improving performance for bottom-line results*. CRC press, 2019.

[35] Jay Lee, Edzel Lapira, Behrad Bagheri, and Hung-an Kao. Recent advances and trends in predictive manufacturing systems in big data environment. *Manufacturing letters*, 1(1):38–41, 2013.

[36] Yaguo Lei, Feng Jia, Jing Lin, Saibo Xing, and Steven X Ding. An intelligent fault diagnosis method using unsupervised feature learning towards mechanical big data. *IEEE Transactions on Industrial Electronics*, 63(5):3137–3147, 2016.

[37] Chuan Li, René-Vinicio Sánchez, Grover Zurita, Mariela Cerrada, and Diego Cabrera. Fault diagnosis for rotating machinery using vibration measurement deep statistical feature learning. *Sensors*, 16(6):895, 2016.

[38] WY Liu, WH Zhang, JG Han, and GF Wang. A new wind turbine fault diagnosis method based on the local mean decomposition. *Renewable Energy*, 48:411–415, 2012.

[39] Xiaoqin Liu, Xing Wu, Chang Liu, and Tao Liu. Research on condition monitoring of speed reducer of industrial robot with acoustic emission. *Transactions of the Canadian Society for Mechanical Engineering*, 40(5):1041–1049, 2016.

[40] Kurt Matyas, Tanja Nemeth, Klaudia Kovacs, and Robert Glawar. A procedural approach for realizing prescriptive maintenance planning in manufacturing industries. *CIRP Annals*, 66(1):461–464, 2017.

[41] John J McCall. Maintenance policies for stochastically failing equipment: a survey. *Management science*, 11(5):493–524, 1965.

[42] Gabriel Michau and Olga Fink. Domain adaptation for one-class classification: monitoring the health of critical systems under limited information. *International Journal of Prognostics and Health Management*, 10:11, 2019.

[43] R Keith Mobley. *An introduction to predictive maintenance*. Elsevier, 2002.

[44] Dimitris Mourtzis, Nikolaos Milas, and Nikolaos Athinaios. Towards machine shop 4.0: a general machine model for cnc machine-tools through opc-ua. *Procedia CIRP*, 78:301–306, 2018.

[45] Nabtesco. RV-N reduction gear reduction gear example. URL https://precision.nabtesco.com/en/products/detail/RV-N.

[46] Tanja Nemeth, Fazel Ansari, Wilfried Sihn, Bernhard Haslhofer, and Alexander Schindler. Prima-x: A reference model for realizing prescriptive maintenance and assessing its maturity enhanced by machine learning. *Procedia CIRP*, 72: 1039–1044, 2018.

[47] Caxton Okoh, Rajkumar Roy, Jorn Mehnen, and Louis E Redding. Overview of remaining useful life prediction techniques in through-life engineering services. 2014.

[48] Charles H Oppenheimer and Kenneth A Loparo. Physically based diagnosis and prognosis of cracked rotor shafts. In *Component and Systems Diagnostics, Prognostics, and Health Management II*, volume 4733, pages 122–132. International Society for Optics and Photonics, 2002.

[49] Suttichai Premrudeepreechacharn, Tawee Utthiyoung, Komkiat Kruepengkul, and Pongsatorn Puongkaew. Induction motor fault detection and diagnosis using supervised and unsupervised neural networks. In *2002 IEEE International Conference on Industrial Technology, 2002. IEEE ICIT'02.*, volume 1, pages 93–96. IEEE, 2002.

[50] Guixiu Qiao and Brian A Weiss. Advancing measurement science to assess monitoring, diagnostics, and prognostics for manufacturing robotics. *International journal of prognostics and health management*, 7(Spec Iss on Smart Manufacturing PHM), 2016.

[51] Guixiu Qiao and Brian A Weiss. Monitoring, diagnostics, and prognostics for robot tool center accuracy degradation. 2018.

[52] Guixiu Qiao and Brian A Weiss. Quick health assessment for industrial robot health degradation and the supporting advanced sensing development. *Journal of Manufacturing Systems*, 2018.

[53] Morgan Quigley, Ken Conley, Brian Gerkey, Josh Faust, Tully Foote, Jeremy Leibs, Rob Wheeler, and Andrew Y Ng. Ros: an open-source robot operating system. In *ICRA workshop on open source software*, volume 3, page 5. Kobe, Japan, 2009.

[54] Bhaskar Saha, Kai Goebel, Scott Poll, and Jon Christophersen. Prognostics methods for battery health monitoring using a bayesian framework. *IEEE Transactions on instrumentation and measurement*, 58(2):291–296, 2008.

[55] Randy R Schoen, Brian K Lin, Thomas G Habetler, Jay H Schlag, and Samir Farag. An unsupervised, on-line system for induction motor fault detection using stator current monitoring. *IEEE Transactions on Industry Applications*, 31(6): 1280–1286, 1995.

[56] Xiao-Sheng Si, Wenbin Wang, Chang-Hua Hu, and Dong-Hua Zhou. Remaining useful life estimation–a review on the statistical data driven approaches. *European journal of operational research*, 213(1):1–14, 2011.

[57] Hoon Sohn, Charles R Farrar, Norman F Hunter, and Keith Worden. Structural health monitoring using statistical pattern recognition techniques. *Journal of dynamic systems, measurement, and control*, 123(4):706–711, 2001.

[58] Lukas Spendla, Michal Kebisek, Pavol Tanuska, and Lukas Hrcka. Concept of predictive maintenance of production systems in accordance with industry 4.0. In *2017 IEEE 15th International Symposium on Applied Machine Intelligence and Informatics (SAMI)*, pages 000405–000410. IEEE, 2017.

[59] E Burton Swanson. The dimensions of maintenance. In *Proceedings of the 2nd international conference on Software engineering*, pages 492–497. IEEE Computer Society Press, 1976.

[60] Prasanna Tamilselvan and Pingfeng Wang. Failure diagnosis using deep belief learning based health state classification. *Reliability Engineering & System Safety*, 115:124–135, 2013.

[61] Fei Tao, Qinglin Qi, Ang Liu, and Andrew Kusiak. Data-driven smart manufacturing. *Journal of Manufacturing Systems*, 48:157–169, 2018.

[62] Ciriaco Valdez-Flores and Richard M Feldman. A survey of preventive maintenance models for stochastically deteriorating single-unit systems. *Naval Research Logistics (NRL)*, 36(4):419–446, 1989.

[63] Hongzhou Wang. A survey of maintenance policies of deteriorating systems. *European journal of operational research*, 139(3):469–489, 2002.

[64] K Wang. Intelligent predictive maintenance (ipdm) system–industry 4.0 scenario. *WIT Transactions on Engineering Sciences*, 113:259–268, 2016.

[65] Lidong Wang and Guanghui Wang. Big data in cyber-physical systems, digital manufacturing and industry 4.0. *International Journal of Engineering and Manufacturing (IJEM)*, 6(4):1–8, 2016.

[66] Yuanhang Wang, Chao Deng, Jun Wu, Yingchun Wang, and Yao Xiong. A corrective maintenance scheme for engineering equipment. *Engineering Failure Analysis*, 36:269–283, 2014.

[67] Achmad Widodo and Bo-Suk Yang. Support vector machine in machine condition monitoring and fault diagnosis. *Mechanical systems and signal processing*, 21(6):2560–2574, 2007.

[68] Wikipedia. Asperities in solid surface asperities. URL https://en.wikipedia.org/wiki/Asperity_(materials_science).

[69] Jihong Yan, Yue Meng, Lei Lu, and Lin Li. Industrial big data in an industry 4.0 environment: Challenges, schemes, and applications for predictive maintenance. *IEEE Access*, 5:23484–23491, 2017.

[70] Bo-Suk Yang, Andy Chit Chiow Tan, et al. Multi-step ahead direct prediction for the machine condition prognosis using regression trees and neuro-fuzzy systems. *Expert systems with applications*, 36(5):9378–9387, 2009.

[71] Xiaomin Zhao, Tejas H Patel, and Ming J Zuo. Multivariate emd and full spectrum based condition monitoring for rotating machinery. *Mechanical Systems and Signal Processing*, 27:712–728, 2012.